University of São Paulo
"Luiz de Queiroz" College of Agriculture

Sugarcane plant detection and mapping for site-specific management

Leonardo Felipe Maldaner

Thesis presented to obtain the degree of Doctor of Science. Area: Agricultural Systems Engineering

Piracicaba
2022

Leonardo Felipe Maldaner
Agricultural Engineering

Sugarcane plant detection and mapping for site-specific management

Versão revisada de acordo com a resolução CoPGr 6018 de 2011

Advisor
Prof. Dr. **JOSÉ PAULO MOLIN**

Thesis presented to obtain the degree of Doctor of Science. Area: Agricultural Systems Engineering

Piracicaba
2022

Dados Internacionais de Catalogação na Publicação
DIVISÃO DE BIBLIOTECA – DIBD/ESALQ/USP

Maldaner, Leonardo Felipe

Sugarcane plant detection and mapping for site-specific management / Leonardo Felipe Maldaner. - - versão revisada de acordo com a resolução CoPGr 6018 de 2011 - - Piracicaba, 2022.

83p.

Tese (Doutorado) - - USP / Escola Superior de Agricultura “Luiz de Queiroz”.

1. Precision agriculture 2. Crop sensing 3. High-resolution image 4. Plant variability. I. Título

ACKNOWLEDGEMENTS

My sincere thanks,

To University of São Paulo - "Luiz de Queiroz" College of Agriculture (USP-ESALQ) and Agricultural Systems Engineering Graduate Program (PPGESA) for providing the infrastructure and the environment necessary to get my Doctor in Science degree.

To Prof. José Paulo Molin, for the opportunity to have you as Master and Ph.D. supervisor. I am very proud to mention him as one of those responsible for my professional academic education. I thank you for your trust, friendship, advice, and patience. You are an example of simplicity, knowledge, and competence.

To National Council for Scientific and Technological Development (CNPq) grant number 168643/2017-0, and also financial support promoted, at the beginning of the doctorate, by the Brazilian Federal Agencies: Coordination for the Improvement of Higher Education Personnel (CAPES) – Finance Code 001.

To companies São Manuel Mill, São Manuel, SP and Agency Paulista Agribusiness Technology (APTA), Piracicaba, SP for the partnership and availability of sugarcane fields for the development of the thesis; and to Solinfitec Incorporated, Araçatuba, SP for the partnership and help in mapping the sugarcane yield over the three years of research.

To Prof. Carlos Tadeu do Santos Dias for the kind contribution and suggestions regarding the methods used for modeling the data.

To all friends from Precision Agriculture Laboratory (LAP), including the guys from the mechanization and precision agriculture group (gMAP), for the pleasant working environment of the last years.

To all employees of the Department of Biosystems Engineering, for cordiality and support during the daily activities, especially to Agnaldo F. Degaspari, Áureo S. de Oliveira, Davilmar A. D. Colevatti, Francisco de Oliveira (Chicão), José G. Gomes, and Juarez R. do Amaral.

To my parents Aroni José and Celeide, for the example of dedication, honesty and perseverance, role models to be followed, and to my wife Rosineide and my son João Miguel for their support and unconditional love. Thank you for your encouragement and patience with me in those very busy days that preceded the delivery of this thesis. This thesis is dedicated to you.

Thank you all!

CONTENTS

RESUMO

Detecção e mapeamento de plantas de cana-de-açúcar para gerenciamento específico do local

O setor de produção de cana-de-açúcar é um dos mais aptos a adotar tecnologia para gerenciar equipamentos e as lavouras de cana-de-açúcar. Desenvolver novas tecnologias e otimizar o uso das tecnologias já utilizadas em outros sistemas de produção é essencial para o sucesso da gestão das lavouras. O uso otimizado de tecnologias ajudará na gestão localizada a aumentar a viabilidade, maximizar a rentabilidade e minimizar os impactos ambientais da produção de cana-de-açúcar. Tecnologias para detectar, medir e espacializar plantas podem ser uma das soluções para o gerenciamento a nível de fileira. Além disso, estes dados podem ser usados para acompanhar temporariamente o desenvolvimento das lavouras de cana-de-açúcar, sendo dados essenciais para o gerenciamento localizado da lavoura. A espacialização das plantas e o espaçamento entre plantas podem ajudar na investigação dos fatores que influenciam a produtividade da cana-de-açúcar. Neste contexto, o objetivo geral da tese foi explorar ferramentas e métodos de detecção de plantas em nível de fileira para melhorar e apoiar o gerenciamento localizado de plantações de cana-de-açúcar. Uma abordagem para a detecção de plantas de cana-de-açúcar usando sensores fotoelétricos e ultrassônicos foi desenvolvida e avaliada. A imagem aérea e os sensores terrestres foram testados para detectar e medir o espaçamento entre plantas de cana-de-açúcar. A avaliação temporal dos sensores e imagens aéreas durante quatro estágios diferentes de desenvolvimento da cana-de-açúcar foi feita para propor o melhor momento para detectar plantas de cana-de-açúcar e medir o espaçamento entre as plantas. Imagens de alta resolução foram usadas para mapear a população e o espaçamento das plantas. Estes dois dados foram utilizados para verificar a relação entre declividade, ângulo do percurso e a população de plantas, além disso, mapear regiões com maior suscetibilidade à redução de plantas ao longo dos anos. Finalmente, foi realizada a análise espacial-temporal da produtividade e espaçamento de plantas para verificar a relação entre estas duas variáveis em regiões com diferentes potenciais produtivos em lavouras comerciais. Os resultados mostram que a fusão de sensores ultrassônico e fotoelétrico associada ao modelo de aprendizagem da máquina tem precisão acima de 95%. Estes dois sensores e imagens de alta resolução tiveram a melhor precisão e acurácia para detectar e medir o espaçamento das plantas em 31 e 47 dias após a colheita. A análise espacial e temporal mostrou que regiões com uma declive do terreno de 5-8% e maior que 8% com percursos curvos têm um número inferior de plantas em comparação com outras regiões. A análise local identificou que regiões com declives mais acentuados e caminhos curvos têm alta suscetibilidade de redução da planta ao longo dos anos, em comparação com outras regiões. Finalmente, a perda de produtividade dentro da fileira da cana de açúcar ocorre com o aumento do espaçamento entre as plantas. Regiões com diferentes potenciais produtivos requerem diferentes populações ótimas para maximizar a produtividade. Regiões de baixa produtividade requerem uma população de plantas maior e são mais suscetíveis a perder produtividade dentro da fileira com o aumento do espaçamento entre plantas.

Palavras-chave: Agricultura de precisão; Sensoriamento da cultura; Imagem de alta resolução; Variabilidade da cultura

ABSTRACT

Sugarcane plant detection and mapping for site-specific management

The sugarcane production sector is one of the most adept at adopting technology to manage equipment and sugarcane fields. Developing new technologies and optimizing the use of the technologies already used in other production systems is essential for successful field management. The optimized use of technologies will help in the localized management to increase viability, maximize profitability, and minimize the environmental impacts of sugarcane production. Technologies to detect, measure, and spatialize plants can be one of the solutions for the row level management.. Moreover, this data can be used to temporally follow the development of sugarcane fields, being essential data for localized field management. The spatialization of plants and plant spacing can help in the investigation of factors that influence sugarcane yield. In this context, the overall objective of the thesis was to explore tools and methods for detecting plants at row level to improve and support localized management of sugarcane plantations. An approach to sugarcane plant detection using photoelectric and ultrasonic sensors was developed and evaluated. Aerial image and ground sensors have been tested to detect and measure sugarcane plant spacing. Temporal evaluation of sensors and aerial images during four different stages of sugarcane development was made to propose the best time to detect sugarcane plants and measure the plant spacing. High-resolution images were used to map plant population and plant spacing. These two data were used to check the relationship between slope, path angle, and the plant population, furthermore, map regions with higher susceptibility to plant reduction over the years. At last, a spatio-temporal analysis of yield and plant spacing was performed to verify the relationship between these two variables in regions with different yield potentials in commercial crops. Results show that ultrasonic and photoelectric sensor fusion associated with the machine learning model has accuracy above 95%. These two sensors and high-resolution images had the best accuracy and precision in detecting and measuring plant spacing at 31 and 47 days after harvest. Spatial and temporal analysis showed that regions with a terrain slope of 5-8% and greater than 8% with curved paths have an inferior number of plants compared to other regions. The local analysis identified that regions with steeper slopes and curved paths have high susceptibility of plant reduction over the years compared to other regions. Finally, yield loss within the sugarcane row occurs with increasing plant spacing. Regions with different yield potentials require different optimum populations to maximize yield. Low-yielding regions require a larger plant population and are more susceptible to lose in yield within the row with increasing plant spacing.

Keywords: Precision agriculture; Crop sensing; High-resolution image; Plant variability.

FIGURE LIST

TABLE LIST

1. GENERAL INTRODUCTION

Raw material to produce sugar, ethanol, and bioelectricity, sugarcane (*Saccharum* spp.) is an important commodity in the Brazilian economy. Brazil is the world's largest sugarcane producer and one of the world's largest ethanol producers. In 2020, Brazil produced 654.8 million tons in a cultivated area of 8.62 million hectares (CONAB, 2020). Sugarcane is considered one of the great alternatives for the biofuels sector due to its great potential in ethanol production. Currently, it is one of the crops with the highest adoption rate of technologies aimed at optimizing the use of inputs, increasing yields, more sustainable and profitable practices.

Sugarcane is a perennial grass with phenological characteristic tillering in early grown stages. After the first harvest, its cycle lasts an average of 12 months. The number of plant and tiller density is important to achieve high yields and have a profitable production. Moreover, the longevity of the sugarcane yield is essential for the amortization of planting costs. However, sugarcane yield declines over the years, and keep high yields over the years is still a challenge. Many factors can cause a reduction in the number of plants and tiller density within the sugarcane field. In Brazil, the longevity is on average 5-6 ratoons, obtaining low economic return after this period, being more feasible to plow out the plants and implement a new sugarcane field.

For many years, the management of sugarcane fields has been based on limited amount of data. Precision agriculture (PA) combines spatial and temporal data with other information to support management decisions according to the estimated variability for better resource utilization efficiency, yield, quality, profitability, and sustainability of agricultural production (ISPA, 2019). It includes many technologies ranging from sensing systems that map crop and soil variability to guidance systems and variable-rate (VR) systems that dose agricultural inputs onto the field (Sanches et al., 2021). In Brazil, PA tools being used are auto-guide of machinery (Passalaqua and Molin, 2020), soil fertility mapping (Sanches et al., 2019), satellite images (Canata et al., 2021), yield monitors (Magalhães and Cerri, 2007; Maldaner et al., 2021; Momin et al., 2019), and canopy sensors for input variable-rate application (Amaral et al., 2018; Portz et al., 2013).

However, there is still a need to develop new systems and methods to identify the variability of sugarcane at the row level and from there to make interventions and decision-making during field management. For this, systems to detecting the plants within the sugarcane rows may be a solution for localized application of inputs. Systems capable of performing plant-by-plant application may be able to maximize the efficiency of input application, applying only the dose necessary to maximize the production of each plant, and minimize environmental impacts, avoiding unnecessary application in places without plants. In other perennial crops such as oranges, grapes, apples, systems with sensors to detect plants and perform localized application can significantly reduce off-target losses (Gil et al., 2007; H. Y. Jeon and H. Zhu, 2012; Llorens et al., 2010; Mahmud et al., 2021). In this sense, new research is important with low-cost sensors capable of detecting sugarcane plants and which is easily accessible to the sugarcane industry, which can assist the adoption of new technologies by producers.

From this point of view, taking advantage of the data generated by these expert systems is a powerful tool to guide and assist in the localized management of sugarcane fields. Plant spacing information together with sugarcane yield information is widely used in decision making for localized replanting of the sugarcane field. Currently, the tool most used by the industry for mapping plant spacing is high-resolution imaging (Luna and Lobo, 2016). However, this methodology still faces major challenges, such as image post-processing, spectral quality of the images, and optimal resolution for plant identification. Furthermore, it is necessary to understand how this

methodology performs in identifying plants in the early grown stages since the canopy of plants can influence the accuracy in identifying and individualizing the sugarcane plants (Souza et al., 2017).

On top of it all, monitoring the sugarcane plant population over the years is very important because mapping brings detailed information that can help in decision-making for replanting regions with low plant counts or applying agricultural inputs appropriately in defective regions (Shirzadifar et al., 2020). Which can help in the optimization of inputs, adjustments in tillage, irrigation, even replanting, reducing costs, maximizing yield, and minimizing environmental impacts. Monitoring the factors that influence yield has become increasingly essential for decision-making. Moreover, identify regions with greater susceptibility to plant reduction can be powerful data to improve the decision-making for partial or total replanting of the sugarcane field and reduce the cost of implementing a new sugarcane field.

This thesis hypothesizes that methodologies capable of detecting, measuring, and spatializing plants can be one of the solutions for the in-row management of sugarcane. Moreover, this information can be used to temporally follow the development of sugarcane fields, being essential data for localized field management. Also, the spatialization of plants and plant spacing can help in the investigation of factors that influence sugarcane yield. In this context, the overall objective of the thesis was to explore tools and methods for detecting plants at row level to improve and support localized management of sugarcane plantations. This thesis is divided into four distinct studies with specific objectives but with the same context of using the spatialization of plants and plant spacing to guide the localized management of sugarcane fields.

1.1. Connection text to chapter 2

Novel precision agriculture approaches that allow real-time intervention within sugarcane rows offer solutions to reduce costs and minimize negative environmental impacts. However, most of the tools utilized in site-specific management demand high investments. The research and investigation for cost-effective solutions present a promising challenge in agriculture. One of the alternatives is to implement low-cost tools as presently operated in other areas, and that can be adapted to agricultural practices. Chapter 2 explores the use of sensors for detecting plants within the sugarcane row. A system was developed and evaluated for its accuracy in detecting sugarcane plants.

The full text of chapter 2 is published in *Computers and Electronics in Agriculture* journal:

Maldaner, L.F.; Molin, J.P.; Martello, M.; Canata, T.F. (2021) A system for plant detection using sensor fusion approach based on machine learning model. *Computers and Electronics in Agriculture, 189: 106382*. https://doi.org/10.1016/j.compag.2021.106382

References

Amaral, L.R., Trevisan, R.G., Molin, J.P., 2018. Canopy sensor placement for variable-rate nitrogen application in sugarcane fields. Precis. Agric. 19, 147–160. https://doi.org/10.1007/s11119-017-9505-x

Canata, T.F., Wei, M.C.F., Maldaner, L.F., Molin, J.P., 2021. Sugarcane Yield Mapping Using High-Resolution Imagery Data and Machine Learning Technique. Remote Sens. 13, 232. https://doi.org/10.3390/rs13020232

CONAB, C.N. do A., 2020. Acompanhamento da safra brasileira - Cana-de-açúcar, Safra 2020/2021, Quarto levantamento. Brasília, DF.

Gil, E., Escolà, A., Rosell, J.R., Planas, S., Val, L., 2007. Variable-rate application of plant protection products in

vineyard using ultrasonic sensors. Crop Prot. 26, 1287–1297. https://doi.org/10.1016/j.cropro.2006.11.003

H. Y. Jeon, H. Zhu, 2012. Development of a Variable-Rate Sprayer for Nursery Liner Applications. Trans. ASABE 55, 303–312. https://doi.org/10.13031/2013.41240

ISPA, I.S. of P.A., 2019. ISPA Precision Ag definition [WWW Document]. URL https://www.ispag.org/about/definition (accessed 6.16.21).

Llorens, J., Gil, E., Llop, J., Escolà, A., 2010. Variable rate dosing in precision viticulture: Use of electronic devices to improve application efficiency. Crop Prot. 29, 239–248. https://doi.org/10.1016/j.cropro.2009.12.022

Luna, I., Lobo, A., 2016. Mapping crop planting quality in sugarcane from UAV imagery: A pilot study in Nicaragua. Remote Sens. 8, 1–18. https://doi.org/10.3390/rs8060500

Magalhães, P.S.G., Cerri, D.G.P., 2007. Yield Monitoring of Sugar Cane. Biosyst. Eng. 96, 1–6. https://doi.org/10.1016/j.biosystemseng.2006.10.002

Mahmud, M.S., Zahid, A., He, L., Choi, D., Krawczyk, G., Zhu, H., Heinemann, P., 2021. Development of a LiDAR-guided section-based tree canopy density measurement system for precision spray applications. Comput. Electron. Agric. 182, 106053. https://doi.org/10.1016/j.compag.2021.106053

Maldaner, L.F., Corrêdo, L. de P., Canata, T.F., Molin, J.P., 2021. Predicting the sugarcane yield in real-time by harvester engine parameters and machine learning approaches. Comput. Electron. Agric. 181, 105945. https://doi.org/10.1016/j.compag.2020.105945

Momin, M.A., Grift, T.E., Valente, D.S., Hansen, A.C., 2019. Sugarcane yield mapping based on vehicle tracking. Precis. Agric. 20, 896–910. https://doi.org/10.1007/s11119-018-9621-2

Passalaqua, B.P., Molin, J.P., 2020. Path errors in sugarcane transshipment trailers. Eng. Agric. 40, 223–231. https://doi.org/10.1590/1809-4430-ENG.AGRIC.V40N2P223-231/2020

Portz, G., Amaral, L.R., Molin, J.P., Adamchuk, V.I., International, Y., Molin, J.P., Adamchuk, V.I., 2013. Field comparison of ultrasonic and canopy reflectance sensors used to estimate biomass and N-uptake in sugarcane, in: Precision Agriculture 2013 - Papers Presented at the 9th European Conference on Precision Agriculture, ECPA 2013. Wageningen Academic Publishers, Wageningen, pp. 111–117. https://doi.org/10.3920/978-90-8686-778-3_12

Sanches, G.M., Graziano Magalhães, P.S., Junqueira Franco, H.C., 2019. Site-specific assessment of spatial and temporal variability of sugarcane yield related to soil attributes. Geoderma 334, 90–98. https://doi.org/10.1016/j.geoderma.2018.07.051

Sanches, G.M., Magalhães, P.S.G., Kolln, O.T., Otto, R., Rodrigues, F., Cardoso, T.F., Chagas, M.F., Franco, H.C.J., 2021. Agronomic, economic, and environmental assessment of site-specific fertilizer management of Brazilian sugarcane fields. Geoderma Reg. 24, e00360. https://doi.org/10.1016/j.geodrs.2021.e00360

Shirzadifar, A., Maharlooei, M., Bajwa, S.G., Oduor, P.G., Nowatzki, J.F., 2020. Mapping crop stand count and planting uniformity using high resolution imagery in a maize crop. Biosyst. Eng. 200, 377–390. https://doi.org/10.1016/j.biosystemseng.2020.10.013

Souza, C.H.W. de, Lamparelli, R.A.C., Rocha, J.V., Magalhães, P.S.G., 2017. Mapping skips in sugarcane fields using object-based analysis of unmanned aerial vehicle (UAV) images. Comput. Electron. Agric. 143, 49–56. https://doi.org/10.1016/j.compag.2017.10.006

2. A SYSTEM FOR PLANT DETECTION USING SENSOR FUSION APPROACH BASED ON MACHINE LEARNING MODEL

Abstract

There is a need for new precision agriculture approaches that allow real-time intervention within sugarcane rows to reduce costs and minimize negative environmental impacts. Therefore, our goal was to test an alternative system for detection within rows of sugarcane plants. The objective was to determine the errors of an alternative system to detect targets of different sizes at different travel speeds. A system with a photoelectric sensor, ultrasonic sensor, and encoder was developed to detect and map the plants within the sugarcane row. The use of sensors separately and simultaneously for plant detection was compared. To improve the accuracy of plant detection, decision tree (DT), random forest (RF), and support vector machine (SVM) models were tested. The three machine learning (ML) models used data generated by the photoelectric and ultrasonic sensors along with the displacement sensor. The models were compared in terms of their precision in detecting plants within sugarcane rows. The approach with the two sensors and the DT model had the best precision (>90%) in plant detection. The sensors have the ability to detect 91% of the total plants (recall = 0.91). The travel speed influenced the performance of the sensors in detecting the targets, especially at 2 m s−1. The accuracy and precision of the plant detection system at different speeds indicate the possibility of the sensors being used in integrating systems for real-time interventions. In addition, the system generates data to plant and gap maps, which are useful information to support the site-specific management of sugarcane fields.

Keywords: Precision agriculture; Ultrasonic sensor; Photoelectric sensor; Plant sensing; Plant variability

2.1. Introduction

Sugarcane (*Saccharum* spp.) is a perennial crop with a growth cycle of 12–18 months. After the first harvest, a gradual decline in yield is common, which leads to the necessity of plowing out at a certain break-even point. Ratooning is a fundamental trait related to the profitability of sugarcane farming (Matsuoka and Stolf, 2012). Thus, the high cost of establishing a plantation can be amortized over a number of lower-cost ratoon crops (Chapman and Wilson, 1996). In this regard, site-specific management within a row based on precision agriculture (PA) techniques can be a solution for sustainable sugarcane production and sustain high yields over the years. Nevertheless, nowadays it is challenging to find new cost-effective approaches that allow site-specific management to increase agricultural yields and reduce production costs (Andújar et al., 2013; Lindblom et al., 2017).

Although technologies to reduce input applications in some perennial crops and reduce production costs (Abbas et al., 2020) have been developed, there is a need for new technologies for localized management at the sugarcane row level. Embedded sensors in agricultural machines are a promising approach that in addition to providing real-time localized applications can provide data for mapping ratoon stands and the lengths of plant gaps within the rows. Map spots within a sugarcane field with low and high gap intensities are important tools to improve management decisions (Molin and Veiga, 2016), for example, in aiding decisions to fully or partially plow out a sugarcane field (Matsuoka and Stolf, 2012). Temporal analysis of sugarcane stand and gap maps provided by sensors during farming operations can help future site-specific applications within sugarcane fields. The data generated

within each row reflects the final sprouting of the plants and allows for the prediction of parameters related to crop yield. In addition, this information can help predict yield within sugarcane fields (Sanches et al., 2018).

The use of sensor systems capable of detecting sugarcane plants to support real-time variable-rate applications may be a solution to reduce application costs. Although there are studies with sensors that measure the reflectance of plants to specific wavelengths within each row to nitrogen variable-rate applications (Amaral et al., 2018, 2015), there are no approaches that allow ON/OFF input application within sugarcane rows. ON/OFF control systems can optimize the application of inputs within sugarcane rows by being applied only where sugarcane plants are detected. In studies with perennial crops such as oranges, apples, and vineyards, this system can significantly reduce off-target losses (Gil et al., 2007; H. Y. Jeon and H. Zhu, 2012; Llorens et al., 2010; Mahmud et al., 2021).

Different sensor systems have been studied for application in perennial crops. Among the sensors, ultrasonic and photoelectric sensors are the simplest for detecting and characterizing plant canopies (Abbas et al., 2020). For agricultural applications, ultrasonic sensors have been used to detect spaces between plants and turn off the spray in the gap between tree canopies (Escolà et al., 2013; Palleja and Landers, 2015; Zürey et al., 2020) and variable rate application (Gil et al., 2007; Moltó et al., 2001; Solanelles et al., 2006). Portz et al. (2013) used an ultrasonic sensor to measure the canopy height and compared it with the canopy reflectance to predict sugarcane biomass and N uptake. A photoelectric sensor was used simultaneously with a capacitive sensor to detect poplar cuttings along a row (Assirelli et al., 2015). Xin et al. (2018) used a photoelectric sensor to detect plant transplant locations in an intelligent transplanting system.

Molin and Veiga (2016) developed the first system based on a photoelectric sensor to map the gap length in sugarcane fields. The performance of the system in measuring the gap between the ratoons was evaluated. However, it is necessary to evaluate these sensors with regard to their ability to detect plants within a row. Not detecting plants could overestimate the size of the gaps, which could influence the final information and consequently lead to an erroneous decision. Thus, our hypothesis is that the use of this system together with one or more sensors simultaneously improves sugarcane ratoon detection capability. Integrating two or more sensors can achieve more reliable, precise, and valuable data than a single sensor (Abbas et al., 2020; Dasarathy, 1997). Therefore, our goal was to test a plant detection system using photometric and ultrasonic sensors simultaneously. Moreover, the objective of this research was to evaluate whether different travel speeds influence the detection of targets of different sizes. Four fields were scanned with the system to map the plants and the gap length for the spatial management of sugarcane fields.

2.2. Material and Methods

2.2.1. Description of system

The plant detection system was composed of a photoelectric sensor (PS), ultrasonic sensor (US), and rotary incremental encoder (Table 1). PS and US were used to detect the plants and the encoder to measure the displacement of the vehicle. The signals generated by the sensors along the vehicle's displacement value were input data from the machine learning (ML) model used to improve the accuracy of sensors in detecting sugarcane plants. The system was mounted on a platform coupled to the back of a tractor (Fig. 1). PS and US were mounted at 0.20 m above ground, allowing for the detection of sugarcane plants without interference from the previous crop's straw.

The sensors were mounted to detect the side of the plants and under their canopy to avoid interference from the leaves during the detection of sugarcane stalks.

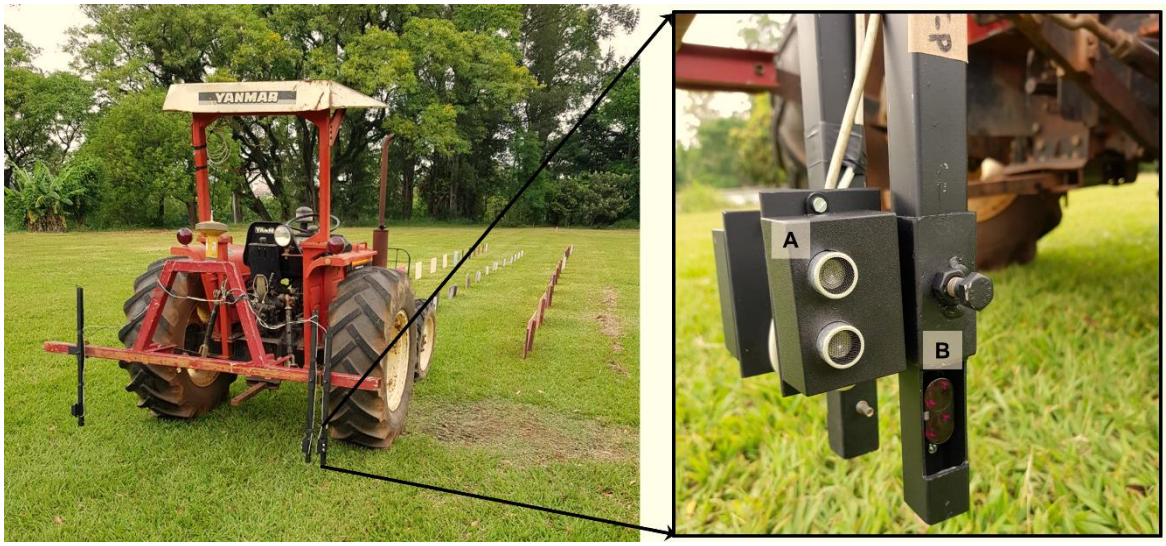

Figure 1. Sugarcane plant detecting system with (A) ultrasonic sensor and (B) photoelectric sensor.

2.2.2. Sensors

The PS used was a diffuse reflective sensor, model BA2M-DDT (Autonics, Yangsan, Korea) (Table 1). It was selected with a focus on the response time. The sensor has electrical noise immunity, detects objects of all sizes, is small, and is easy to install. The sensor detects the absence or presence of an object using a light transmitter with a limited effect from ambient light (sunlight and incandescent). It emits infrared light, modulated at 850 nm, which passes through the object and then reflects the receiver. The sensitivity was adjusted to detect plants at a distance of 1.5 m to overcome the interference of plants in the back row.

Table 1. Sensor specifications.

	Photoelectric	Ultrasonic
Model	BA2M-DDT	HC-SR04
Detection Method	Direct reflection	Distance
Operation principle	Infrared LED light (850 nm)	Ultrasonic sound pulses
Max range	2.0 m	4.0 m
Object Detection	Opaque, translucent material	Minimum area of 0.5 m^2 *
Response rate	1 ms	10 ms
Supply voltage	12–24 V DC	5 V DC

*Round objects or sound-absorbing materials reflect less energy or nothing directly back to the sensor.

The US used was an active ultrasonic sensor containing a transmitter and a receiver of high-frequency sound waves (HC-SR04, Elecfreaks, Shenzhen, China). This sensor estimates the distance from the sensor to the first obstacle according to the time-of-flight principle, that is, the amount of time that a wave travels, reflects, and returns to the receiver sensor (Madli et al., 2015). The model used sent a high-level trigger pulse of 10 µs, indicating the beginning of data transmission. After that, eight pulses of 40 kHz were sent, and the sensor waited for the return. If the receiver identifies any return signal, then the sensor generates a high-level signal on the output pin whose

duration is equal to the time calculated between sending and returning the ultrasonic signal. The ultrasonic method allows for measuring distances between 0.02 and 4.0 m with an angle of detection of 15°.

The rotary incremental encoder was a model 5820 (Hohner, Artur Nogueira, SP, Brazil) installed on a nonactivated tractor front wheel. An incremental encoder immediately reports changes in the position of the tractor wheel. The rotary incremental encoder used had a resolution of 60 counts with approximately 0.0523 rad per count. The encoder signal was input to the real-time controller through a Mega 2560 board.

2.2.3. Hardware and software development

The Mega 2560 board has an AT-megaprocessor-based prototyping platform and was developed using the C++ software language (Zhang et al., 2019). The selection of the board was based on its processing speed, compatibility, and the number of pins required to connect the sensors (Fig. 2). The US was connected to the corresponding pins on the Mega 2560 board: PWM pins 2, 4, and 6 to the TRIG signals (data input) and PWM pins 3, 5, and 7 to the ECHO signals (data output). The output signals of the PS were connected to three PWM pins (16, 17, and 18). The rotary incremental encoder was connected to pin 19 on Mega 2560. The Mega 2560 board supplies power at 5 V; therefore, only the three USs were connected to the power pin. The three PSs and rotary encoder were connected to an AC-DC adapter powered by 12 V DC.

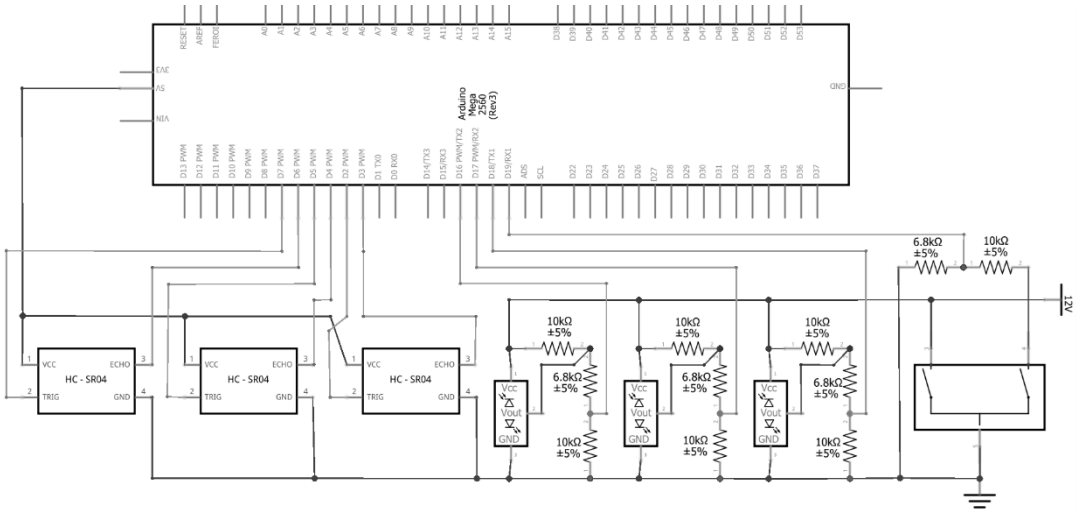

Figure 2. Block diagram of connections of three photoelectric, three ultrasonic, and one encoder on Mega 2560 (Arduino).

The Arduino Integrated Development Environment (IDE) was used to write a code to connect, read the signal, and send sensor data output via a universal serial bus (USB). A typical Arduino code consists of two functions (setup and loop) that are compiled and linked with a program stub main() into an executable cyclic executive program (Wishkerman and Wishkerman, 2017). The *Ultrasonic.h* library was used to convert the US signal into a metric distance value. All information gathered from the US, PS, and rotary encoder was transmitted at 40 Hz through the Mega 2560 board USB port and recorded in a text file (.txt) on a laptop using the Processing freeware software (Reas and Fry, 2006). In addition to the data generated by the sensors, the coordinates generated by a global navigation satellite system (GNSS) model GR-3 (Topcon, Tokyo, Japan) with an accuracy of 0.017 m with real-time kinematic (RTK) differential correction in a dynamic condition (Maldaner et al., 2021) was recorded in the text file. This allowed for georeferencing of sensor data within sugarcane rows during field trials.

2.2.4. Plant detection

The signals from each sensor were converted into binary numbers (0 and 1). By default, the signal output of the PS is already 0 for the gap and 1 for the presence of the plant. A cutoff value was used for the output of the US for conversion into a binary number. Distance values above 1.25 m and below 0.75 m were considered a gap (value 0). Distances between these two values were considered plants (value 1). Owing to the spacing between rows (usually 1.5 m) and the traffic control used to avoid damage to the ratoons, almost no deviations were observed in the path of the equipment. Thus, the variation in the distance between the sensor and the target (plant) was not sufficiently representative (within the collected data) to produce variations above the cutoff limits proposed in this study.

In addition to using the sensors separately to detect plants, the simultaneous use of both sensors was tested. Simple logic was used to simultaneously detect plants using the sensors. If one of the sensors has an output value of 1, a plant is detected. Otherwise, if both sensors have zero output, no plant is detected (gap). Three other methods for detecting plants using the ML model were tested (Fig. 3). These methods are an extension of the previously mentioned methods with the addition of an encoder sensor. For the detection of plants, the count (C) of the binary values over the distance *i* traveled by the vehicle was calculated. The encoder sensor provides the distances from the vehicle (C10, C15, C20, C25, and C30), which were 0.10, 0.15, 0.20, 0.25, and 0, respectively. The counts were used as input to the ML model, which classifies data in a plant or gap class.

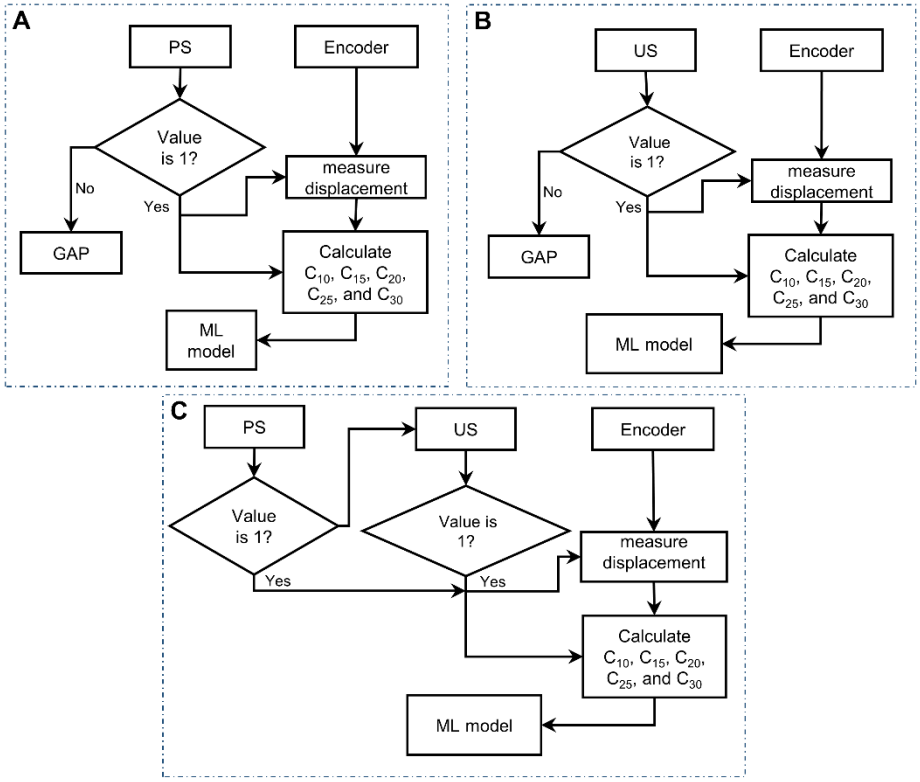

Figure 3. Model to plant detection using (A) only photoelectric sensor (PS), (B) only ultrasonic sensor (US), and (F) both sensors simultaneous (PS+US). These three ways to plant detect use the count (C) of binary values within the distances 0.10, 0.15, 0.20, 0.25, and 0.30 m as input to machine learning (ML) model.

2.2.5. Machine learning classification models

2.2.5.1. Decision tree

A decision tree (DT) classification model generated by supervised learning was used to improve plant detection by the sensors. This model was used because the learning and classification steps are simple, fast (Nanda and Patra, 2021), and accurate. In addition, high-dimensional data, typically generated by sensors used in agriculture (Poteko et al., 2021), can be easily handled using DT. The DT classifier is one of the simplest ML models used for discrete quantitative data, as used in this study. Furthermore, the model resulting from supervised training can be implemented in algorithms used in hardware that require high processing performance, such as sensors used in on-the-go applications in agriculture.

A DT presents the sequence of interrelated decisions and the expected results according to the chosen alternative. It consists of nodes and branches that organize the path to be followed for decision-making (Fig. 4). Each tree has a root node that has the highest hierarchical level (the starting point). In this study, a root node represents all independent variables C*i* under analysis. Starting at the root node, the independent variables were split according to C_{10}. The condition at the root node is that if there is no detection by the sensors when the vehicle traveled 0.10 m (C_{10} = 0), then the decision is that there is a gap. Otherwise, if C_{10} >= 1, then the independent variables are linked to a new branch. The C*i* generated by the sensors was tested at each decision node within each branch. Decision nodes are represented by logical conditions (if/else) that determine the path within the tree. The leaf node (or terminal node) represents the final result of a combination of decisions. In this case, the leaf nodes denote whether the data generated by the sensor are considered plants or gaps. The DT models were built using the *rpart* package (Therneau et al., 2015) in RStudio. The model parameters were chosen to minimize validation errors. The Gini index was used as the splitting criterion. The Gini index determines the purity of a specific class after splitting it along a particular attribute. The best split increases the purity of the sets resulting from the splitting (Tangirala, 2020). The Gini index at node *t* is determined by $1 - \sum_i p_i^2$, where *p* is the probability of assigning the class *i* (Breiman et al., 1984). In addition, the minimum number of observations that must exist in a node for a split to be attempted (*minsplit*) was set to 2.

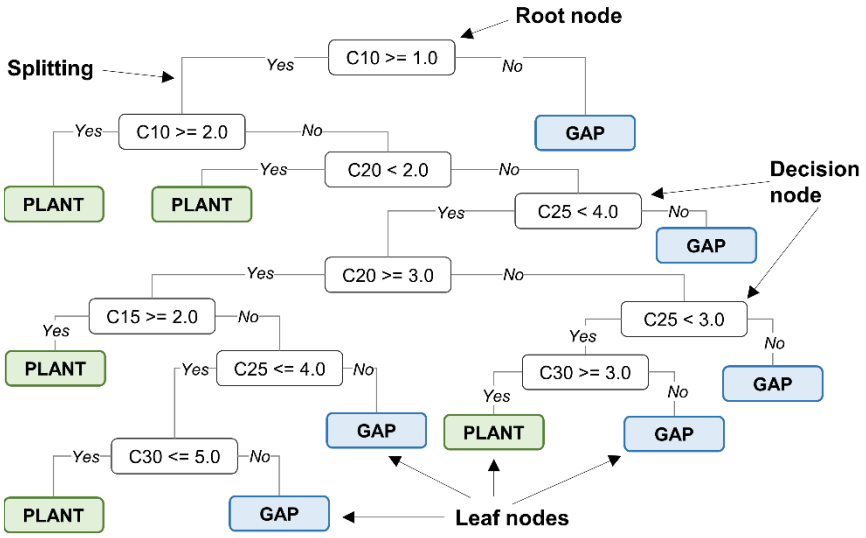

Figure 4. Representation of decision tree model generated by supervised learning. Inputs are number of times sensors detected a target inside 0.10 m (C_{10}), 0.15 m (C_{15}), 0.20 m (C_{20}), 0.25 m (C_{25}), and 0.30 m (C_{30}) distances traveled by vehicle.

2.2.5.2. Random Forest

Random forest is a combination of tree predictors such that each tree depends on the values of a random vector sampled independently and with the same distribution for all trees in the forest (Breiman, 2001). Training a random forest classifier is equivalent to training several independent decision trees. RF was used because it is suitable for both binary problems, such as multiclass problems and the one considered here. It is also considered a very easy and accessible algorithm to deploy because of the small number of hyperparameters to be tuned (Marins et al., 2021). The RF models were built using the *randomForest* package (Liaw and Wiener, 2002) in RStudio. The hyperparameter of the model was chosen to minimize validation errors. The best combination of the number of variables randomly sampled as candidates at each split (*mtry* = 1, 2, 3, 4, and 5) and the number of trees to grow (*ntree* = 3 to 50) was tested. The metric "accuracy" (as described in Section 2.5) was used to evaluate the classification performance of each parameter combination in the model. The RF classification model was built using *ntree* = 7 and *mtry* = 5. The model with these parameters performed better than the other combinations.

2.2.5.3. Support vector machine

The support vector machine (SVM) classifier is a supervised learning algorithm that aims to classify a given set of data points that are mapped to a multidimensional feature space using a kernel function. Its application advantages include good generalization performance, mathematical treatability, geometric interpretation, and the use of unlabeled data. The goal of SVM is to maximize the distance between the hyperplane and the margins on which the closest data points of the two classes are called support vectors (Kumar et al., 2020). SVM can classify features in a training set into categories that use either linear or nonlinear models. The *e1017* package in RStudio was used to implement the SVM model. A linear kernel function was used to obtain a lower classification error rate. The kernel function is a function that maps data to a larger dimensional space in the hope that the data will have a better structure, making it easier to separate.

2.2.6. Training data

A total of 14,217 data points were collected in a controlled trial. To create the amount of data for training and validation of the models, targets with sizes 0.10 m to 1.0 m simulating sugarcane plants were used. The dataset contains the dependent variables resulting from the observed independent variables. In this case, the independent variables were the C*i* of each sensor, and the dependent variable was the class (plant or gap). The dependent variable in this dataset was annotated using the appropriate class. The dataset was randomly split in a 70:30 ratio. The same dataset was used to train and validate the six proposed models. No preprocessing of the original data, such as normalization and filtering, was performed.

2.2.7. Sensors performance

For the performance of the sensors, targets with lengths ranging from 0.10 m to 1.0 m were used to verify the influence of the target size on detecting the targets. The sensors were subjected to tests with five travel speeds: 0.7, 1.0, 1.3, 1.6, and 2.0 m s^{-1}. Twenty repetitions were performed for each travel speed. The performance of plant detection was measured using metrics such as accuracy, precision, and recall. Accuracy is the ratio of correctly

predicted observations to the total number of observations (Equation 1). Precision is the proportion of true positives among the true and false positives (Equation 2), also called a positive predictive value. Recall is the proportion of correctly classified true positives among the total number of plants (Equation 3).

$$\text{Accuracy} = (TP + TN)/(TP + TN + FP + FN) \quad (1)$$

$$\text{Precision} = TP/(TP + FP) \quad (2)$$

$$\text{Recall} = TP/(TP + FN) \quad (3)$$

where TP (true positive) is the target correctly recognized as a plant, TN (true negative) is the target correctly recognized as a gap, FP (false positive) is a plant assigned as a gap, and FN (false negative) is a gap assigned as a plant.

2.2.8. Field trial

The evaluated sugarcane fields 1 and 2 were located in the municipality of Piracicaba, State of São Paulo, Brazil (22°40'33.6' S, 47°38'10.1 W; 523 m altitude) (Fig. 5). Fields 3 and 4 are located in the municipality of São Manuel, State of São Paulo, Brazil (22°41'30.9" S, 48°16'45.3" W; 523 m altitude). The characteristics of the four field trials are presented in Table 2. All fields were planted with a row spacing of 1.5 m. Data acquisition was carried out at the plant growth stage, approximately 40 days after harvesting.

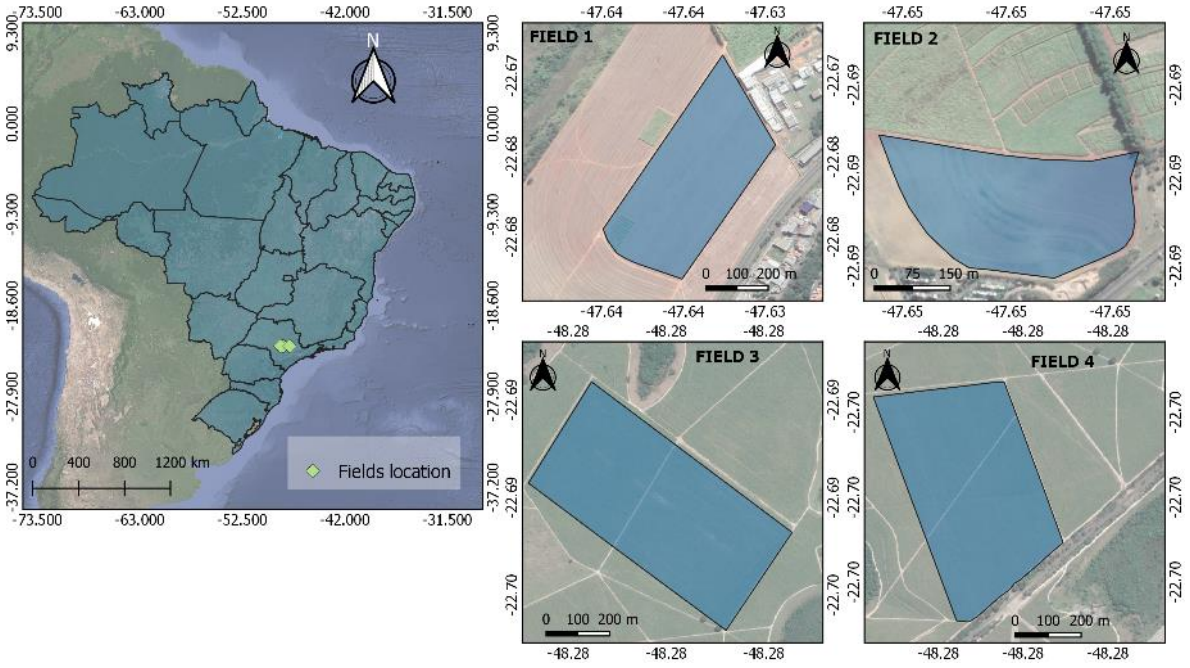

Figure 5. Location of four sugarcane fields in this study.

Table 2. Characteristics of field trials and collection dates.

Field	Area (ha)	Variety	Ratoon	Soil*	Collection date
1	21.1	RB96-6928	Fifth	Eutrophic Red Oxisol with clay texture	October 22, 2018
2	14.6				October 22, 2018
3	31.2	SP83-2847	Third	Argisol with a sandy texture	January 18, 2019
4	26.3				January 11, 2019

*Santos et al. (2018)

Data collection in the field was performed with the US, PS, an encoder prototype, and the DT with two sensors. Data were generated from all sugarcane rows in each field. We used the data stored in the text file to measure the length of the gaps and create the maps. The gap is the distance between ratoons and was measured by tractor displacement generated by an encoder sensor, as described by Molin and Veiga (2016). As each data contained its coordinates, it was possible to create maps of the size of the gaps. To create the ratoon stand map, the number of plants detected in each meter traveled by a tractor during field scaling was calculated.

2.3. Results

2.3.1. Sensor performance

The ML models improved the performance of the sensors for detecting targets (Table 3). The PS and US have 61% and 65% precision, respectively, with a recall of 70% and 72%, respectively. PS and US simultaneously without the ML model did not increase the precision or accuracy of target detection. Target detection with PS, US, and DT models had better efficacy than the other methods, with 94% precision. Although using US and PS alone with a DT model also had equal accuracy, this approach detected 91% of all plants (recall = 0.91), which is the best result compared to the other models. Target detection using RF and SVM also yielded good results with a precision above 90%. The ability of the models to detect targets was approximately 81%. This is equivalent to 9% below the approach to target detection using the DT.

Table 3. Overall performance metrics of sensors in detection of targets.

	Only senor			Decision Tree			Random Forest			SVM		
	US	PS	Fusion	US	PS	Fusion	US	PS	Fusion	US	PS	Fusion
Accuracy	0.73	0.75	0.78	0.88	0.88	**0.92**	0.85	0.85	0.89	0.84	0.84	0.88
Precision	0.61	0.65	0.76	0.92	0.94	**0.94**	0.89	0.90	0.91	0.89	0.89	0.91
Recall	0.72	0.70	0.74	0.73	0.71	**0.91**	0.71	0.69	0.82	0.70	0.67	0.81

PS: Photoelectric sensor; US: Ultrasonic sensor; SVM: Support Vector Machine.

The speed of data collection affected the performance of the target detection system (Fig. 6). The superiority of target detection using ML models is evident when compared to using PS and US alone. Plant detection using DT, RF, and SVM had a small accuracy range at speeds from 0.7 to 1.3 m s^{-1}. The precision decreased with travel speeds up to 1.3 m s^{-1}, reaching values under 90% at 2.0 m s^{-1}. The ability of the sensors to detect all targets decreased with increasing speed. Target detection using PS and US with DT showed the best results, with recall ranging from 91% at a speed 0.7 m s^{-1} to 84% at a speed of 2.0 m s^{-1}.

The system using only PS or US has low precision in detecting targets smaller than 0.2 m, with values smaller than 20% (Fig. 7). The use of ML models has increased the precision of sensors for detecting targets. However, the precision of the sensors in detecting small plants (<0.20 m) is lower than that of plants above 0.20 m. The precision of detecting targets above 0.4 m in size is more than 90%. However, the system with ML models had less than 80% accuracy in detecting the 0.10-m target. In this case, the PS sensor with DT performed better, with a precision of 79%. The US with ML models has the highest efficiency in detecting all plants from 0.1 m with a recall of 71%.

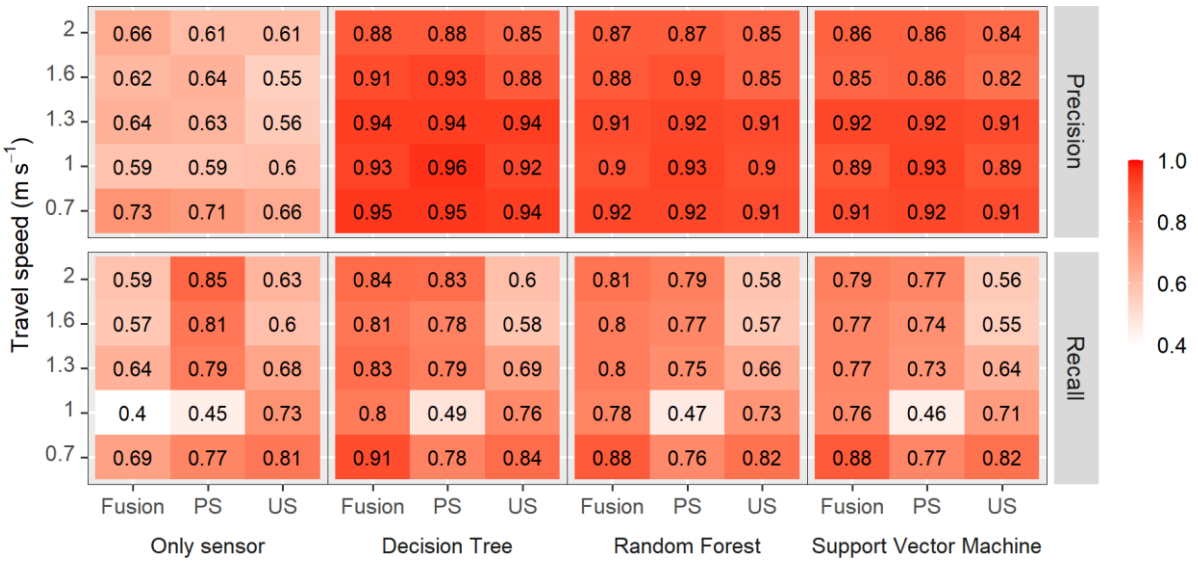

Figure 6. Precision and Recall of different approaches at different travel speeds (m s^{-1}). PS: Photoelectric sensor. US: Ultrasonic sensor.

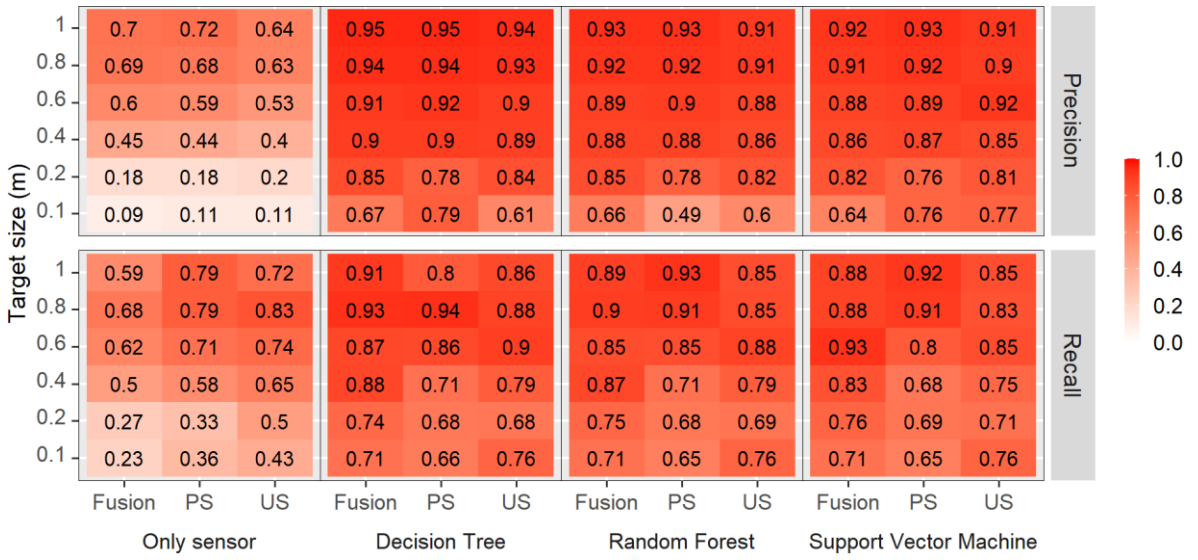

Figure 7. Precision and Recall of approaches in detecting targets with different sizes. PS: Photoelectric sensor; US: Ultrasonic sensor.

2.3.2. Field spatial data

Sensors can generate spatial data and can be used for ON/OFF applications through plant detection. Table 4 lists the data generated by the sensors during data collection in the four study fields. The sensors allowed for the counting and measurement of the length of the gaps within each row of sugarcane, which can help characterize the crop field in terms of crop row and gap incidence. The study field had a high number of gaps. The higher gap rate in Fields 1 and 2 (61% and 71% of the crop rows) was probably related to the number of times the harvest occurred (fifth ratoon). On the other hand, Fields 3 and 4 had 49% and 55% of the crop rows as gaps, probably related to their third ratoon. In addition, the average gap size of Fields 1 and 2 was more extensive, with an average

of 2.1 and 1.6 m, respectively, compared to fields with a lower number of ratoons, which had an average gap length of 0.6 and 0.5 m.

Table 4. Global features obtained from data collection with sensors.

Field	n	Minimum	Maximum	Mean	Total length	Gap Rate
		m				%
Field 1	29874	0.05	90.10	2.14	45921	61
Field 2	78340	0.05	117.51	1.58	99837	71
Field 3	298723	0.04	30.20	0.61	209080	49
Field 4	229058	0.10	15.30	0.49	219021	55

n: Number of gaps.

The maps created at the end of the procedure show the spatial distribution of gaps in sugarcane fields (Fig. 8). Because the data are georeferenced, they can be used to direct field verification to the most relevant points, optimizing the effort in the field. Fields 1 and 2 present more evident spatial distribution spots of the gaps within the rows. There are greater gaps above 3.8 m in these two fields than in Fields 3 and 4, which have a more significant number of gaps but with a shorter length. Field 3 presents small regions with gaps. Unlike in Field 4, there were no gap spots within the field. However, in Field 4, the gaps are evenly distributed within the field; that is, there is uniformity in the distances between plants in this field.

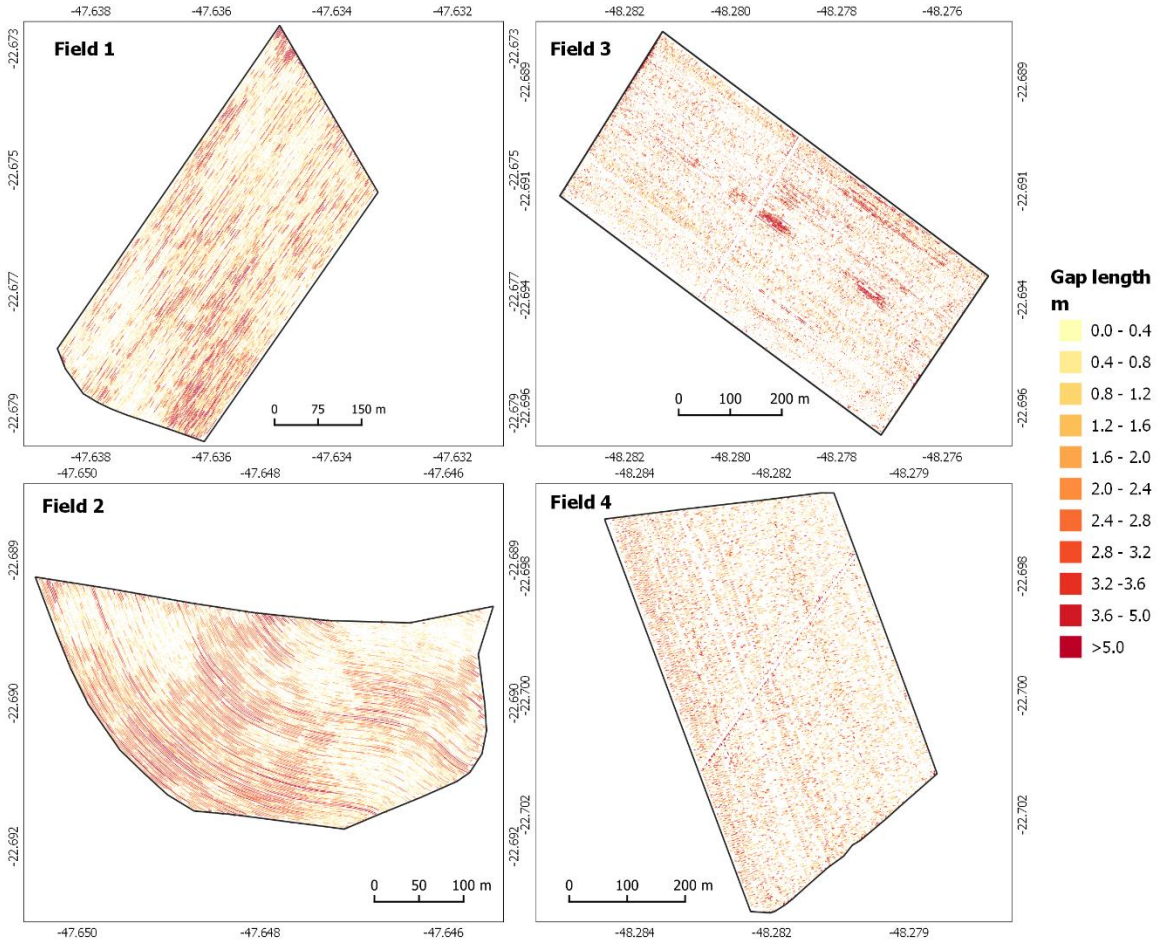

Figure 8. Map of length of gaps for four fields evaluated in this study.

The amount and length of the gaps directly affected the number of plants within the sugarcane row. Fields 1 and 2 have a smaller number of plants per linear meter than Fields 3 and 4. Field 1 presents a high amplitude in the density values (m of plants in a linear m), ranging from 0.0 to 1.0 m m^{-1}. In this field, it is possible to check areas with a high density of plants (Fig. 9), with values above 0.75 m m^{-1}. However, 59% of the entire field has several plants below 0.5 m m^{-1} (Fig. 10). Field 2 had 92% of its total with values below 0.5 m m^{-1}. Although Fields 3 and 4 have a higher frequency of gaps within the field, on the maps in Fig. 9, it is evident that there is uniformity in the distribution of gaps within the fields. On the other hand, Fields 1 and 2 have a lower frequency of gaps than the other two. Field 3 has 29% of the density values of less than 0.5 m m^{-1}, and Field 4 has 31% lower values than Fields 1 and 2, which has five ratoons.

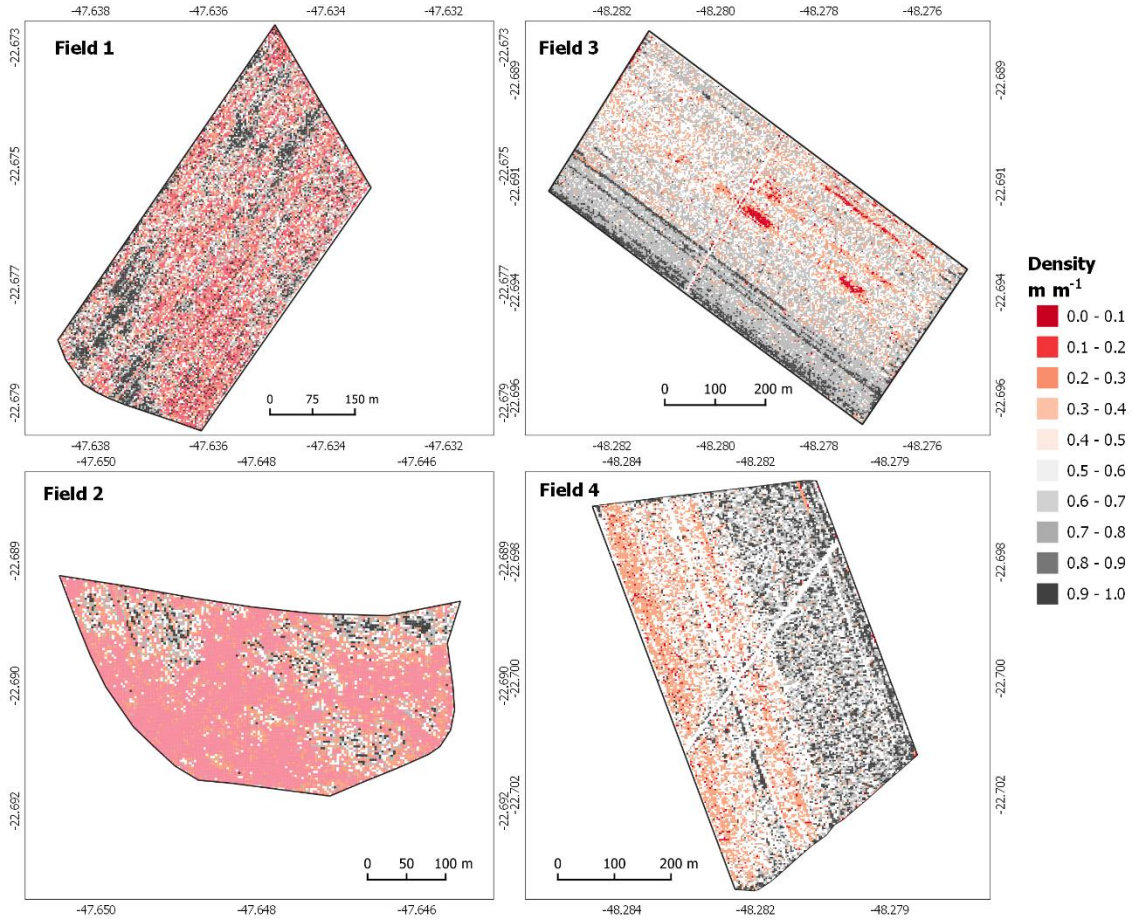

Figure 9. Sugarcane plant density (m m^{-1}) in each field in this study.

2.4. Discussion

The results show that the detection methods tested in this study differ in their performance and are affected by the travel speed, while ML techniques can improve the plant detection capability. Using only the US and PS sensors produced a low detection rate of the plants, which does not make the use of these sensors viable. However, with the addition of an ML model, it was possible to obtain an accuracy above 90% for plant detection. The DT model proved to be more accurate in the detection of plants, which is expected of a system to detect plants for agricultural site-specific applications. SVM and RF perform well in plant detection with similar accuracy to the DT model. RF and SVM are known to work very well on high-dimensional data, unlike that found here, where the

amount of data generated by PS and US in real time was small. The configuration of the PS and US in this study was such that they do not depend on each other for their operation, but their data were combined to solve the incompleteness of a single sensor (Yang and Hu, 2007). The DT model is a simple and efficient method for combining sensor data to detect plants. Furthermore, it is easy to implement algorithms that process signals from sensors.

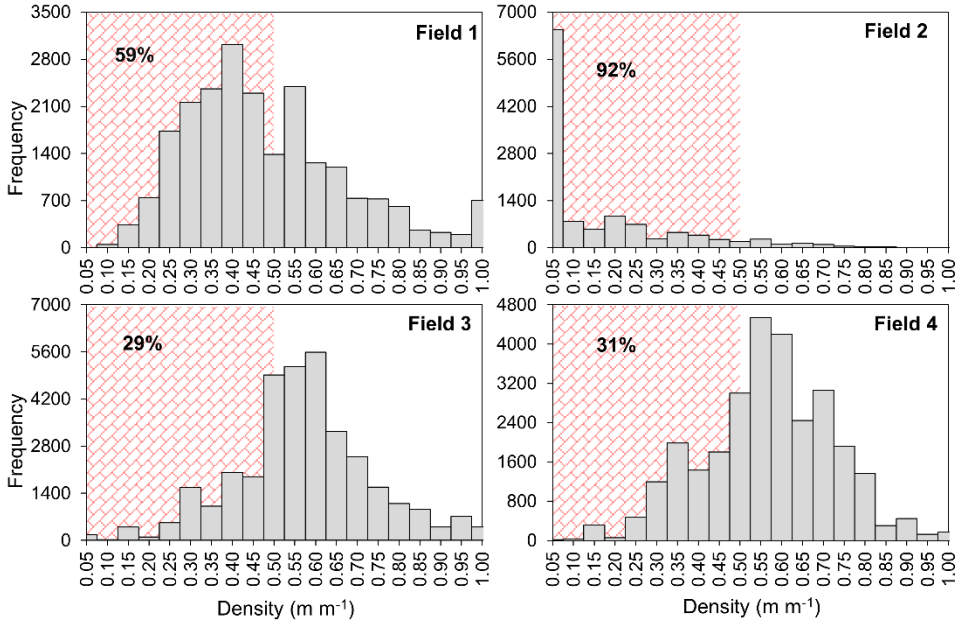

Figure 10. Histogram of plant in-row density (m m^{-1}). Area in red identifies amount of data below 0.50 m m^{-1}.

The system approach had difficulty detecting plants as small as 0.1 m. A sugarcane plant is composed of tillers that can vary in density within sugarcane fields. This phenological characteristic of sugarcane may be one of the reasons for the lack of systems that detect plants in site-specific applications. The proposed system can detect up to 79% of plants with a size of 0.10 m. This can lead to the nondetection of plants with lower development or low tiller numbers. The travel speed influenced the performance of the sensors in detecting the targets, especially at 2 m s^{-1}. This can make it challenging to use these sensors over 2 m s^{-1} to detect small sugarcane plants, especially in fields where there are small ratoons with late sprouting. In studies conducted on other crops, Páez et al. (2017) and Zaman and Salyani (2004) also showed that the ability to detect plants by ultrasonic sensors decreases with increasing displacement speed. By contrast, in a study conducted by Liu and Zhu (2016) with laser scanning, the displacement speed did not influence the laser to detect complex-shaped targets for variable-rate sprayer development.

The accuracy and precision of the plant detection system at the different speeds (0.7 to 2.0 m s^{-1})—which are expected during the application of inputs within sugarcane fields—shows the possibility of the sensors being integrated into equipment with real-time systems for variable-rate inputs, thus allowing for ON/OFF automatic section control. This low-cost system for sugarcane plant detection would allow growers to increase operability, as there is no need for two dedicated operations. According to Tona et al. (2018), ON/OFF automatic section control can reduce product losses and minimize the environmental impact of input applications while avoiding excessive expenditures. In addition, the system of plant detection can be used for spray applications. Some studies on ultrasonic sensors (Escolà et al., 2011; Gil et al., 2007; Páez et al., 2017; Pawlowski et al., 2017) and laser scanning sensors (Li et al., 2018; Liu and Zhu, 2016; Salcedo et al., 2020) for off-target systems and variable-rate applications

have shown an intelligent solution to maximize spray application efficiency during field operations. Sugarcane is a crop with high input costs (Cardoso et al., 2018), and new sensor systems that help with the application of inputs more accurately can bring significant economic and environmental returns.

In addition to detecting the plants, the use of a GNSS enabled the georeferencing of the plants, and together with an encoder installed on the tractor wheel, it was possible to measure the number of plants per linear meter within the sugarcane rows and map the gaps. It was evident that Fields 1 and 2 with fifth ratoons had a higher gap rate (61% and 71%, respectively) than Fields 3 and 4 with third ratoons (49% and 55%, respectively). Some studies showed that with an increase in the number of ratoons, there is a decrease in the number of plants within each row, that is, an increase in the length and number of gaps. Consequently, there is a reduction in the average yield of the field over the years (Matsuoka and Stolf, 2012; Stolf, 1986). It is evident that in Fields 1 and 2, there is a higher incidence of spots, that is, regions with spatial dependence on gaps; while in Fields 3 and 4, there was a uniform distribution of gaps within the field. According to Luna and Lobo (2016), mapping the gap density is critical in guiding the replanting process. Although there are tools for plant detection, map gaps, and technologies such as presprouted sugarcane seedlings (Santos et al., 2020; Teixeira et al., 2020) for localized replanting, there is still a lack of mechanical equipment capable of performing local replanting within the sugarcane row. Spatial data provided by the sensor system tested in this study show that in Fields 3 and 4, there is a higher frequency in plant density above 0.5 m m^{-1}, which can assist in local replanting decisions. Although cost analysis is still necessary, these two fields have a greater possibility of local replanting than Field 2, reducing the cost of plowing out an old stubble field. Field 2 has a high incidence of gaps, and 92% of the field has a plant density lower than 0.5 m of plant per linear meter. Thus, it could be more economical to plow out an old stubble field and establish a new planting.

Additionally, this plant detection system can minimize the time and cost of data collection to generate gap maps. It does not require a dedicated data collection operation, as is currently done through high-resolution images captured by cameras coupled to a unmanned aerial vehicle (Luna and Lobo, 2016; Souza et al., 2017). Moreover, the data generated by the system proposed in this study are already georeferenced with length values generated by the encoder installed in the tractor wheel or other devices, unlike other methodologies that require postprocessing (Luna and Lobo, 2016; Souza et al., 2017). Detecting gaps within sugarcane rows is an effective strategy for optimizing inputs using site-specific approaches. According to Souza et al. (2017), it is possible to compare gap maps with other maps such as vegetation maps, yield maps, and ground and slope maps, generating additional information to assist in decision-making.

The approach followed in this study demonstrates the usefulness of combining two sensors to detect plants across real-time interventions. Crops such as oranges and vineyards already have commercial solutions for real-time interventions within the fields; however, interventions in real-time row-by-row in sugarcane fields still face significant challenges. The system to detect plants tested in this study, along with sensors used by Amaral et al. (2015) for nitrogen variable rate recommendation, has excellent potential to provide high-resolution information for real-time intervention within sugarcane rows. However, the challenge is to develop a dosing system capable of varying high amplitudes of rate in a small interval of time, row-by-row. On the contrary, georeferenced data generated by sensors, such as plant and gap maps, are fundamental in the context of PA, especially for decision-making and management of the variability of sugarcane fields. This study certainly highlighted the weaknesses and strengths of the photoelectric and ultrasonic combinations and the ML model in these two scenarios. Of course, the adaptation of these sensors in agricultural practices to improve or facilitate the management of inputs and mapping of plants and gaps is worthwhile, but this remains a topic for further research.

2.5. Conclusion

Sugarcane plants can be easily detected within sugarcane rows using a system with low-cost sensors and a decision tree model. Using sensors simultaneously associated with a decision tree model is the best approach to sugarcane plant detection, with an accuracy above 90% up to speeds of 2.0 m s^{-1}. Sugarcane lacks technologies for localized row-to-row applications. Although the sensors have the ability to detect 91% of the total plants (recall = 0.91), the benefits of using sensors can be greater than the error in plant detection. Overall, systems with a combination of sensors generate valuable real-time support for the site-specific management of sugarcane fields. Tools such as these sensors can be used in management practices to increase sugarcane yield, profitability, and improve environmental stewardship. These sensors can be used in equipment that performs cropping operations such as spraying or fertilizing to obtain gap information without a dedicated operation and in real time. In addition to the use of sensors to detect plants for in-row ON/OFF applications in real time, with a GNSS it is possible to spatialize the plants within the field, generating a spatialized information gap size and quantity of plants per linear meter. There are few studies on sugarcane with the development of new tools for localized applications, and this study can be a starting point for further studies.

2.6. Connection text to chapter 3

Spacialized data from gaps generate important information in the management of sugarcane fields. Moreover, identifying gaps within sugarcane rows is an effective strategy to optimize inputs using site-specific approaches. High-resolution RGB image is the most widely used approach to mapping this data. Images generated by cameras onboard to unmanned aerial vehicle (UAV) provide information about the canopy of sugarcane plants. However, the crop grown stage is an important factor that can affect the results of gap data collection. In this sense, Chapter 3 discusses the comparison of techniques for detecting and measuring sugarcane gaps at different stages of crop development. More specifically, it was analyzed three strategies with sensors (vegetative index, ultrasonic, photoelectric) mounted on a tractor, and one strategy using an RGB camera on-boarded to an UAV.

Chapter 3 has been published in *Biosystems Engineering* Journal, as can be seen below.

Maldaner, L. F.; Molin, J. P.; Martello, M.; Tavares, T. R.; Dias, F. L. F. (2021) Identification and measurement of gaps within sugarcane rows for site-specific management: comparing different sensor-based approaches. *Biosystems Engineering*. https://doi.org/10.1016/j.biosystemseng.2021.06.016

References

Abbas, I., Liu, J., Faheem, M., Noor, R.S., Shaikh, S.A., Solangi, K.A., Raza, S.M., 2020. Different sensor based intelligent spraying systems in Agriculture. Sensors Actuators, A Phys. 316, 112265. https://doi.org/10.1016/j.sna.2020.112265

Amaral, L.R., Molin, J.P., Schepers, J.S., 2015. Algorithm for variable-rate nitrogen application in sugarcane based on active crop canopy sensor. Agron. J. 107, 1513–1523. https://doi.org/10.2134/agronj14.0494

Amaral, L.R., Trevisan, R.G., Molin, J.P., 2018. Canopy sensor placement for variable-rate nitrogen application in sugarcane fields. Precis. Agric. 19, 147–160. https://doi.org/10.1007/s11119-017-9505-x

Andújar, D., Rueda-Ayala, V., Moreno, H., Rosell-Polo, J.R., Escolà, A., Valero, C., Gerhards, R., Fernández-Quintanilla, C., Dorado, J., Griepentrog, H.W., 2013. Discriminating crop, weeds and soil surface with a terrestrial LIDAR sensor. Sensors (Switzerland) 13, 14662–14675. https://doi.org/10.3390/s131114662

Assirelli, A., Liberati, P., Santangelo, E., Del Giudice, A., Civitarese, V., Pari, L., 2015. Evaluation of sensors for poplar cutting detection to be used in intra-row weed control machine. Comput. Electron. Agric. https://doi.org/10.1016/j.compag.2015.06.001

Bramley, R.G.V., Ouzman, J., Gobbett, D.L., 2019. Regional scale application of the precision agriculture thought process to promote improved fertilizer management in the Australian sugar industry. Precis. Agric. 20, 362–378. https://doi.org/10.1007/s11119-018-9571-8

Breiman, L., 2001. Random forests. Mach. Learn. 45, 5–32. https://doi.org/10.1023/A:1010933404324

Breiman, L., Friedman, J., Stone, C., Olshen, R., 1984. Classification algorithms and regression trees. Boca Raton: CRC Press.

Cardoso, T.F., Watanabe, M.D.B., Souza, A., Chagas, M.F., Cavalett, O., Morais, E.R., Nogueira, L.A.H., Leal, M.R.L.V., Braunbeck, O.A., Cortez, L.A.B., Bonomi, A., 2018. Economic, environmental, and social impacts of different sugarcane production systems. Biofuels, Bioprod. Biorefining 12, 68–82. https://doi.org/10.1002/bbb.1829

Chapman, L.S., Wilson, J.R., 1996. Economics of ratoon cycle length in sugarcane, in: Wilson, J., Hogartsh, D., Campbell, J., Garside, A. (Eds.), Sugarcane: Research Towards Efficient and Sustainable Production. CSIRO Division of Tropical Crops and Pastures, pp. 169–171.

Dasarathy, B. V., 1997. Sensor fusion potential exploitation-innovative architectures and illustrative applications. Proc. IEEE 85, 24–38. https://doi.org/10.1109/5.554206

Escolà, A., Planas, S., Rosell, J.R., Pomar, J., Camp, F., Solanelles, F., Gracia, F., Llorens, J., Gil, E., 2011. Performance of an ultrasonic ranging sensor in apple tree canopies. Sensors 11, 2459–2477. https://doi.org/10.3390/s110302459

Escolà, A., Rosell-Polo, J.R., Planas, S., Gil, E., Pomar, J., Camp, F., Llorens, J., Solanelles, F., 2013. Variable rate sprayer. Part 1 - Orchard prototype: Design, implementation and validation. Comput. Electron. Agric. 95, 122–135. https://doi.org/10.1016/j.compag.2013.02.004

Gil, E., Escolà, A., Rosell, J.R., Planas, S., Val, L., 2007. Variable rate application of plant protection products in vineyard using ultrasonic sensors. Crop Prot. 26, 1287–1297. https://doi.org/10.1016/j.cropro.2006.11.003

H. Y. Jeon, H. Zhu, 2012. Development of a Variable-Rate Sprayer for Nursery Liner Applications. Trans. ASABE 55, 303–312. https://doi.org/10.13031/2013.41240

Kumar, S.D., Esakkirajan, S., Bama, S., Keerthiveena, B., 2020. A microcontroller based machine vision approach for tomato grading and sorting using SVM classifier. Microprocess. Microsyst. 76, 103090. https://doi.org/10.1016/j.micpro.2020.103090

Li, L., He, X., Song, J., Liu, Y., Zeng, A., Yang, L., Liu, C., Liu, Z., 2018. Design and experiment of variable rate orchard sprayer based on laser scanning sensor. Int. J. Agric. Biol. Eng. 11, 101–108. https://doi.org/10.25165/j.ijabe.20181101.3183

Liaw, A., Wiener, M., 2002. Classification and Regression by randomForest. R News 2, 18–22.

Lindblom, J., Lundström, C., Ljung, M., Jonsson, A., 2017. Promoting sustainable intensification in precision agriculture: review of decision support systems development and strategies. Precis. Agric. 18, 309–331. https://doi.org/10.1007/s11119-016-9491-4

Liu, H., Zhu, H., 2016. Evaluation of a laser scanning sensor in detection of complex-shaped targets for variable-rate sprayer development. Trans. ASABE 59, 1181–1192. https://doi.org/10.13031/trans.59.11760

Llorens, J., Gil, E., Llop, J., Escolà, A., 2010. Variable rate dosing in precision viticulture: Use of electronic devices to improve application efficiency. Crop Prot. 29, 239–248. https://doi.org/10.1016/j.cropro.2009.12.022

Luna, I., Lobo, A., 2016. Mapping crop planting quality in sugarcane from UAV imagery: A pilot study in Nicaragua. Remote Sens. 8, 1–18. https://doi.org/10.3390/rs8060500

Madli, R., Hebbar, S., Pattar, P., Golla, V., 2015. Automatic detection and notification of potholes and humps on roads to aid drivers. IEEE Sens. J. 15, 4313–4318. https://doi.org/10.1109/JSEN.2015.2417579

Mahmud, M.S., Zahid, A., He, L., Choi, D., Krawczyk, G., Zhu, H., Heinemann, P., 2021. Development of a LiDAR-guided section-based tree canopy density measurement system for precision spray applications. Comput. Electron. Agric. 182, 106053. https://doi.org/10.1016/j.compag.2021.106053

Maldaner, L.F., Canata, T.F., Dias, C.T. dos S., Molin, J.P., 2021. A statistical approach to static and dynamic tests for Global Navigation Satellite Systems receivers used in agricultural operations. Sci. Agric. 78. https://doi.org/10.1590/1678-992x-2019-0252

Marins, M.A., Barros, B.D., Santos, I.H., Barrionuevo, D.C., Vargas, R.E.V., de M. Prego, T., de Lima, A.A., de Campos, M.L.R., da Silva, E.A.B., Netto, S.L., 2021. Fault detection and classification in oil wells and production/service lines using random forest. J. Pet. Sci. Eng. 197, 107879. https://doi.org/10.1016/j.petrol.2020.107879

Matsuoka, S., Stolf, R., 2012. Sugarcane tillering and ratooning: key factors for a profitable cropping, in: Goncalves, J.F., Correia, K.D. (Eds.), Sugarcane: Production, Cultivation and Uses. Nova Science Publishers.

Molin, J.P., Veiga, J.P.S., 2016. Spatial variability of sugarcane row gaps: measurement and mapping. Cienc. e Agrotecnologia 40, 347–355. https://doi.org/10.1590/1413-70542016403046915

Moltó, E., Martín, B., Gutiérrez, A., 2001. Pesticide loss reduction by automatic adaptation of spraying on globular trees. J. Agric. Eng. Res. 78, 35–41. https://doi.org/10.1006/jaer.2000.0622

Nanda, M.K., Patra, M.R., 2021. Intrusion detection and classification using decision tree-based feature selection classifiers, in: Smart Innovation, Systems and Technologies. Springer Science and Business Media Deutschland GmbH, pp. 157–170. https://doi.org/10.1007/978-981-15-6202-0_17

Páez, F.C., Rincón, V.J., Sánchez-Hermosilla, J., Fernández, M., 2017. Implementation of a low-cost crop detection prototype for selective spraying in greenhouses. Precis. Agric. 18, 1011–1023. https://doi.org/10.1007/s11119-017-9522-9

Palleja, T., Landers, A.J., 2015. Real time canopy density estimation using ultrasonic envelope signals in the orchard and vineyard. Comput. Electron. Agric. 115, 108–117. https://doi.org/10.1016/j.compag.2015.05.014

Pawlowski, A., Guzmán, J.L., Sánchez-Hermosilla, J., Rodríguez, C., Dormido, S., 2017. A low-cost embedded controller design for selective spraying vehicle. IFAC-PapersOnLine 50, 5404–5409. https://doi.org/10.1016/j.ifacol.2017.08.1074

Portz, G., Amaral, L.R., Molin, J.P., Adamchuk, V.I., International, Y., Molin, J.P., Adamchuk, V.I., 2013. Field comparison of ultrasonic and canopy reflectance sensors used to estimate biomass and N-uptake in sugarcane, in: Precision Agriculture 2013 - Papers Presented at the 9th European Conference on Precision Agriculture, ECPA 2013. Wageningen Academic Publishers, Wageningen, pp. 111–117. https://doi.org/10.3920/978-90-8686-778-3_12

Poteko, J., Eder, D., Noack, P.O., 2021. Identifying operation modes of agricultural vehicles based on GNSS measurements. Comput. Electron. Agric. 185, 106105. https://doi.org/10.1016/j.compag.2021.106105

Q. U. Zaman, M. Salyani, Zaman, Q.U., Salyani, M., 2004. Effects of foliage density and ground speed on ultrasonic measurement of citrus tree volume. Appl. Eng. Agric. 20, 173–178. https://doi.org/10.13031/2013.15887

Reas, C., Fry, B., 2006. Processing: Programming for the media arts. AI Soc. 20, 526–538. https://doi.org/10.1007/s00146-006-0050-9

Salcedo, R., Zhu, H., Zhang, Z., Wei, Z., Chen, L., Ozkan, E., Falchieri, D., 2020. Foliar deposition and coverage on young apple trees with PWM-controlled spray systems. Comput. Electron. Agric. 178, 105794. https://doi.org/10.1016/j.compag.2020.105794

Sanches, G.M., Duft, D.G., Kölln, O.T., Luciano, A.C. dos S., De Castro, S.G.Q., Okuno, F.M., Franco, H.C.J., 2018. The potential for RGB images obtained using unmanned aerial vehicle to assess and predict yield in sugarcane fields. Int. J. Remote Sens. 39, 5402–5414. https://doi.org/10.1080/01431161.2018.1448484

Santos, H.G. dos, Jacomine, P.K.T., Anjos, L.H.C. dos, Oliveira, V.A. De, Lumbreras, J.F., Coelho, M.R., Almeida, J.A. de, Araujo Filho, J.C. de, Oliveira, J.B. de, Cunha, T.J.F., 2018. Sistema brasileiro de classificação de solos, 5th ed, Embrapa Solos.

Santos, L.S., Braga, N.C.C., Rodrigues, T.M., Neto, A.R., Brito, M.F., da Costa Severiano, E., 2020. Pre-sprouted Seedlings of Sugarcane Using Sugarcane Industry By-products as Substrate. Sugar Tech 22, 675–685. https://doi.org/10.1007/s12355-020-00798-y

Solanelles, F., Escolà, A., Planas, S., Rosell, J.R., Camp, F., Gràcia, F., 2006. An Electronic Control System for Pesticide Application Proportional to the Canopy Width of Tree Crops. Biosyst. Eng. 95, 473–481. https://doi.org/10.1016/j.biosystemseng.2006.08.004

Souza, C.H.W. de, Lamparelli, R.A.C., Rocha, J.V., Magalhães, P.S.G., 2017. Mapping skips in sugarcane fields using object-based analysis of unmanned aerial vehicle (UAV) images. Comput. Electron. Agric. 143, 49–56. https://doi.org/10.1016/j.compag.2017.10.006

Stolf, R., 1986. Metodologia de avaliação de falhas nas linhas de cana-de-açúcar. Stab 4, 22–36.

Tangirala, S., 2020. Evaluating the impact of GINI index and information gain on classification using decision tree classifier algorithm. Int. J. Adv. Comput. Sci. Appl. 11, 612–619. https://doi.org/10.14569/ijacsa.2020.0110277

Teixeira, G.C.M., de Mello Prado, R., Rocha, A.M.S., dos Santos, L.C.N., dos Santos Sarah, M.M., Gratão, P.L., Fernandes, C., 2020. Silicon in Pre-sprouted Sugarcane Seedlings Mitigates the Effects of Water Deficit After Transplanting. J. Soil Sci. Plant Nutr. 20, 849–859. https://doi.org/10.1007/s42729-019-00170-4

Therneau, T., Atkinson, B., Ripley, B., 2015. rpart: Recursive Partitioning and Regression Trees. R package version. R Packag. version 4.1-11 https//CRAN.R-project.org/package=rpart.

Tona, E., Calcante, A., Oberti, R., 2018. The profitability of precision spraying on specialty crops: a technical–economic analysis of protection equipment at increasing technological levels. Precis. Agric. 19, 606–629. https://doi.org/10.1007/s11119-017-9543-4

Wishkerman, A., Wishkerman, E., 2017. Application note: A novel low-cost open-source LED system for microalgae cultivation. Comput. Electron. Agric. 132, 56–62. https://doi.org/10.1016/j.compag.2016.11.015

Xin, J., Kaixuan, Z., Jiangtao, J., Xinwu, D., Hao, M., Zhaomei, Q., 2018. Design and implementation of Intelligent transplanting system based on photoelectric sensor and PLC. Futur. Gener. Comput. Syst. 88, 127–139. https://doi.org/10.1016/j.future.2018.05.034

Yang, G.-Z., Hu, X., 2007. Multi-Sensor Fusion, in: Yang, G. (Ed.), Body Sensor Networks. Springer London, pp. 239–285. https://doi.org/10.1007/1-84628-484-8_8

Zhang, P., Hu, S., Li, W., Zhang, C., 2020. Parcel-level mapping of crops in a smallholder agricultural area: A case of central China using single-temporal VHSR imagery. Comput. Electron. Agric. 175, 105581. https://doi.org/10.1016/j.compag.2020.105581

Zhang, Z., Zhu, H., Guler, H., Shen, Y., 2019. Improved premixing in-line injection system for variable-rate orchard sprayers with Arduino platform. Comput. Electron. Agric. 162, 389–396. https://doi.org/10.1016/j.compag.2019.04.023

Zürey, Z., Sabanci, K., Balci, S., 2020. Automatic nozzle control system with ultrasonic sensor for orchard sprayers. Eur. J. Tech. 10, 264–273. https://doi.org/10.36222/ejt.715015

3. IDENTIFICATION AND MEASUREMENT OF GAPS WITHIN SUGARCANE ROWS FOR SITE-SPECIFIC MANAGEMENT: COMPARING DIFFERENT SENSOR-BASED APPROACHES

Abstract

Identifying gaps within sugarcane rows is an effective strategy to optimize inputs using site-specific approaches. This work aimed to compare four different sensor-based techniques to identify and measure sugarcane gaps. Specifically, it was analyzed three strategies with sensors (vegetative index, ultrasonic, photoelectric) mounted on a tractor, and one strategy using an RGB camera on-boarded to a unmanned aerial vehicle (UAV); the latter being the current commercial method. Field trials were performed during four crop stages of development: 19, 31, 47, and 59 days after harvest (DAH). The successful gap identification was evaluated by accuracy, precision, and recall. We use the root-mean-square error (RMSE) to evaluate sensors in measuring the length of the gaps. All sensor-based techniques had accuracy between 80% and 92% in identifying the gaps at 31 and 47 DAH. At 19 DAH, the sensor-based methods overestimate the number of gaps, and at 59 DAH, there was an underestimation of gaps. The photoelectric sensor has the best performance in measuring the length of the gaps (RMSE $\leq$ 0.18 m) with the least variation in RMSE over the stage of sugarcane development. The vegetative index sensor (VIS) and UAV images had similar performance, with the RMSE ranging between 0.11 and 0.40 m. The canopy of the plants in the 47 and 59 DAH affected these two methodologies. The larger is the plant canopy, the lower is their ability to identify and measure the gaps.

Keywords: High-resolution images; Ultrasonic sensor; Photoelectric sensor; Crop sensor; Proximal sensing

3.1. Introduction

Sugarcane (*Saccharum* spp.) is used to produce sugar, ethanol, and bioelectricity, and it plays a fundamental role in the Brazilian economy and energy matrix (Bordonal et al., 2018). Sugarcane is a perennial crop with a growth cycle ranging between 12 and 18 months. After the first harvest, it is common for a gradual yield decline with an increasing number of gaps within sugarcane rows, leading to the necessity of ploughing out at a certain break-even point. According to (Matsuoka & Stolf, 2012), the decision to plough out an old stubble field and establish a new planting is not an easy task. The decline in yield is generally related to an increasing number and length of sugarcane gaps that promote the reduction of plants in the field (Matsuoka & Stolf, 2012; Souza, Lamparelli, Rocha, & Magalhães, 2017).

Identifying and quantifying gaps in sugarcane fields is of great importance because it can allow the development of site-specific management strategies to correct gaps (e.g., localized replanting). It is typical to replant the entire field based on the average number of gaps in the field. The traditional method to assess gaps in sugarcane rows is based on Stolf (1986), which associates gap rates with a prediction of yield reduction in the field. The methodology mentioned above is based on evaluating the total number of gaps and the sum of the lengths above 0.5 m per 100 m of sugarcane row. However, this methodology is applied using small random samples within the field, conducting the measurements manually, which hinders the accomplishment of a reliable characterization of the spatial variability of gaps.

A current methodology, which aims at a more reliable characterization of sugarcane field gaps, uses unmanned aerial vehicle (UAV) images to map, quantify and measure sugarcane gaps in agricultural fields (Luna & Lobo, 2016; Souza et al., 2017). Outsourced imaging for this purpose has been under considerable demand in the sugarcane industry. The use of UAV to monitor agricultural fields has the advantage of large imaging areas relatively quickly. However, the use of this technology still faces some challenges. The high-resolution images require a laborious post-processing procedure to extract data from images and transform it into information for site-specific applications (Peña, Torres-Sánchez, Serrano-Pérez, de Castro, & López-Granados, 2015; Souza et al., 2017; Torres-Sánchez, Ló Pez-Granados, Castro, & Peñ A-Barragán, 2013).

A practical alternative to manual mapping and the UAV image gap map is the use of proximal sensors mounted on agricultural machines (Molin & Veiga, 2016). This strategy allows data acquisitions during normal field operations, enabling site-specific applications using real-time diagnostics. Different sensors that work proximally have a compatible operation to be instrumented in agricultural machines to identify and measure gaps, among them, ultrasonic, photoelectric sensors, and vegetative index sensors of plants. Ultrasonic sensors are commonly used embedded in machines for measuring the height of crops (Escolà et al., 2011; Portz, Amaral, Molin, & Adamchuk, 2013). Vegetative index sensor (VIS) scan plant canopies providing vegetation indices, consisting of mathematical relationships of the reflectance values recorded by these sensors in different spectral regions (e.g., visible and near-infrared region). VIS can also be used to identify sugarcane gaps (Frasson et al., 1999) since the absence of plants is easily obtained by interpreting the vegetation indices. Molin & Veiga (2016) identified and measured gaps within the sugarcane row using photoelectric sensors, which showed promising results for this application.

To the best of our knowledge, no previous research has compared the above-mentioned sensor-based strategies' performance to assess sugarcane gaps. In this way, the present work used three proximal sensors, ultrasonic, VIS, and photoelectric, all mounted on a tractor, comparing the performance of each of these sensors to identify and measure the length of sugarcane gaps. The performance of the sensors mounted on a tractor was also compared with the gap monitoring carried out via UAV images, the current commercial method adopted by sugarcane growers.

3.2. Materials and Methods

3.2.1. Gap monitoring with proximal sensors mounted on a tractor

The PS, VIS, and US were adapted to a platform mounted on the rear of a tractor (Fig. 11). The PS and US were mounted at 0.20 m above soil height with an average distance of 0.75 m from the targets (sugarcane plants), while the VIS was positioned at 0.50 m above the targets. The sensors operate in three rows simultaneously, being used in three units of each sensor type. During the operation, the tractor moved at an average displacement speed of 1.2 ms^{-1}. The sensors' specifications and how gap locations were identified and measured are described in the following sections. In this work, gaps were considered all spaces between stalks and close to the ground that was greater than 0.06 m. This threshold value is the smallest length measured given the sensors' resolution (Table 5).

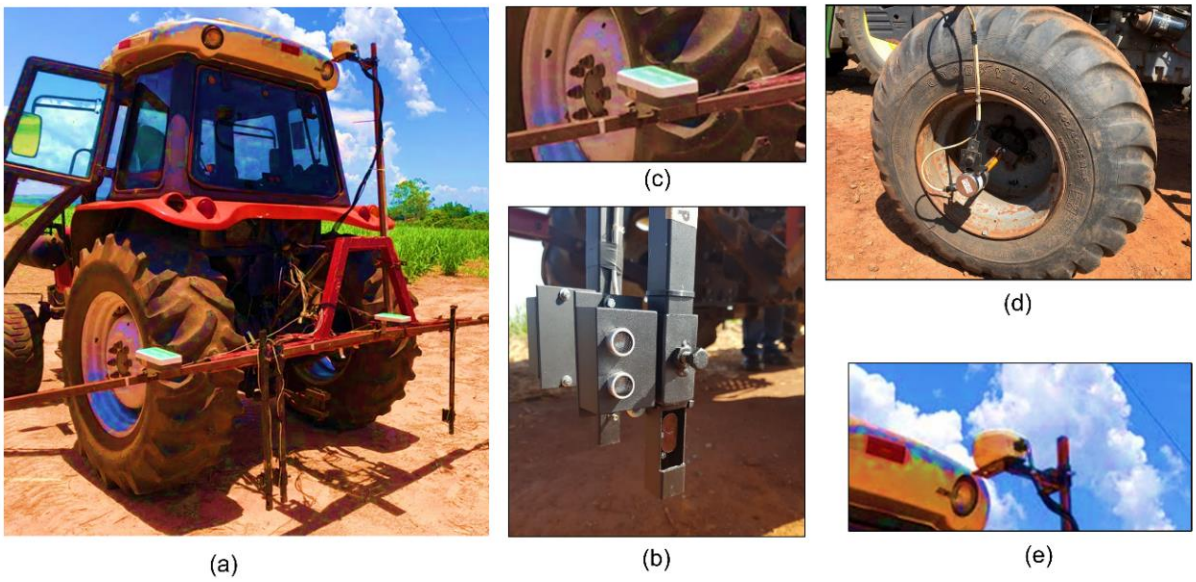

Figure 11. Position of the sensors mounted on the tractor (a). Ultrasonic and photoelectric sensors (b) and vegetative index sensor used to detect gaps (c). Rotary encoder used to measure the gap lengths (d). Global Navigation Satellite System used to georeferenced the gaps within sugarcane rows (e).

3.2.2. Ultrasonic and photoelectric sensors

The US selected was an HC-SR04 (Elecfreaks, Shenzhen, China), an active ultrasonic sensor containing a transmitter and a receiver of high-frequency sound waves. This sensor provides an estimation of the distance from the sensor to the first obstacle according to the time-of-flight principle; in other words, the US measure the time that waves take to travel, reflect, and come back to the receiver sensor, which is used to calculate the distance travelled (Carullo & Parvis, 2001; Madli, Hebbar, Pattar, & Golla, 2015). The US worked at a frequency of 40 kHz, allowing it to measure distances in the range between 0.02 and 4.0 m, with an angle of detection of 15°.

Table 5. Information related to sensors' working position, as well as the density and spatial resolution of data acquired.

Sensor	Working position	Data acquisition frequency[1]	Spatial density	Resolution[2]
		Hz	points m^{-1}	m
Ultrasonic sensor	beside of the plants and under their canopy	20	16.6	0.06
Photoelectric sensor		20	16.6	0.06
Vegetative index sensor (VIS)	zenith position above the canopy	5	4.2	0.24

[1] Data acquisition frequency of ultrasonic and photoelectric sensors was limited by the maximum frequency of the GNSS receiver and the VIS by the recording frequency of its data logger. [2] The resolution was calculated regarding the tractor operational speed (1.2 ms^{-1}).

The PS used was a diffuse reflective sensor; model BA2M-DDT (Autonics, Yangsan, Korea). It emits an infrared LED light (modulated at 850 nm), which reflects back to the sensor's receiver (detector) when it comes into contact with an object. The receiver detects the amount of light reflected by the object, activating the sensor when the light intensity reaches a predetermined threshold value. The photoelectric has an adjusted sensitivity related to a

distance between sensor and target; in this work, this parameter was set up for 1.5 m. The photoelectric used has a response time of approximately 1.0 ms, which can detect small objects, such as sugarcane stalks.

Both the US and the PS were connected with a rotary encoder, and a data acquisition system operated by an Arduino Mega 2560 (Arduino, Budapest, HU).

3.2.3. Vegetative index sensor (VIS)

Three VIS model ACS-430 (Holland Scientific Inc., Lincoln, NE, USA) were used. It is an active sensor that measures the diffuse reflectance reflected in three wavelengths positioned in red (at 670 nm), red-edge (at 730 nm), and NIR (at 780 nm) regions of the electromagnetic spectrum. This sensor's system provides the Normalised Difference Red Edge (NDRE) vegetation index as output (Amaral, Molin, & Schepers, 2015). NDRE data was recorded at a frequency of 5 Hz. The VIS data was recorded using the GeoSCOUT data logger (Holland Scientific Inc., Lincoln, NE, USA), its data acquisition system. The recorded data was also associated with the GNSS receiver's position information.

3.2.4. Identify and measure the gaps with the proximal sensors

To measure the gap lengths, we used one 60 pulses rotary encoder model 5820 (Hohner, Artur Nogueira, SP, Brazil) placed on the front wheel of the tractor (Fig. 11). Figure 12 showing the flowchart of the detection and measurement of gaps within sugarcane rows. The measurement of gap lengths made using the US and PS and system was carried out through the following sequence of actions: (i) sensor identified the absence of cane stalks (letter X in Fig. 12); (ii) the encoder begins to measure the gap length (letter Z in Fig. 12); (iii) sensor identify the next sugarcane stalk (letter Y in Fig. 12); (iv) the encoder stop measuring the gap length; and (v) gap length is the tractor displacement between point X and point Y in Figure 12. The GNSS receiver acquires the coordinates, and the georeferenced gap length is recorded in a text file. The PS and US working position allows gap identification besides the plants and under their canopy (Fig. 12b). On the other hand, VIS scans the canopy of plants; that is, the working position is in zenith position above the plant canopy (Fig. 12c).

For the VIS, the detection of the plants is done by the NDRE index value. Data with NDRE values above 0.01 were considered sugarcane plants. This threshold value allowed us to separate the plants from the crop residues and soil. There were no weeds with crop residues and control in this crop condition that could be detected. The model of the sensor used in this study did not allow the integration of the data in real-time with the hardware communication of the PS and US because its data has priority encryption. Thus, it was impossible to process it in real-time, so the identification of gaps by threshold value was made by post-processing the data.

3.2.5. Gap monitoring with UAV images

The UAV system used was an Advanced Phantom 4 (SZ DJI Technology Co., Ltd., Shenzhen, China). The on-board camera has a 2.54 cm focal length and CMOS sensor (2.54 cm and 20 Megapixels) and stores the acquired images on a compact flash card. The UAV system acquired georeferenced images using its GNSS receiver that allows the accuracy of ± 3.00 m. The georeferencing of the images was refined using inertial measurement units by positioning seven control points in the ground, where their positions were obtained using a receiver SMART6-

L™ (NovAtel Inc., Calgary, Canada) with TerraStar-C correction that allows the accuracy of ± 0.09 m (Maldaner, Canata, Dias, & Molin, 2021).

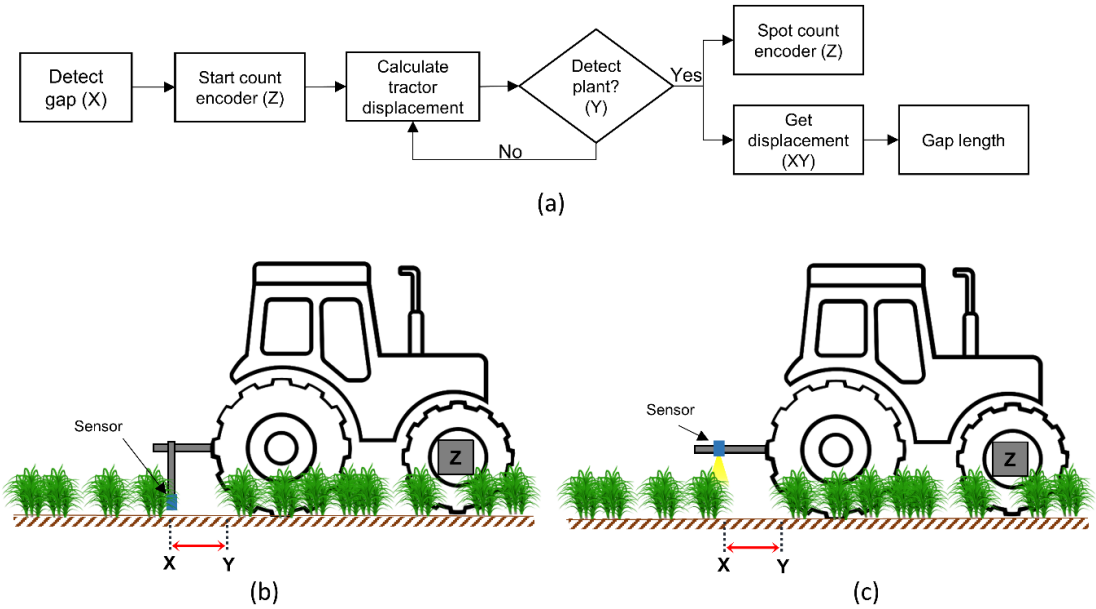

Figure 12. Flowchart of detecting and measuring gaps within sugarcane rows (a). Working position to detecting gaps by photoelectric and ultrasonic sensors (b) and vegetative index sensor (c). X - Point where the sensors detect the absence of plants; Y - the point where the sensors detect the presence of plants; Z – encoder on the front wheel of the tractor that measures the tractor's displacement between points X and Y.

The flight plan for image acquisition was made using DroneDeploy (DroneDeploy, San Francisco, USA), conducted with 70 m of height, acquiring images with a front overlap of 75% and a side overlap of 65%. The camera features associated with the executed flight plan's characteristics allowed the acquisition of images with 0.03 m of spatial resolution. Figure 13 shows image processing steps from creating a mosaic image to gap lengths. The first processing stage (mosaic image generation) was carried out with PhotoScan v. 1.5 software (Agisoft LLC, St. Petersburg, Russia) (Garilli, Bruno, Autelitano, Roncella, & Giuliani, 2021; Peña-Villasenín, Gil-Docampo, & Ortiz-Sanz, 2020). The software adopts a standardized processing pipeline: camera alignment and georeferencing with control points, generation of a 3D point cloud, generation of a triangular mesh model from the point cloud, and creation of a mosaic image. The mosaicked images were generated with a resolution of 0.03 m per pixel (Fig. 14a), which was the maximum resolution allowed from images captured by the on-board camera in UAV.

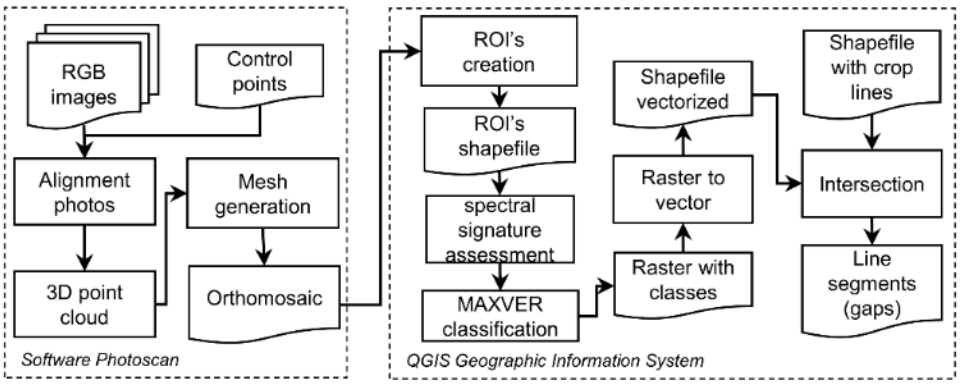

Figure 13. A flowchart describes the steps to identify spaces between plants by segmenting RGB images with a resolution of 0.03 m and a shapefile with the sugarcane lines (rows).

The identification of gaps was performed through supervised classification pixel by pixel (Luna & Lobo, 2016) of the mosaics using the Semi-Automatic Classification Plugin (SCP), a free, open-source plugin for QGIS (QGIS Geographic Information System, v. 3.4.4-Madeira, QGIS 2019) that allows for classification of pixels to differentiate targets. The first stage was to define two classes, sugarcane and background, in the mosaicked image by selecting samples manually. The regions of interest (ROI's) were identified, and a training file (shapefile) was created. After creating a file with ROI's, the SCP automatically assesses and records the spectral signatures of each ROI. Finally, the entire mosaicked image classification was carried out using the Maximum Likelihood (MAXVER) algorithm (Richards & Jia, 2006). The classification process resulted in a raster, where pixel values correspond to sugarcane and background class (Fig. 14b), which has been vectorised using the QGIS "Polygon" tool. In this study, the file with crop rows was available from the planting operation (planting was done with RTK-GNSS guidance), requiring no extra processing to extract the lines in the images (Fig. 14c). In the next step, the QGIS "Intersection" tool was used to create the intersection between the classified vector file (background and sugarcane) to the crop row file. This way, the segment of the crop rows that are background and features of the rows that are sugarcane were identified (Fig. 14d). Finally, the length of the features considered gaps were calculated through the tool "field calculator".

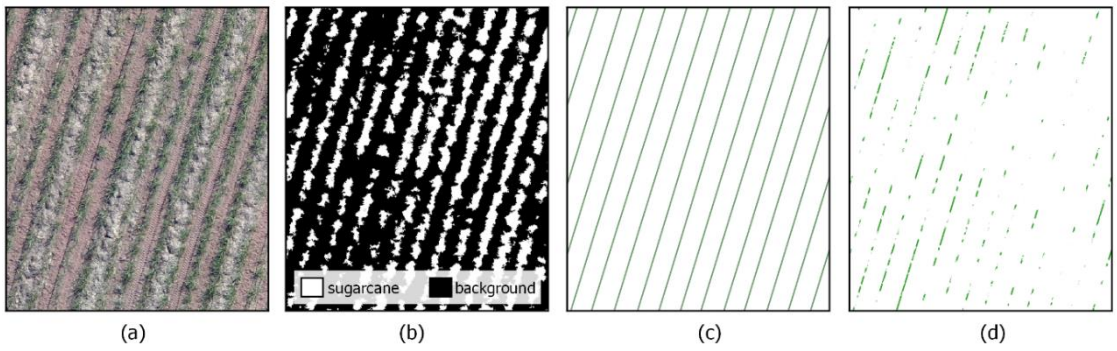

Figure 14. Single mosaicked image created by PhotoScan software (a), raster with two classes after image segmentation (b), shapefile with crop lines (c), and segment lines that are considered gaps (d).

3.2.6. Field trials and evaluation of sensors system's performance

The evaluated sugarcane field is located in Piracicaba, State of São Paulo, Brazil (22°40'33.6" S, 47°38'10.1" W; 523 m altitude) (Fig. 15). The sugarcane crop (variety RB966928) was spaced 1.5 m between rows. The experiment was conducted during the 2017/18 season when the harvest was in the fifth year of the ratoon cane. The data collection was evaluated on four different dates after harvesting (DAH) (Fig. 16) to verify the influence of the plant canopy size (stages of crop development) on the identification of gaps within the rows.

The sensor based on strategies were compared concerning their ability to identify and to measure the gap, using the manual method of gap assessment as a reference. For the reference method, 520 validation points were assessed in the field, 50% of them positioned in locations with sugarcane plants, and the remaining 50% were located in places with gaps. The gaps were measured manually by using a tape measure and, for the temporal evaluations, the validation points were georeferenced every time in the same place.

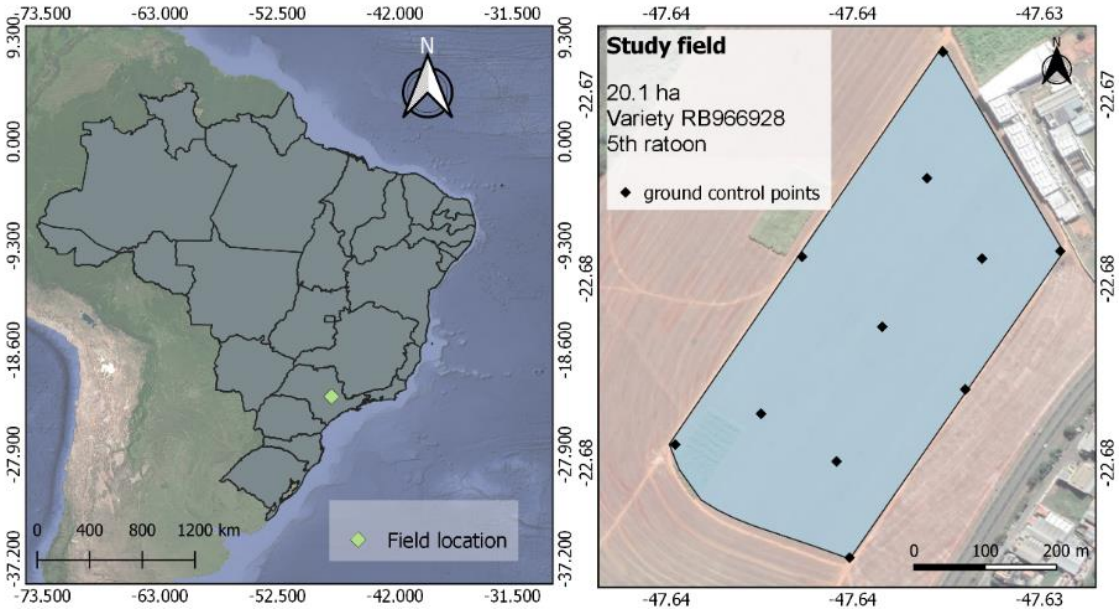

Figure 15. Location of the field trial in this study.

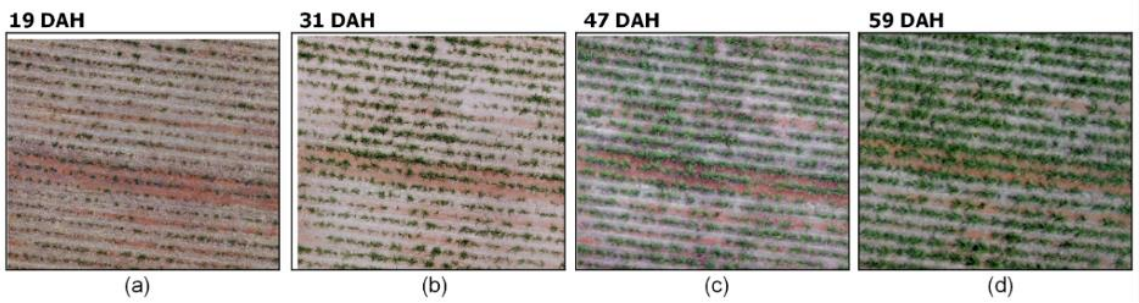

Figure 16. The characteristic of sugarcane canopy closure in different crop development stages at data collection date: September 24, 2018 (a), October 06, 2018 (b), October 22, 2018 (c), and November 03, 2018 (d). DAH – days after harvester.

To assess the sensors system's ability for gap identification, the quality indicators suggested by Olson & Delen (2008) were calculated, as follows:

$$Accuracy\ (\%) = \frac{TP + TN}{TP + TN + FP + FN} \times 100 \quad (4)$$

$$Precision\ (\%) = \frac{TP}{TP + FP} \times 100 \quad (5)$$

$$Recall\ (\%) = \frac{TP}{TP + FN} \times 100 \quad (6)$$

TP denotes the number of true positives, FP represents the number of false positives, TN is the number of true negatives, and FN shows the number of false negatives. A true positive indicates the number of points correctly recognized as a gap, and false positives indicate a point with a gap identified as a sugarcane plant. A true negative was the point correctly identified as a sugarcane plant, and a false negative indicates a point with a plant recognized as a gap. These four counts constitute a confusion matrix of binary classifications (Sokolova & Lapalme, 2009).

The methodology proposed by Souza et al. (2017) was used to assess the ability of the sensors system for gap measurement, whereby the gap length obtained through the sensors (estimated) was compared with the length

obtained via ground measurements (observed). The metrics used for performance evaluation were Pearson's correlation coefficient (r), and the root means square error (RMSE).

3.3. Results and discussion

3.3.1. Sensors system's performance for gap identification

The performance results of the sensor systems in identifying gaps are shown in Figures 17 and 18. In the first stage of development evaluated (19 DAH), an accuracy of 88%, 94%, 96%, and 93% was obtained for VIS, US, PS, and UAV images, respectively (Fig. 17). Lower performance than at 31 and 47 DAH when the PS and US had an accuracy of approximately 98%. At this growth stage (31 DAH), VIS and UAV image had 88% and 95% accuracy. In the later growth stage (59 DAH), an accuracy of 75%, 75%, 82%, and 80% was obtained for VIS, UAV image, PS and US, respectively; smaller than the other growth stages.

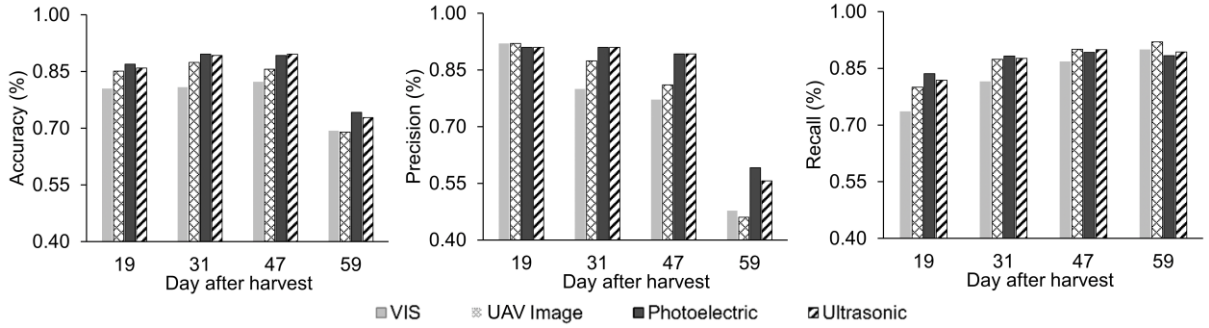

Figure 17. Sensor system's performance for gap identification accuracy, precision, and recall of the different sensor-based techniques over the days after harvest. VIS – Vegetative index sensor. UAV - Unmanned Aerial Vehicles.

The best of all sensor-based techniques performance was at 31 and 47 DAH, since in the initial stage (19 DAH) and the late stage (59 DAH) of development there was an influence due to uneven in the ratoon sprouting. Sugarcane is characterized as a crop with different tillering stages after the beginning of the ratoon sprouting (Moore, 1987; Van Dillewijn, 1952) and it makes it difficult to identify small ratoons with late sprouting. It happened especially with VIS and UAV images, resulting in fewer identified gaps than the other two sensor-based techniques. The late sprouting made the methodologies overestimated the number of gaps identified within the field at 19 DAH. With an increase in sugarcane growth, the relationship between the identified gaps and the unidentified plants (recall) increased (Fig. 17). Consequently, the greater the development of the canopy of the plant, the greater the recall.

On the other hand, there was a reduction in the number of gaps identified with the increase in the ratoon's growth stage to VIS, PS, US, and UAV images. All sensor-based methodologies have 100% precision in identifying the gaps at 19 DAH, i.e., identifying all the gaps (True positive-TP in Fig. 18). However, a significant point to be mentioned is many false negatives in 19 DAH (Fig. 18). VIS and UAV image approaches identify 25% and 15% of plants as gaps, and PS and US identity 9% and 11% of plants as gaps. These values are very high; that is, there was a significant overestimation of the gaps within the study field, compared to other growth stages. The number of false negatives in the VIS was more significant than the other three approaches at 19 and 31 DAH due to its ability to identify small plants. VIS data collection resolution was only 0.26 m; this was much more than PS and US with a 0.06 m resolution. It is overestimating the number of gaps within the field in the initial stages of the ratoon sprouting influences this decision-making information.

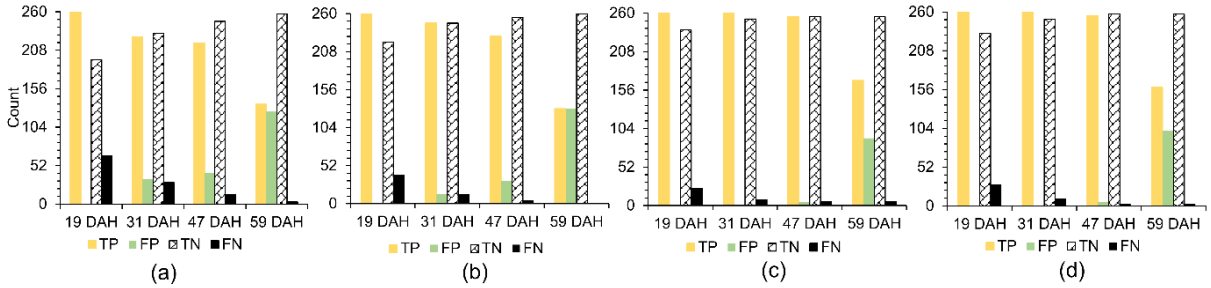

Figure 18. Performance of the vegetative index sensor (VIS) (a), UAV image (b), photoelectric sensor (c), ultrasonic sensor (d), in the gap and plant identification. True positive (TP) - points correctly recognised as a gap. True negative (TN) - points correctly recognised as sugarcane. False positive (FP) - point with gap identified as a plant. False negative (FN) – the point with a plant recognised as a gap. DAH – Day after harvesting.

The performance of the sensor system for gap identification was reduced as the plant developed. At 31 DAH, the PS and US successfully identified 100% of the gaps (True positive), being more efficient than the VIS and UAV imaging system, which identified only 87% and 95% of the gaps (Fig. 18), respectively. The UAV image and the VIS identified only 51% and 52% of the gaps 59 DAH, while the PS and US identified 65% and 61%. In a more canopy growth stage (at 59 DAH), the PS and US performed better in identifying the gaps within the sugarcane rows compared to the other two approaches. At 59 DAH, the VIS and the UAV image did not identify gaps smaller than 0.4 m. The non-identification of small gaps by VIS and UAV images in more advanced crop growth stages (47 and 59 DAH) should be related to the canopy characteristics of the ratoon. In Fig. 18, it is evident that with the increase in canopy growth, there was also a greater identification of plants by the four approaches in this study. At 41 and 59 DAH, the UAV image identified 98% and 100% of the plants, and in this same stage, the VIS identified 95% and 99% of the plants (True negative in Fig. 18a and b). Matsuoka & Stolf (2012), at a particular stage of growth, sugarcane has a characteristic to cover the gaps between ratoons.

Moreover, the ability to cover the small gaps is determined by combining the tillering and leaf arrangement. Which facilitates plants identification by RAP image and VIS. Nevertheless, when it comes to mapping the gaps, the underestimation of the number of gaps at 47 and 59 DAH by VIS and UAV images can influence decision-making, such as the necessity of ploughing out partial or total of the field.

3.3.2. Sensors system's performance for gap measurement

The length of the estimated gaps, using the four sensor-based techniques, showed a strong coefficient of correlation ($r \geq 0.93$) based on observed values obtained with the reference method (Fig. 19). It was observed that this correlation decreases as the sensor survey is conducted with a more developed crop; for example, a reduction from 0.99 to 0.93 was observed for the VIS and US between 19 and 59 DAH measurements; a similar pattern was observed for the other techniques.

RMSE values ranging from 0.09 to 0.18 m were obtained in the tests with PS, having the best performance in measuring the length of the gaps compared to other sensors. VIS and UAV images had similar performance, with the RMSE ranging between 0.11 and 0.40 m. The US has RMSE ranging from 0.10 to 0.27 m. The smallest error in the measurement of gaps during data collection in the first stage of development (19 DAH) of sugarcane. In this stage of developing the sugarcane ratoon, the sensor-based techniques performed similarly. This result shows that at 19 DAH, there was little interference from the canopy of the plants in the measurement of the

gaps. VIS has a greater RMSE than the other sensors at 31 DAH, which indicates that gap measurement by this sensor is being affected by the canopy of the plants at this stage of development. It is evident that with a more advanced stage of development, the greater the RMSE of the VIS and UAV image. At 59 DAH, coinciding when the sugarcane covered the inter-row area, VIS and UAV images had the RMSE much larger than the PS. PS was the methodology with the least variation in RMSE over the stage of sugarcane development.

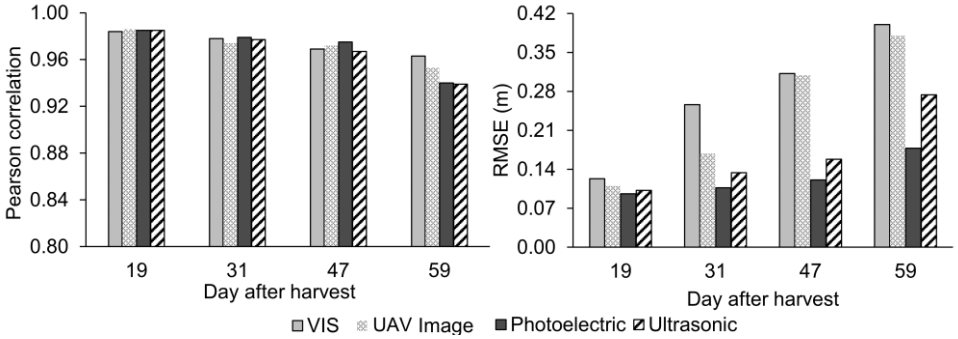

Figure 19. Pearson correlation and Root Mean Square Error (RMSE) of the four sensor-based techniques over the days after harvest. VIS – Vegetative index sensor. UAV - Unmanned Aerial Vehicle.

The dispersion of the error below zero showed that the sensor-based techniques underestimated the actual size of the gaps (Fig 20). The similarity between the distribution of errors between the VIS and UAV images is evident in Fig. 10. Both methodologies show the increase in the error negatively over the time of data collection, meaning that the higher the growth stage, the greater the measurement error. The VIS and UAV image, which measures the sugarcane canopy's reflectance, has difficulties identifying the stalks of sugarcane underestimating the length of the gaps. Also, at 47 and 59 DAH, there is a linear trend of increasing the error with the increase of the observed length of the gaps. The PS and US, which identify the gaps on the side of the plant, under the canopy, had lower measurement errors at 19 DAH compared to the VIS and UAV image. The PS and US had similar performance; both have the most positive errors, meaning that these two methodologies estimated values greater than the actual size. There was a greater dispersion of the error with the increase in the gap length observed for these two methodologies.

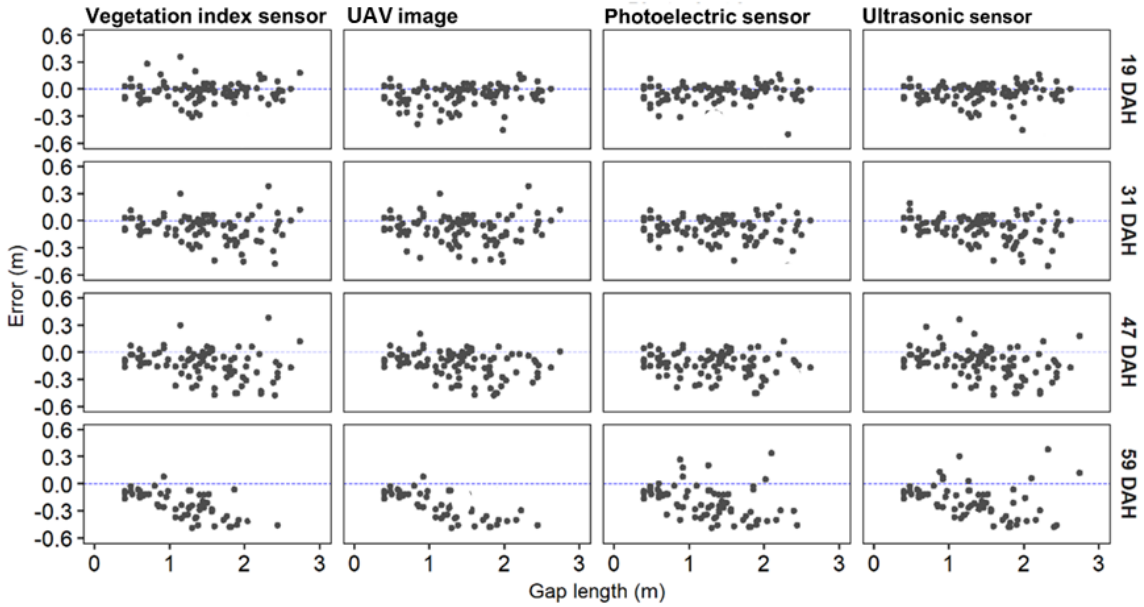

Figure 20. Scatter plot of the error vs the gap length for the four methodologies. UAV - Unmanned Aerial Vehicles. DAH – Days after harvester.

Another critical factor to highlight is the spatial resolution in each sensor system. The VIS presented the highest RMSE and the lowest correlation with field validations at all times, and the resolution is the highest due to the limited frequency for data collection. This factor will influence the system's ability to identify and measure soil-plant variation. For sugarcane, a crop that grows quickly, the time for data acquisition must be taken into account. The capacity to cover large areas with UAV imaging can be seen as a positive aspect concerning the other methodologies studied here. It is essential to highlight that additional information can be generated with the same images collected to identify the gaps. As already seen in other studies, the UAV images can also be used to detect weeds (Tanut & Riyamongkol, 2020), plant diseases (Matese & Di Gennaro, 2018), perform plant count estimations (Koh, Hayden, Daetwyler, & Kant, 2019), among others. To this point of view, UAV images are significant in identifying the gaps, even if there is a loss of accuracy and precision in identifying and measuring gaps.

In this work, the economic return of each operation was not observed. Notably, a dedicated operation to map gaps using sensors attached to a tractor has the disadvantage of a time-mapped area related to the UAV image. However, PS and US be easily coupled to equipment that performs cropping operations, such as spray or fertilizing, to obtain gap information without a dedicated operation. In real-time, it is still a challenge for data from UAV, for example. Such sensors can assist in optimizing inputs only in locations where there are plants, thus reducing input costs. Ultrasonic sensors to detecting spaces between plants, and then manipulating nozzle activations in real-time were studied by Palleja and Landers (2015) and (Escolà et al., 2013). According to the review published by Abbas et al. (2020), infrared and ultrasonic sensors technology can reduce the use of inputs, and unwanted losses, and therefore their usage is beneficial for farmers, consumers, and the environment. Another interesting application would be the association of these sensors with a VIS for N management; this permits avoiding the applications where there is no sugarcane combined with applying the appropriate doses on cane ratoon by using algorithms that transform the reflectance values in nitrogen doses (Amaral, Trevisan, & Molin, 2018). Gap maps allow optimizing inputs, reducing costs, and minimizing environmental impacts.

3.4. Conclusion

The sensor-based techniques using photoelectric and ultrasonic sensors with the best accuracy (98%) and precision (100%) identify gaps within sugarcane rows. As mentioned in this study, the sensors work beside the plants and under their canopy to identify the sugarcane stalks and identify and measure gaps in the sugarcane rows without the plant canopy interference. The sensor-based techniques performed better in identifying the gaps at 31 and 47 days after harvest (DAH). More advanced growth stages (59 DAH) result in greater underestimation of the gap length by the sensor-based techniques, especially for UAV images and vegetative index sensor (VIS), which had RMSE above 0.38 m. Furthermore, these two methodologies underestimate the number of gaps when the canopy of the plant covers the inter-row area.

3.5. Conection text to chapter 4

Sugarcane plant population is crucial to achieving high yields over the years. Monitoring spatial and temporal plant populations within sugarcane field is essential to site-specific management. However, because of phenological characteristics, there are challenges for the detection and mapping of plants within the sugarcane fields. Unmanned aerial vehicles (UAV), already used for mapping gaps, can be an alternative tool for counting and

mapping the plants within the field. In this sense, the Chapter 4 addresses spatial and temporal analysis of the plant population using UAV images in sugarcane commercial fields. Moreover, analyses were performed to verify the relationship between slope, path angle, and the plant population, as sloping areas and curved paths are more likely to cause plant damage by machinery wheels.

Chapter 4 has been submitted in Biosystems Engineering Journal and its status is under review, as can be seen below.

Maldaner, L.F., Molin, J.P., Dias, C.T.S., Martello, M., Canata, T.F. (2021) Mapping sugarcane spatial patterns using spatial and temporal analysis of features extracted from UAV images. *Biosystems Engineering*. **Under review**.

References

Abbas, I., Liu, J., Faheem, M., Noor, R.S., Shaikh, S.A., Solangi, K.A., & Raza, S.M. (2020). Different sensor based intelligent spraying systems in Agriculture. *Sensors Actuators*, A Phys. 316, 112265. https://doi.org/10.1016/j.sna.2020.112265

Amaral, L. R., Molin, J. P., & Schepers, J. S. (2015). Algorithm for Variable-Rate Nitrogen Application in Sugarcane Based on Active Crop Canopy Sensor. *Agronomy Journal*, *107*(4), 1513–1523. https://doi.org/10.2134/agronj14.0494

Amaral, L. R., Trevisan, R. G., & Molin, J. P. (2018). Canopy sensor placement for variable-rate nitrogen application in sugarcane fields. *Precision Agriculture*, *19*(1), 147–160. https://doi.org/10.1007/s11119-017-9505-x

Bordonal, R. de O., Carvalho, J. L. N., Lal, R., de Figueiredo, E. B., de Oliveira, B. G., & La Scala, N. (2018, April 1). Sustainability of sugarcane production in Brazil. A review. *Agronomy for Sustainable Development*. Springer-Verlag France. https://doi.org/10.1007/s13593-018-0490-x

Carullo, A., & Parvis, M. (2001). An ultrasonic sensor for distance measurement in automotive applications. *IEEE Sensors Journal*, *1*(2), 143–147. https://doi.org/10.1109/JSEN.2001.936931

Escolà, A., Rosell-Polo, J.R., Planas, S., Gil, E., Pomar, J., Camp, F., Llorens, J., & Solanelles, F., (2013). Variable-rate sprayer. Part 1 - Orchard prototype: Design, implementation and validation. *Computers and Electronics in Agriculture*. 95, 122–135. https://doi.org/10.1016/j.compag.2013.02.004

Escolà, A., Planas, S., Rosell, J. R., Pomar, J., Camp, F., Solanelles, F., … Gil, E. (2011). Performance of an ultrasonic ranging sensor in apple tree canopies. *Sensors*, *11*(3), 2459–2477. https://doi.org/10.3390/s110302459

Frasson, F. R., Salvi, J. V., Povh, F. P., Molin, J. P., Salvi1, F. R. F. J. V., Molin1, F. P. P. J. P., & Motomiya, A. V. de A. (1999). Quantificação de falhas de plantio em cana-de-açúcar utilizando um sensor ótico ativo. In *Simpósio Brasileiro De Sensoriamento Remoto* (Vol. 8, p. 160). https://doi.org/10.1017/CBO9781107415324.004

Garilli, E., Bruno, N., Autelitano, F., Roncella, R., & Giuliani, F. (2021). Automatic detection of stone pavement's pattern based on UAV photogrammetry. Automation in Construction, 122, 103477. https://doi.org/10.1016/j.autcon.2020.103477

Koh, J. C. O., Hayden, M., Daetwyler, H., & Kant, S. (2019). Estimation of crop plant density at early mixed growth stages using UAV imagery. *Plant Methods*, *15*(1), 1–9. https://doi.org/10.1186/s13007-019-0449-1

Luna, I., & Lobo, A. (2016). Mapping crop planting quality in sugarcane from UAV imagery: A pilot study in Nicaragua. *Remote Sensing*, *8*(6). https://doi.org/10.3390/rs8060500

Madli, R., Hebbar, S., Pattar, P., & Golla, V. (2015). Automatic detection and notification of potholes and humps on roads to aid drivers. *IEEE Sensors Journal*, *15*(8), 4313–4318. https://doi.org/10.1109/JSEN.2015.2417579

Maldaner, L. F., Canata, T. F., Dias, C. T. dos S., & Molin, J. P. (2021). A statistical approach to static and dynamic tests for Global Navigation Satellite Systems receivers used in agricultural operations. *Scientia Agricola*, *78*(5). https://doi.org/10.1590/1678-992x-2019-0252

Matese, A., & Di Gennaro, S. F. (2018). Practical applications of a multisensor UAV platform based on multispectral, thermal, and RGB high-resolution images in precision viticulture. *Agriculture (Switzerland)*, *8*(7). https://doi.org/10.3390/agriculture8070116

Matsuoka, S., & Stolf, R. (2012). Sugarcane Tillering And Ratooning: Key Factors For A Profitable Cropping. In ão F. Goncalves and Kauê D. Correia (Ed.), *Sugarcane: Production, Cultivation, and Uses*. Nova Science Publishers.

Molin, J. P., & Veiga, J. P. S. (2016). Variabilidade espacial de falhas em cana-de-açúcar: Mensuração e mapeamento. *Ciencia e Agrotecnologia*, *40*(3), 347–355. https://doi.org/10.1590/1413-70542016403046915

Moore, P. H. (1987). Anatomy and morphology. In *Developments in Crop Science* (Vol. 11, pp. 85–142). Elsevier. https://doi.org/10.1016/B978-0-444-42769-4.50008-4

Olson, D. L., & Delen, D. (2008). *Advanced data mining techniques*. *Advanced-Data Mining Techniques*. https://doi.org/10.1007/978-3-540-76917-0

Palleja, T., & Landers, A.J. (2015). Real-time canopy density estimation using ultrasonic envelope signals in the orchard and vineyard. *Computers and Electronics in Agriculture*. 115, 108–117. https://doi.org/10.1016/j.compag.2015.05.014

Peña, J. M., Torres-Sánchez, J., Serrano-Pérez, A., de Castro, A. I., & López-Granados, F. (2015). Quantifying efficacy and limits of unmanned aerial vehicle (UAV) technology for weed seedling detection as affected by sensor resolution. *Sensors (Switzerland)*, *15*(3), 5609–5626. https://doi.org/10.3390/s150305609

Peña-Villasenín, S., Gil-Docampo, M., & Ortiz-Sanz, J. (2020). Desktop vs cloud computing software for 3D measurement of building façades: The monastery of San Martín Pinario. *Measurement: Journal of the International Measurement Confederation*, 149, 106984. https://doi.org/10.1016/j.measurement.2019.106984

Portz, G., Amaral, L. R., Molin, J. P., & Adamchuk, V. I. (2013). Field comparison of ultrasonic and canopy reflectance sensors used to estimate biomass and N-uptake in sugarcane. In *Precision Agriculture 2013 - Papers Presented at the 9th European Conference on Precision Agriculture, ECPA 2013* (pp. 111–117). Wageningen Academic Publishers, Wageningen. https://doi.org/10.3920/978-90-8686-778-3_12

Peña-Villasenín, S., Gil-Docampo, M., & Ortiz-Sanz, J. (2020). Desktop vs cloud computing software for 3D measurement of building façades: The monastery of San Martín Pinario. *Measurement: Journal of the International Measurement Confederation*, *149*, 106984. https://doi.org/10.1016/j.measurement.2019.106984

Richards, J. A., & Jia, X. (2006). *Remote sensing digital image analysis: An introduction*. *Remote Sensing Digital Image Analysis: An Introduction*. Springer Berlin Heidelberg. https://doi.org/10.1007/3-540-29711-1

Sokolova, M., & Lapalme, G. (2009). A systematic analysis of performance measures for classification tasks. *Information Processing and Management*, *45*(4), 427–437. https://doi.org/10.1016/j.ipm.2009.03.002

Souza, C. H. W. de, Lamparelli, R. A. C., Rocha, J. V., & Magalhães, P. S. G. (2017). Mapping skips in sugarcane fields using object-based analysis of unmanned aerial vehicle (UAV) images. *Computers and Electronics in Agriculture*, *143*, 49–56. https://doi.org/10.1016/j.compag.2017.10.006

Stolf, R. (1986). Metodologia de avaliação de falhas nas linhas de cana-de-açúcar. *Stab*, *4*(6), 22–36.

Tanut, B., & Riyamongkol, P. (2020). The development of a defect detection model from the high-resolution images of a sugarcane plantation using an unmanned aerial vehicle. *Information (Switzerland)*, *11*(3). https://doi.org/10.3390/info11030136

Torres-Sánchez, J., Ló Pez-Granados, F., Castro, D., & Peñ A-Barragán, A. I. (2013). Configuration and Specifications of an Unmanned Aerial Vehicle (UAV) for Early Site Specific Weed Management. *PLoS ONE*, *8*(3), 58210. https://doi.org/10.1371/journal.pone.0058210

Van Dillewijn, C. (1952). *Botany of Sugarcane*. Chronica Botanica, Waltham, Mass., and William Dawson & Sons, London. https://doi.org/10.1126/science.116.3013.333

4. MAPPING SUGARCANE SPATIAL PATTERNS USING SPATIAL AND TEMPORAL ANALYSIS OF FEATURES EXTRACTED FROM UAV IMAGES

Abstract

Sugarcane plant population is crucial to achieving high yields over the years. Monitoring spatial and temporal plant populations within sugarcane field is essential to site-specific management. However, because of phenological characteristics, there are challenges for the detection and mapping of plants within the sugarcane fields. Unmanned aerial vehicles (UAV), already used for mapping gaps, can be an alternative tool for counting and mapping the plants within the field. The objective of this study was to perform the spatial and temporal analysis of the plant population using UAV images in sugarcane commercial fields. Moreover, we check the relationship between slope, path angle, and the plant population, as sloping areas and curved paths are more likely to cause plant damage by machinery wheels. The UAV imagery was collected in two successive sugarcane seasons (2019 and 2020). Unsupervised segmentation with the k-means algorithm was used to process the RGB image. From the RGB images, the slope, path angle, plant population, and gap length were extracted. Analysis of variance was performed to verify the influence of slope and path angle factors on plant population and gap length. Principal components analysis (PCA) and cluster analysis were made to classify and map the susceptibility of occurrence of plant reduction over the years. Unsupervised segmentation with the k-means algorithm demonstrated an accuracy of 91% in detecting the sugarcane plants in the RGB image. Overall, there was a 16% reduction in the plant population and increases of 0.7 m in the gap length over the two years of study. Regions with a terrain slope of 5-8% and greater than 8% with curved paths have an inferior number of plants compared to other regions. The greater the terrain slope in the study fields, the greater the probability to reduce plant population over the years. The patterns with susceptibility to plant reduction over the years were mapped, creating useful data to subsidize decision-making as the maintenance of sugarcane, identification of the regions where they should be replanted, and the provision for the renovation of sugarcane fields.

Keywords: Precision agriculture; Plant variability; High-resolution images; Terrain slope

4.1. Introduction

In virtue of the increased adoption of novel tools and the ability of machines to generate data, it is more feasible to collect data with high spatial resolution from the fields. This provides an opportunity to realize more accurate and complex applications that are difficult to accomplish with non-spatialized data. Precision agriculture (PA) combines spatial and temporal data with other information to support management decisions according to the estimated variability for better resource utilization efficiency, yield, quality, profitability and sustainability of agricultural production (ISPA, 2019). For many years, the management of sugarcane fields has been based on data generated from the manual and punctual sampling, such as the percentage of gaps used for the decision to plough out and implement new sugarcane fields, inputs application, and yield estimation.

Sugarcane (*Saccharum* sp.) is one of the crops with the highest rate of adoption of innovative technologies, mainly for the management of equipment and application of inputs. Because it is a perennial crop, longevity is essential for the implementation of cost amortization over a number of ratoon crops (Matsuoka & Stolf, 2012). One of the challenges is to maintain a profitable yield over the years since several factors cause a decremental yield. Therefore, it is essential to monitor spatial and temporal parameters related to sugarcane to assist in management and decision-making. Among these parameters, the commonly used is the percentage of gaps present in the sugarcane field (Molin & Veiga, 2016; Souza, Lamparelli, Rocha, & Magalhães, 2017). The percentage of gaps and the plant

spacing are metrics that correlated with the decrease of plants throughout the harvests, which consequently affects the final yield (Matsuoka & Stolf, 2012).

Among the technologies used by the sugarcane industry, the use of the unmanned aerial vehicle (UAV) has been highlighted and is increasingly used mainly for obtaining RGB images for gap mapping in the sugarcane field. Imaging sugarcane row allow to extract information as the map of sugarcane planting and ratoon quality (Luna & Lobo, 2016) and compare with yield, slope, and soil maps, generating information necessary for crop monitoring and decision making (Souza et al., 2017). Besides that, UAV imaging has been studied for several other applications in the sugarcane industry, like weed detection (Girolamo-Neto et al., 2019), phenotyping (Natarajan, Basnayake, Wei, & Lakshmanan, 2019), variable nitrogen application (Shendryk et al., 2020; Sofonia et al., 2019), yield estimation (Sanches et al., 2018; Sumesh, Ninsawat, & Som-ard, 2021), additionally, directly for spray application (Song et al., 2020; Zhang et al., 2020).

On the other hand, studies related to plant population of the sugarcane fields are limited. The mapping distribution of the plant population is commonly used in other crops such as maize (Gnädinger & Schmidhalter, 2017; Shirzadifar, Maharlooei, Bajwa, Oduor, & Nowatzki, 2020), cotton (Chen, Chu, Landivar, Yang, & Maeda, 2018), and potato (Li et al., 2019). Plant population mapping brings detailed information that can help in decision-making for replanting regions with low plant counts or applying agricultural inputs appropriately in defective regions (Shirzadifar et al., 2020). Monitoring the sugarcane plant population is very important because maintaining the same number of plants throughout the harvests is essential for the longevity of the sugarcane plantation (Matsuoka & Stolf, 2012). Identify regions with greater susceptibility to plant reduction can help in making decisions for partial or total replanting of the sugarcane field. In addition, it can reduce the cost of implementing a new sugarcane field and guide to the most efficient spatialized management.

Sugarcane is a grass and its phenological characteristic is tillering in the early stages of sprouting (Van Dillewijn, 1952). A sugarcane plant is composed of several tillers that may vary in density within the field (Kapur, Duttamajumder, & Krishna Rao, 2011). These characteristics may be one of the reasons for the low uptake of UAV imagery for plant identification and plant counting within the sugarcane field. Unlike other crops such as maize that have a single plant, which facilitates the identification and counting of plants by high resolution images. The tiller density within the field is influenced by factors such as primary tiller germination, underground branching, tiller senescence due to light competition (Bezuidenhout, O'Leary, Singels, & Bajic, 2003), climate (Laclau & Laclau, 2009), row spacing (Singels & Smit, 2009), and agronomic practices (Bell & Garside, 2005). Some studies show that the amount of straw remaining from the previous year influences tillering density and final plant population (Lisboa et al., 2019; Sandhu et al., 2017).

The hypothesis is that in addition to these factors, the sugarcane plant population is also affected by the terrain, especially the slope and the angle of the sugarcane planting rows. Sugarcane is a crop that has traffic of heavy machinery mainly due to the mechanized harvesting operation that can lead to soil compaction (Cherubin, Franchi, Lima, Moraes, & Luz, 2021) and direct damage to the plants (Paula & Molin, 2013). Although sugarcane planting is done at a level that follows the terrain contour and with machines with automatic pilot system, sloping areas and curved paths are more likely to cause damage to plants by machinery wheels. A previous study by (Passalaqua & Molin, 2020), shows that the greater the terrain slope and the smaller the angle of the path, the greater the path error. In other words, higher probability of the machine's wheels hitting the sugarcane plant.

However, mapping the population of sugarcane plants and identifying patterns within the commercial fields is still a challenge. Using high-resolution images from UAV cameras that are already used for gap mapping can

be an alternative tool for counting and mapping the plants within the field. UAV images provide the opportunity to generate high-resolution spatial and temporal information with convenient and cost-effective crop access. Thus, the objective of this study was to perform the spatial and temporal analysis of the stand using UAV images in sugarcane commercial fields. The specific objectives were (i) check the relationship between slope, type of path, and the plant population, (ii) identify regions within the field that have the highest probability to present low plant population, and (iii) locate regions with high probability of reduction compared to the previous year.

4.2. Material and Methods

4.2.1. Study sites

The experiment was conducted on a commercial site composed of 36 sugarcane fields with a combined area of 496 ha located in the South-Central region of São Paulo, Brazil (22°42'06.8"S 48°19'12.7"W) (Fig. 21). The predominant soil class is the Argisol with sandy texture (Santos et al., 2018). The variety RB966928 was mechanically planted with 1.5 m row spacing in May 2014. The harvesting operation consisted of four mechanicals harvesters and a series of tractors pulling in-field wagons with a capacity of 12.0 Mg. The harvest operation was carried out at the beginning of the period of low rainfall with accumulated rainfall in May 2019 of 36.6 mm and May 2020 of 28.6 mm. The harvest in both years of study was with single row harvesters and the infield wagons with three axels each running with auto-steering with accurate traffic control. The average speed of the harvesters was 1.4 m s^{-1}. After the harvest, straw raking and fertilizer application are the remaining machine traffic operations in the field. The UAV imagery was collected in two successive sugarcane grown seasons (2019 and 2020). Considering the previous study by (Maldaner, Molin, Martello, Tavares, & Dias, 2021), the images were captured when the sugarcane was at the tillering stage, approximately 40 days after harvest with an average canopy height of 0.35 m (Fig. 21). Based on the harvesting time, the data collected were on June 24, 2019 (Day 1), July 15, 2019 (Day 2), July 6, 2020 (Day 1), and July 7, 2020 (Day 2).

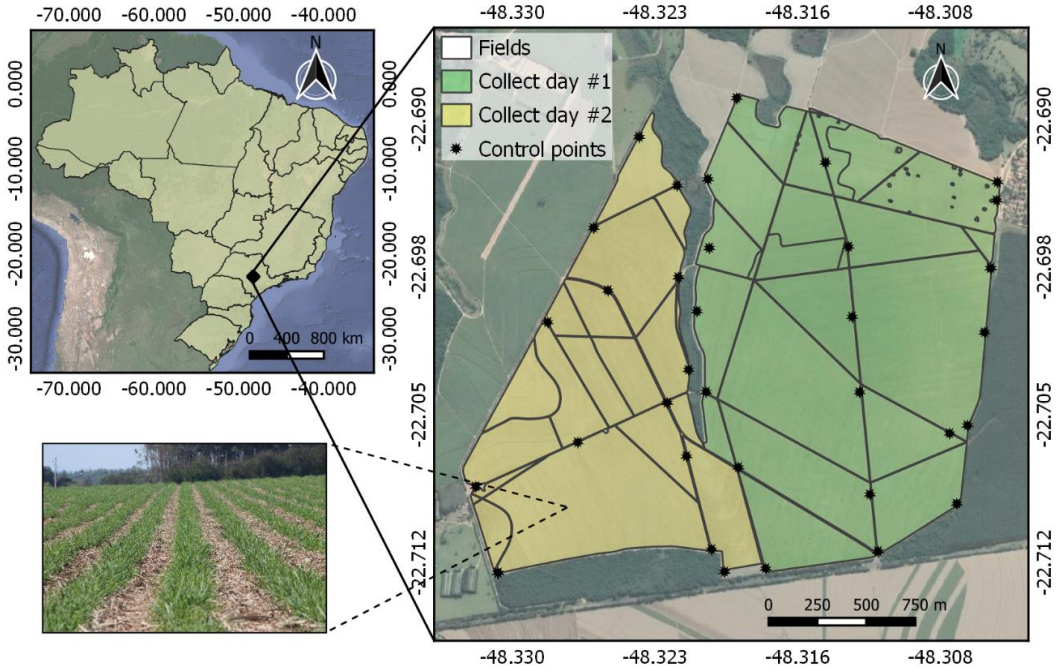

Figure 21. Study field location and the growth stage when data collection happened.

4.2.2. Data acquisition

The UAV images were captured over the fields from 8:40 to 15:10. Although the highest quality imagery is at noon with low humidity (cloudless sky) (Kedzierski et al., 2019), this period is typical in commercial image collections to increase the collection time and consequently the imaged area. The RGB image processing used only the original digital value of each band pixel, and there was no need to perform the radiometric correction of the images captured during the collection time. In addition, a local analysis was performed to identify plants in the RGB image in order to minimize the effect of difference of light intention and reflectance in the images due to the long day period of image collection. The low altitude Phantom 4 Advanced UAV (DJI, Shenzhen, Guangdong, China) with an in-built RGB 20 MP camera was used to acquire the images. This UAV with the onboard navigation-grade GNSS receiver is capable of flying autonomously. DroneDeploy app version 4.1 was used for flight planning and flight operation. To provide images with a spatial resolution of 0.03 m pixel^{-1}, the flight was performed with 100 m flight height, 70% forward, and 60% side overlap. The georeferencing of the images was by positioning thirty-four ground control points (GCP - Fig. 21) and their positions were obtained using a Topcon GR-3 receiver with real time kinematic (RTK) correction that allows the accuracy of ±0.03 m.

4.2.3. Image mosaicking

The image mosaicking was carried out with PhotoScan v.1.5 software (Agisoft LLC, St. Petersburg, Russia). The software adopts a standardized processing pipeline: camera alignment and georeferencing with control points, generation of a 3D point cloud, generation of a triangular mesh model from the point cloud, and creation of a mosaic image (Fig. 22). To georeferencing the mosaic image and accuracy assessment, the GPC was imported. The digital elevation model (DEM) of the study field was subtracted from the triangular mesh. The DEM resolution was 1.0 m pixel^{-1}. The mosaicked images were generated with a resolution of 0.03 m pixel^{-1}, which was the maximum resolution allowed from images captured by the onboard camera in the UAV.

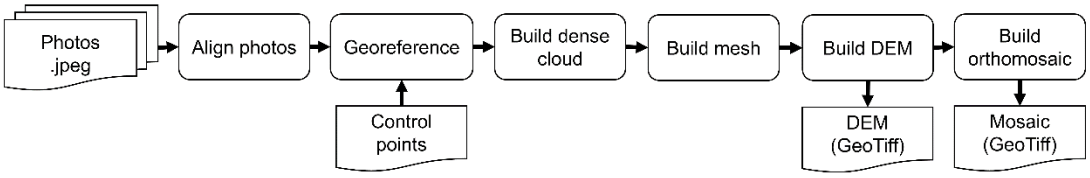

Figure 22. Unmanned aerial vehicle (UAV) image mosaicking workflow.

4.2.4. Image processing

The identification of sugarcane plants in the RGB mosaic consisted of six stages: (i) split the mosaic into tiles; (ii) split each tile into *n* windows; (iii) convert RGB to L*a*b* colour space; (iv) unsupervised classification; (v) identification of the plant class; (vi) and mask layer filtering (Fig. 23). To reduce the size and facilitate the process, the mosaic was splinted into tiles with 40000 square pixels. The segmentation of each tile was done through a local analysis by dividing each tile into 50 square pixel windows. Thus, it was possible to reduce the effect on the

difference in reflectance between the same class (plant or background) in different parts of the study field (Appendices A). The small windows (50x50 pixels) facilitated the discrimination between classes during the unsupervised classification. The methodology described by (Shirzadifar et al., 2020) was used to identify the plant class in each RGB window using unsupervised classification.

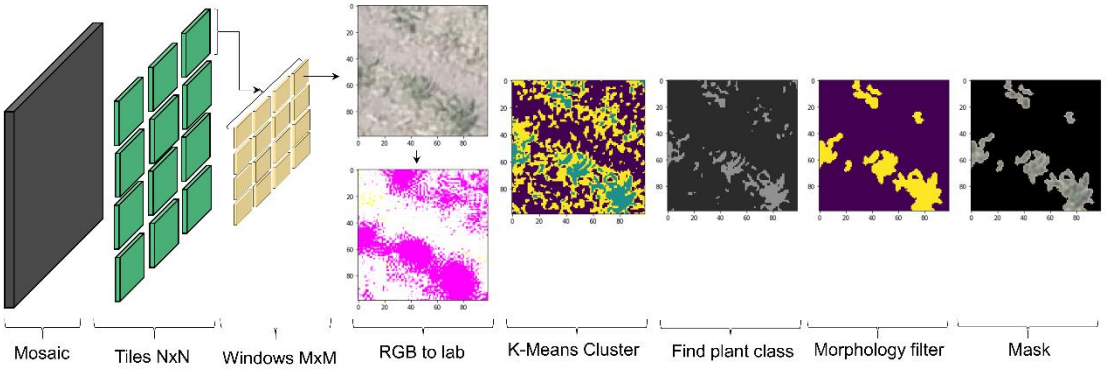

Figure 23. RGB mosaic segmentation flowchart.

4.2.4.1. RGB to L*a*b*

The windows with RGB values were converted to the L*a*b* colour model using the "rgb2lab" function. These components represent the lightness of the colour (L*), its position between red and green (a*), and its position between blue and yellow (b*). Instead of using two-colour components as input data for the unsupervised classification, as suggested by (Shirzadifar et al., 2020), we used only the colour component a* because the distribution of the colour area was sufficient to discriminate the plant pixels from the other pixels (background) (Appendices A). This provided a simple metric for clustering using the k-means algorithm.

4.2.4.2. K-Means algorithm

K-Means is one of the simplest algorithms for the automatic classification of data. The main idea is to choose randomly a set of centres fixed a priori and iteratively seeking the optimal partition (MacQueen, 1967). In this study, a K-means-based image segmentation algorithm for sugarcane plant detection was realized in Python Scikit-learn (Pedregosa et al., 2011) library using the *KMeans* function. The *KMeans* cluster data by trying to separate samples in four groups (n_clusters=4) of equal variance. *KMeans* function used the Elkan algorithm to group the data. The algorithm used the triangular inequality to avoid many distance calculations when assigning pixels to clusters. The k-means++ algorithm (Arthur & Vassilvitskii, 2006) was used to select initial cluster centres. The number of iterations for the *KMeans* function was 3 (interaction=3), as utilized by (Shirzadifar et al., 2020) to identify and count maize plants.

The median of the component a* was calculated for each cluster resulting from the unsupervised classification. The cluster with the smallest median was classified as plant and the others as background (Appendices A). This resulted in a binary image.

4.2.4.3. Morphological filter

Three morphological operations were applied to remove the noise around the central plants and improve the quality of the binary image using Python skimage.morphology library (Pedregosa et al., 2011). We used the function "remove_small_objects" to remove objects smaller than 15 pixels. After that, the "dilation" function was used to enlarge plant regions and shrink background regions. Morphological dilation sets a pixel at (i, j) to the neighbourhood's maximum overall pixels centred at (i, j). Finally, the function "remove_small_holes" has been applied to remove contiguous holes smaller than 15 pixels.

4.2.5. Features extraction

From the binary image was extracted the plant population (stand ha^{-1}), and the plant spacing (m). Sugarcane row (path) was extracted from the RGB mosaic using the software InfoRow 2.0 (SOMO, Piracicaba, Brazil), commonly used by farmers, and then the path angle (α) was calculated. Firstly, the software extracts an approximate vegetation index from an RGB mosaic and applies a filter to identify pixel values in the plant rows center. In the next step, the software extracted lines (straight and curved) using a procedure of building line segments along with points for multiple parallel lines and adjustable offsets (Spekken & Molin, 2018).

The extraction of each feature is detailed below:

Path angle (a) – Is the angle α between two segments of the lines and is calculated by following the Eq. 7:

$$\alpha = \left[\frac{m_2 - m_1}{1 - m_1 m_2}\right] \quad (7)$$

$$m_1 = \frac{y_b - y_a}{x_b - x_a} \quad (8)$$

$$m_2 = \frac{y_c - y_b}{x_c - x_b} \quad (9)$$

where *x* and y are the metric coordinates of the two line segments $\underline{ab}$ and $\underline{bc}$, *m* is the slope of each line segment. After calculating α, the vertices of the lines were extracted with their corresponding α value.

Plant population (stand ha^{-1}) – The binary image was vectorised with the *rasterio* library using the *shape* function (Gillies, Ward, & Petersen, 2013). The shapefile was split in two to separate the polygons as background and plant. To mapping the plant population, the centroids of polygons classified as plants were extracted. A square grid with 5 m x 5 m was created and then the stand ha^{-1} was calculated using the equation 10:

$$stand\ ha^{-1} = \frac{number\ of\ counted\ centroid\ within\ grid}{area\ of\ grid\ (ha)} \quad (10)$$

Plant spacing (m) – The shapefile with the lines was cropped with the polygons classified as plant using *geopandas* library (Jordahl et al., 2020) with *intersection* function. Then, the length of each segment was calculated, and this length was considered the plant spacing within each row of sugarcane.

Slope (%) - Slope gradient was calculated using the QGIS r.slope.aspect command. The DEM resulting from UAV image processing was used as command input. The r.slope.aspect command uses a finite difference method to compare the height of a pixel cell in the DEM with that of its eight immediate neighbours (Horn, 1981). The resulting raster layer (spatial resolution of 1 m) with slope gradient values in percentage was converted to points using the QGIS r.to.vect command.

4.2.6. Data analysis

The performance of plant detection using the RGB image was analyzed using the metrics: accuracy, precision, recall, and f1-score as described by (Sokolova & Lapalme, 2009). Nineteen sample plots were randomly selected within all study fields considering regions with different slopes and types of paths. In each of the nineteen plots, the manual annotation and counting of sugarcane plants was performed in the RGB images collected. A comparison between the plant count estimates by image versus the manual count was made using the Pearson correlation coefficient and fitting a linear model. Descriptive statistics and geostatistics followed by a visual assessment of the maps of plant population and plant spacing were made to identify patterns in the spatial variability (Colaço, Molin, Rosell-Polo, & Escolà, 2019). Spatial dependence index (SDI) was calculated as C0/(C0+C1), where C0 is the nugget variance (non-spatial variance), and C0+C1 is the sill variance (spatially dependent variance). SDI was interpreted as strong (<0.25), moderate (between 0.25 and 0.75), or weak (>0.75) (Cambardella et al., 1994).

The slope layer was classified into five classes, <2%, 2-3%, 3-5%, 5-8%, and >8% (Appendices A). Path with angle *a* upper to 179.6° was classified as straight and below 179.6° was considered as curved. In the analysis of variance (ANOVA), we evaluated the occurrence of the effects of the five slope classes and the two path types on the plant population and plant spacing for both years of study. ANOVA was also applied in the difference of the values of plant population and plant spacing between the years 2019 and 2020. In the presence of treatment effect (slope and path), the means were compared using the Tukey test at the level of 5% probability.

Principal component analysis (PCA) was used to characterize the relationship between these variables on different slopes and path types. Cluster analysis was performed to group of regions within field of greatest similarity. From this, it was possible to identify regions that are more susceptible to plant population reduction over the years. A dendrogram was created using a final partition of five clusters, which occurs at an average distance between clusters of approximately 0.15. The five clusters were classified between low and high susceptibility of reduction of plants over the years, with Group 1 being highly susceptible and Group 5 lowly susceptible. Finally, the susceptibility degree map was created from the classification of the five groups.

4.3. Results and discussion

4.3.1. UAV image prediction accuracy

The green dots in the plant map indicate the plant that was correctly detected by the approach (Fig. 24A). The fraction of the plant correctly detected by the image was 84% (recall). The red dots on the plant map indicate the non-detected plants by the methodology, which represents 2% of the total number of plants. Overall, the approach using RGB images and the k-means algorithm has an accuracy of 91%. Results similar to those found by (Shirzadifar et al., 2020), which was used as the basis for image segmentation in this study. The result of the plant counting using image versus manual count shows a strong correlation, with r=0.956 (Fig. 24B). The coefficient of determination (R^2 =0.89) and slope (0.95) of the linear model fitted in the data show the approach using the image and the k-means algorithm has high accuracy in estimating plant population within sugarcane field. Image processing based on RGB images can be an alternative for counting and mapping sugarcane plants within commercial fields. One advantage is the large photographed area over the time of flight. Moreover, high-resolution image provides

information in the early stages of development that is impossible to detect with the spatial resolution of the current satellite image used. On the other hand, the stage of sugarcane development is an important factor in planning the collection of UAV imagery (Maldaner et al., 2021).

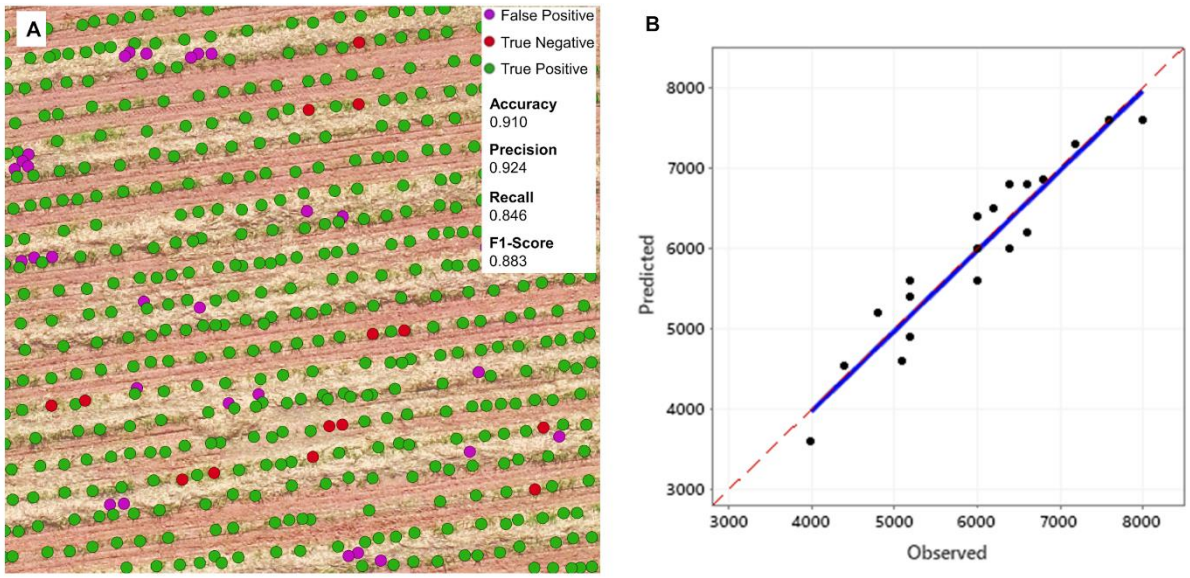

Figure 24. Plant map overlaid on aerial imagery (A) and predicted plant population using aerial image versus manual count (observed) (B). The red dashed line shows 1:1 (x=y) and the blue line shows the linear model fitted (y=0.95x+262 and R^2=0.89).

4.3.2. Geospatial analysis

The plant population ranges from 2400 to 8000 sand ha^{-1} in the two years of studies (Table 6). In 2020, the average plant population was 4904 stand ha^{-1}, lower than the previous year (5843 stand ha^{-1}). There was a reduction from 0 to 5200 stand ha^{-1} within the study area. An average reduction in the plant population of 939 stands ha^{-1}, equivalent to 16% compared to the 2019 average. There was a high variation in the difference between the two years of study with a coefficient of variation of 93%. Although there was a large amplitude in the reduction of the number of plants, there was no change in the spatial variability of the plant population. The plant population showed low spatial dependence, with a range of 24 m in 2019 and 2020. This may indicate that there is no regionalization in plant reduction, i.e., plant reduction may have occurred spatially random within the field of study.

Table 6. Descriptive statistics and geostatistical analysis of the variables plant spacing (m) and stand ha^{-1}.

Variable	Year	Min	Mean	Max	SD	CV (%)	model	range (m)	SDI
Plant population (stand ha^{-1})	2019	2400.0	5843.8	8001.0	965.2	16.5	Exp	24.2	weak
	2020	2400.0	4904.8	8000.0	858.1	17.5	Gau	24.9	weak
	Difference	0.0	-939.0	-5200.0	-877.8	93.5	Exp	8.8	weak
Plant spacing (m)	2019	0.1	0.8	31.7	0.7	84.4	Exp	12.7	strong
	2020	0.1	1.1	184.4	2.1	191.0	Exp	7.0	moderate
	Difference	0.0	0.7	183.8	2.1	315.9	Sph	17.3	moderate

SD – standard deviation. CV - coefficient of variation (%). RMSE – root mean square error of the model fit in the variogram. Variogram theoretical models: exponential (Exp), Gaussian (Gau), and spherical (Sph). SDI – Spatial dependence index according to (Cambardella et al., 1994).

In 2019, the plant spacing ranged between 0.1 m and 31 m, with an average of 0.8 m. In 2020, the length ranged from 0.1 m to 184 m, with an average of 1.1 m. The increase of 0.7 m over the previous year is related to the reduction in plant population. The increase in the plant spacing influenced the spatial dependence over the two years of study. In 2019, the plant spacing presented strong spatial dependence while 2020 had moderate spatial dependence. The reduction of plants at short distances may have increased the variability of the data (nugget effect) compared to the previous year and there was a reduction in the range from 12.7 m to 7 m. Moderate spatial dependence was observed in the difference data between the two years, indicating that the occurrence of an increase may have occurred in specific spots inside the sugarcane field.

It is evident between the maps of 2019 and 2020 the reduction of plants within the field of study (Fig. 25). However, through the maps, it was not possible to identify any site with a higher probability of plant reduction over the years. There was a reduction of plants throughout the study area and there were no predominant locations. It was evident in the maps of plant population and plant spacing of the second year the increase in length with the decrease in the number of plants. In general, there was an increase in plant spacing throughout the study area. The increase in the plant spacing over the years of harvest is already expected, as plants are subject to damage due to machine traffic, pests, diseases, and climate factors (Luna & Lobo, 2016; Matsuoka & Stolf, 2012). In addition, the distance between plants within the row can increase as the vigor of plants decreases (Maldaner et al., 2021).

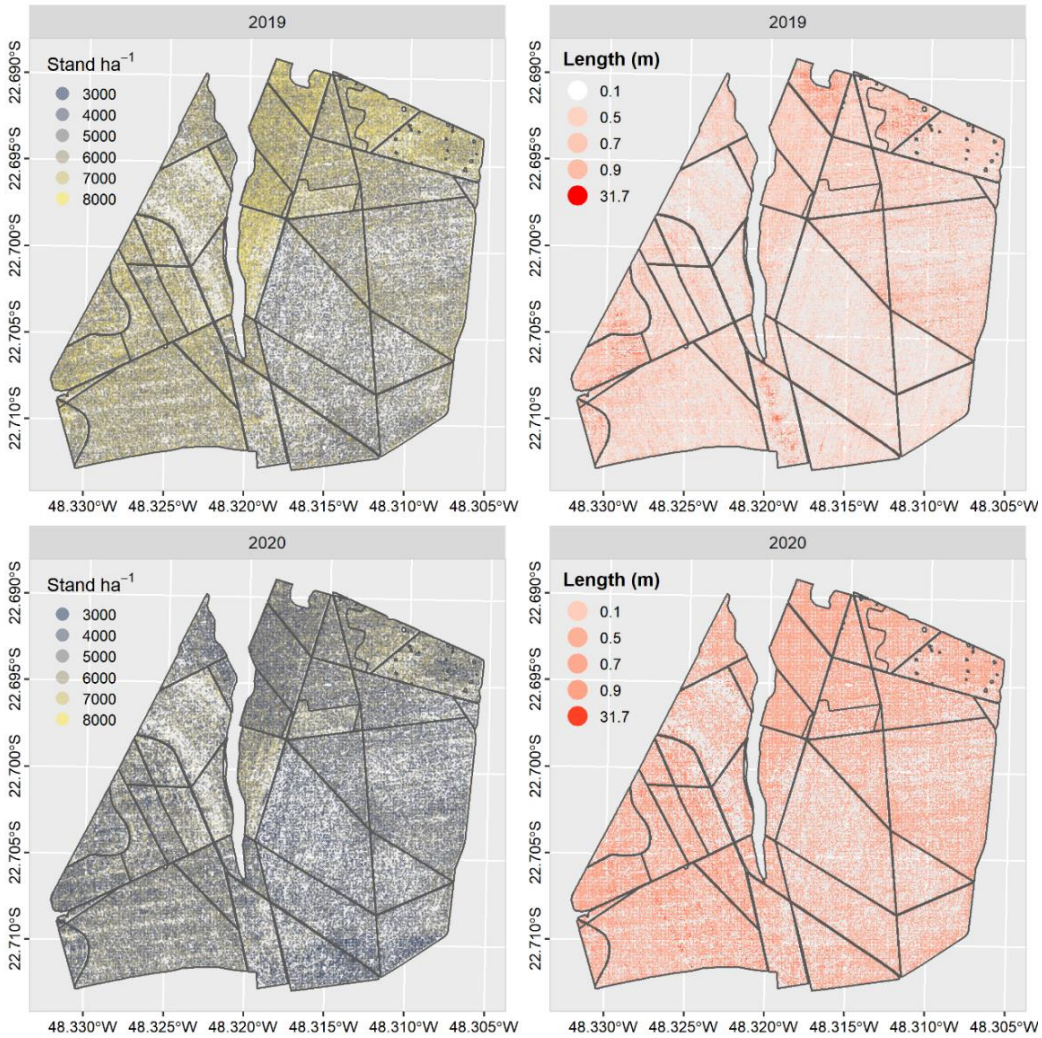

Figure 25. Maps of the variables plant population and plant spacing during the years 2019 and 2020 generated from RGB image of a camera coupled to an unmanned aerial vehicle.

4.3.3. Investigation of the relation among terrain slope, path angle, plant population, and plant spacing

The correlation matrix helps to understand the relationship of plant population and plant spacing in the two study years (Fig. 26). The plant population has a moderate correlation between the two study years (r=0.81). There is a strong correlation between the plant spacing difference between the two study years and the 2020 plant spacing (r=0.95). Not considering the spatial variability of the data, there was no correlation between plant population and plant spacing. The difference in plant spacing and plant population between the two study years had no relationship with these two features.

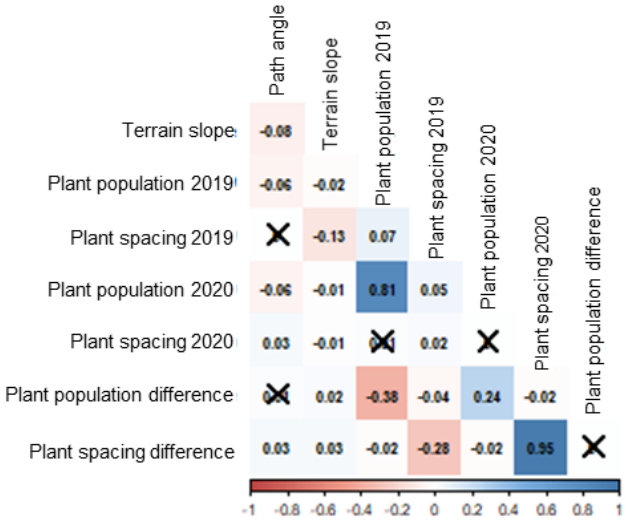

Figure 26. Correlation matrix of the features studied. "X" inside of the cell represents no significant correlation between the two features at a level of 0.05 (p=0.05).

A mean comparison test of the plant population in the different classes of slope shows that there was no significant difference between straight and curved pathways in <2% and in regions with the slope of 2-3% in both years of study (Fig. 27). In 2019, there was a difference in the number of plants between the straight and curved path with 3-5% and 5-8% of the slope. Moreover, the plant population was smaller in regions where there was a curved route and 5-8% of the slope. In both years of the study, regions with 5-8 and >8%, have a larger plant spacing compared to the other regions. Sloping regions within the sugarcane field with the curved route are more likely to cause damage to plants by the wheels due to the machine's path inaccuracy and lack of parallelism between the planting rows in this region (Souza, Souza, Cooper, & Tormena, 2015). The greatest decrease in plant population occurred on slope >8% with curved path, differing on slope <2% with the curved path which had the least plant population reduction over the two years of study (Fig. 28). Consequently, the plant spacing was greater on slopes >8% and smaller on slopes <2%. At the other slopes, there was no difference in plant population reduction and plant spacing increase.

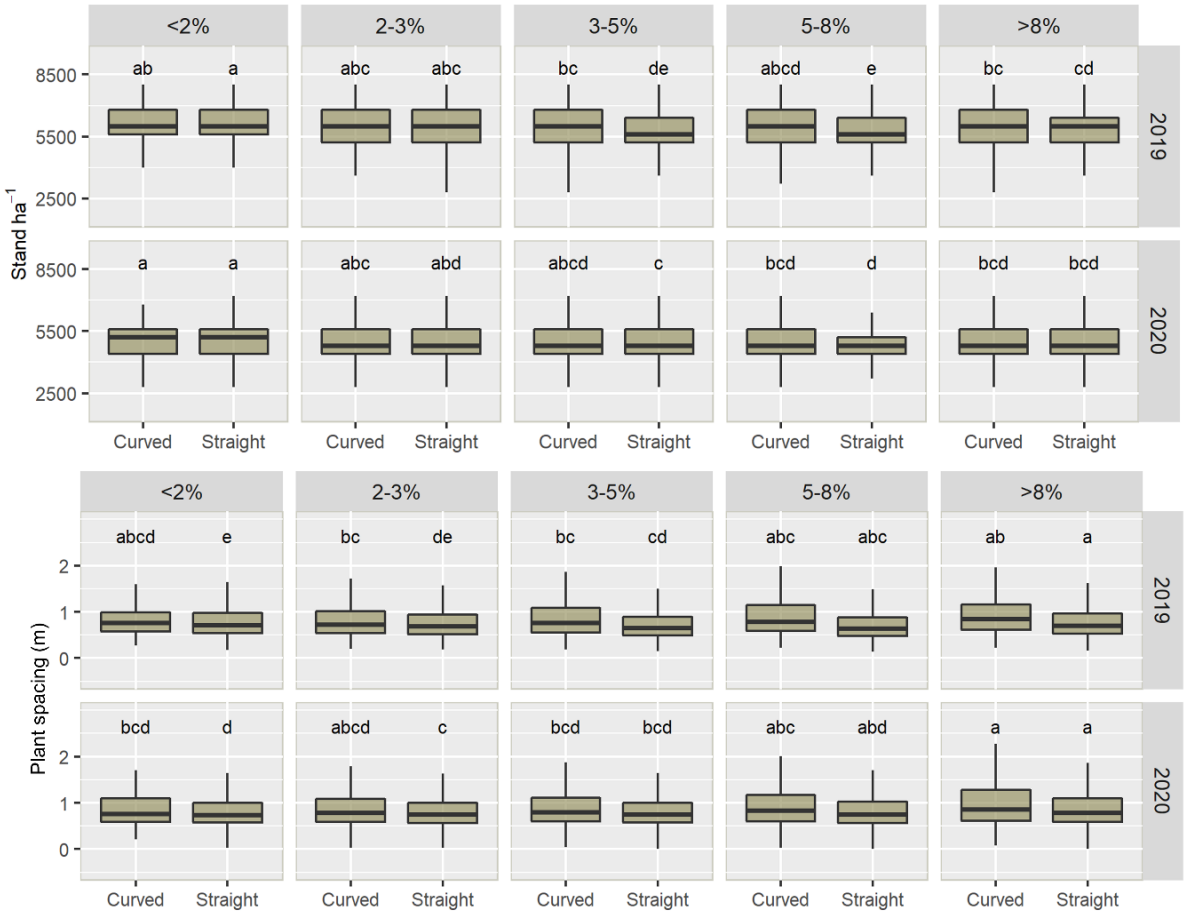

Figure 27. Boxplot of the variation of the plant population and the plant spacing between regions within the study field with different slopes of the terrain and paths. Different letters above the box indicate a significant difference between the groups in the same year (Tukey test; $p<0.05$).

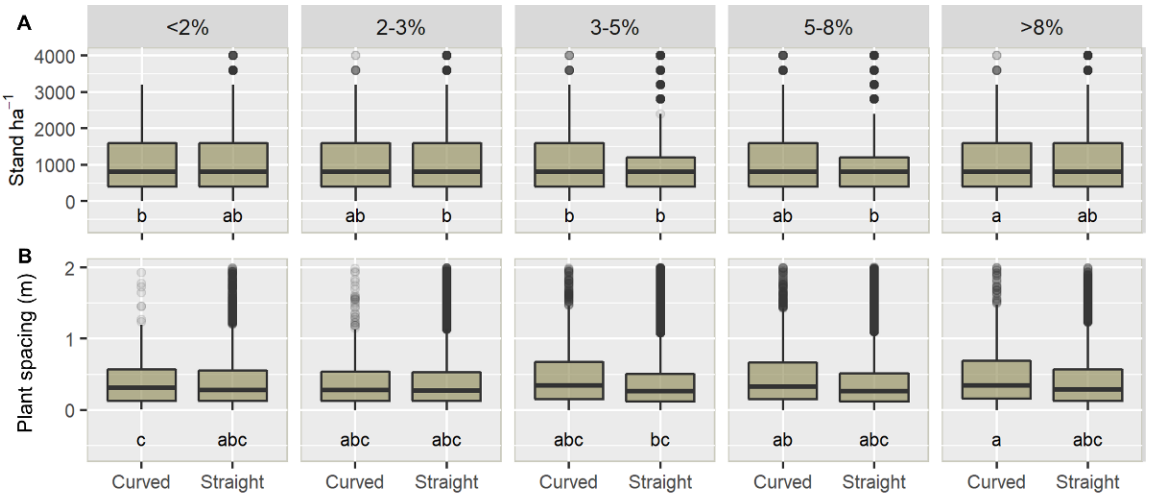

Figure 28. Boxplot of the difference over the two years of the study of the plant population (A) and the plant spacing (B) layers. Different letters below the box indicate a significant difference between the groups of slopes and paths in the same year (Tukey test; $p<0.05$).

The principal component analysis shows an exploratory overview of the ten groups (Fig. 29). The first two components explain 86% of the data variance (56.7% component 1 and 30.2% component 2). The two vectors

next to the variables plant population and plant spacing show a positive correlation between them. This indicates that the reduction of plants within sugarcane rows increases the plant spacing between the remaining plants. The opposite vectors indicate that the sugarcane plant population has a negative correlation with the terrain slope, the higher the slope, the lower the sugarcane plant populations. Plant damage is more likely due to machine drift and traffic over the ratoon in regions which slope is perpendicular to the sugarcane rows (Passalaqua & Molin, 2020), besides the slope increases the damage caused by the base cutting system of the harvester. The reduction in plant density in these regions can cause a decremental yield over the years and, consequently, decreasing the economic returns. In addition, a reduced vegetation density can affect soil quality, especially chemical, physical and biological soil indicators, due to the lack of soil cover (Cherubin et al., 2021).

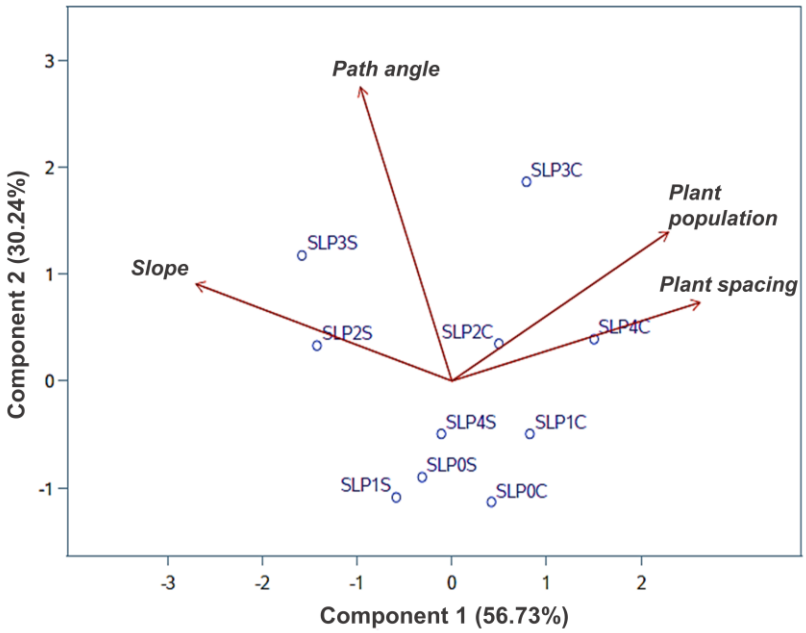

Figure 29. Principal component scores for the ten groups analyzed. Slope <2% (SLP0), 2-3% (SLP1), 3-5% (SLP2), 5-8% (SLP3), and >8% (SLP4). C – Curved path. S – Straight path.

Through the cluster analysis, it was possible to rank the data according to the susceptibility of occurrence of plant reduction over the years (Fig. 30). Group 1 and Group 2 that contain regions with curved paths were classified as regions with a higher probability of occurrence of plant reduction, while the other groups with straight paths as regions with lower probability of plant reduction occurring. Groups with straight percussion were ranked with low susceptibility to plant reduction. The map presented in Figure 31 shows the location of the groups generated through cluster analysis. Group 1 was ranked as highly susceptible to plant reduction and Group 5 as lowly susceptible to plant reduction over the two years of study. The early detection of the remaining plant count is important to evaluate the sprouting rate, to provide details of irregular sprouting of the ratoons, and to be used as a qualitative indicator of management and harvesting practices. Plant population density and uniformity associated with post-harvest ratoon sprouting are considered the main factors contributing to sugarcane yield (Matsuoka & Stolf, 2012). RGB image of the regions ranked with the highest susceptibility (Fig. 31) shows curved paths, with the presence of terraces, and with the edges of the sugarcane rows ending within the field. Terraces can accumulate rainwater, hindering the sprouting and development of the plant, besides making the soil more likely to be

compacted by the traffic of machinery. Regions with the edges of the rows ending within the field, called "dead rows", have a greater probability of plants being damage by machinery. In these regions, part of the harvester and field wagon maneuvering is done inside the field during harvest. This can cause damage from compaction and uprooting of plants during harvest. Sugarcane has heavy machinery traffic during agronomic management and mainly during harvesting, which can accumulate along the ratoons greater soil compaction and damage to plants. Unlike regions with straight paths, that have a higher concentration of soil compaction in inter-row due to the controlled traffic of the machinery (Esteban et al., 2019).

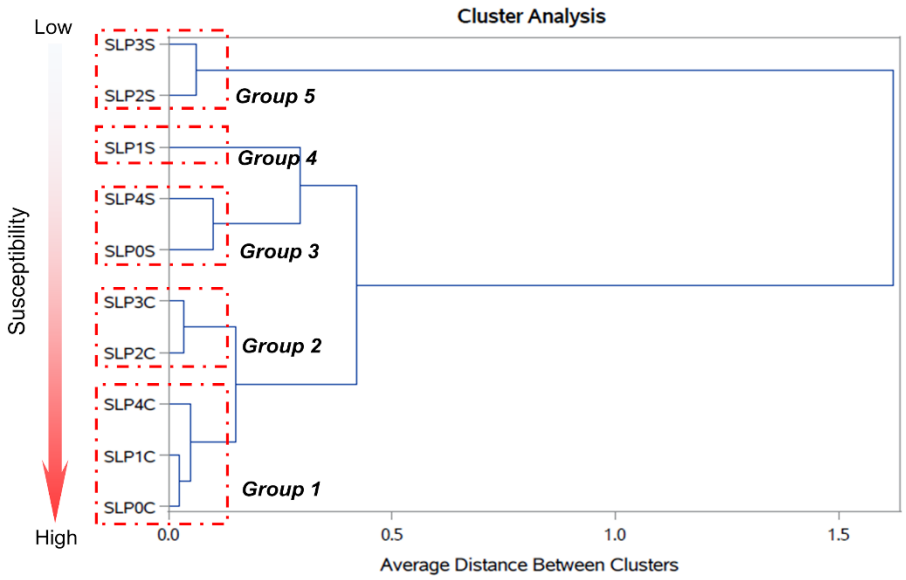

Figure 30. Cluster analysis with five groups (red box) that were ranked according to the susceptibility to plant reduction over the years. The red scale shows the susceptibility of each group, with Group 1 being most susceptible and Group 5 being least susceptible. Slope <2% (SLP0), 2-3% (SLP1), 3-5% (SLP2), 5-8% (SLP3), and >8% (SLP4). C – Curved path. S – Straight path.

The approach followed in this study demonstrates the usefulness of using parameters extracted from an RGB image in a real scenario. The maps of plant population and plant spacing together with information on slope and path type allowed a spatial and temporal evaluation of plant reduction in a crop that the longevity of the ratoon is important. This spatialized information is essential for the implementation and success of PA practices in sugarcane fields. Plant population maps can guide planning for more accurate site-specific applications of the inputs. Susceptibility maps may generate information such as areas where there may be less competition among sugarcane plants, which may increase the incidence of weeds in these areas (Girolamo-Neto et al., 2019), helping in the planning of spatialized control of weeds within sugarcane fields. In addition, the spatialization of regions with greater susceptibility to plant reduction can help in the planning of planting rows for the implementation of a new crop to minimize poor mechanization practices in these regions. The spatialization of the plant population can be valuable information to predict the yield of sugarcane. A recent study by (Neto et al., 2018) shows that the density of sugarcane plants can influence the final yield. From this, regions with a higher probability of income loss over the years can be identified. However, the authors show that in some fields with larger in-row plant spacing there is a greater tillering in relation to fields with higher plant density. Of course, studies using spatialized yield data correlating with the spatialization of the plant population should still be carried out.

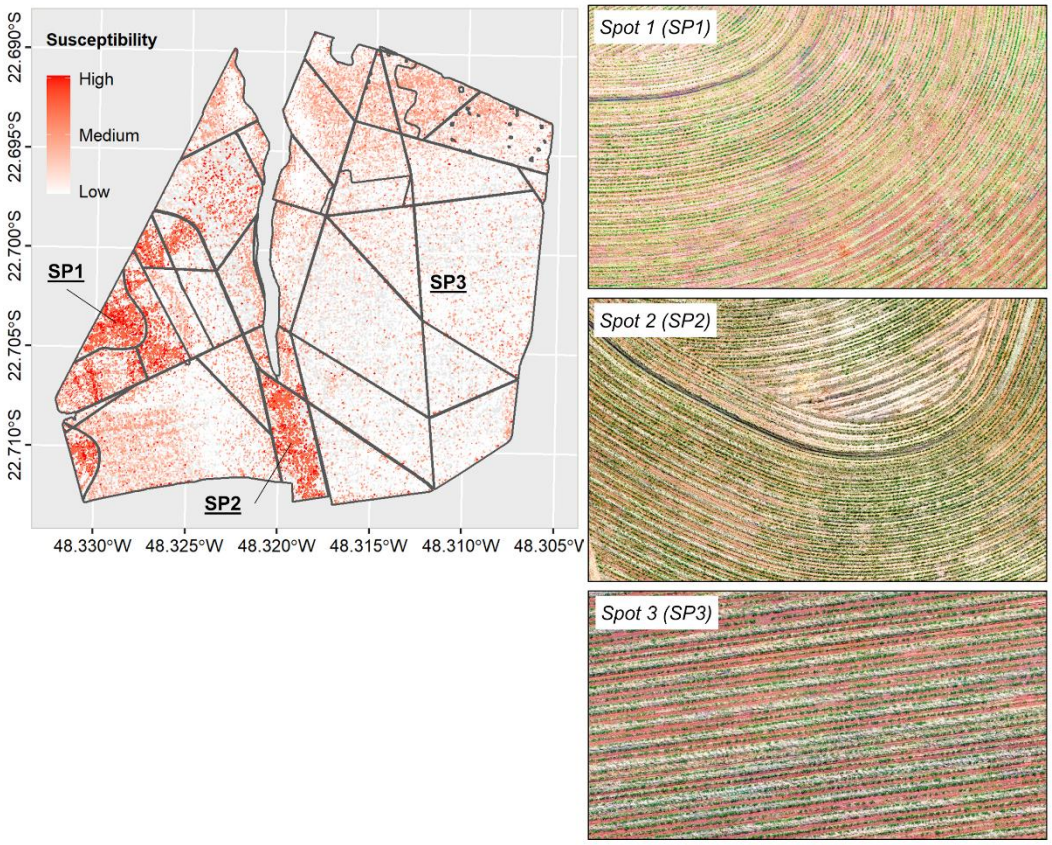

Figure 31. Map of the susceptibility rank of reduction of plants within the study fields.

4.4. Conclusion

In this study was possible to identify through field and crop parameters extracted from RGB images the probability of a lower plant population. The hypothesis that the slope and path type influence the plant population was confirmed. The local analysis identified that regions with steeper slope and curved paths have lower plant populations compared to other regions. The greater the terrain slope in the study fields, the greater the probability of reduction of the plant population over the years. In addition, it was possible to characterize through georeferenced RGB images the spatial and temporal distribution of the plant population and plant spacing within the field of study. The regions within the field most likely to occur plant reduction over the years were mapped through multivariate and cluster analysis. This type of information can be utilized as a subsidy for decision makings like the maintenance of the crop, identification of the places where they should be replanted, and the provision for the renovation of sugarcane fields. High-resolution RGB images are increasingly being used by the sugarcane industry, and extracting useful information for the site-specific management of sugarcane fields is essential to enable the use of this approach.

4.1. Connection text to chapter 5

Monitoring the factors that influence yield has become increasingly essential for decision-making. Defining the best row spacing and plant spacing to obtain higher yields throughout the harvests is complex. However, it is necessary to verify the extent to which the increase in plant spacing influences the loss of yield in regions with different productive potentials within the same field. In this sense, Chapter 5 addresses the relationship

between sugarcane yield and plant spacing in regions with different yield potentials in commercial fields. Chapter 5 is written in the format of a scientific article to be submitted to a peer-reviewed journal.

Maldaner, L.F., Molin, J.P. (2021) Mapping sugarcane spatial patterns using spatial and temporal analysis of features extracted from UAV images.

4.2. Appendix A.

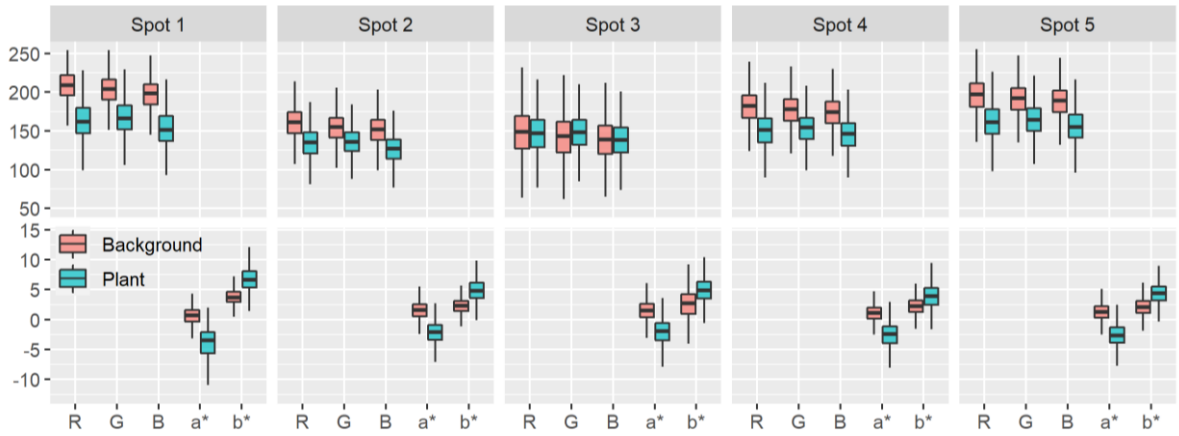

Figure 32. Visualization of RGB, a*, and b* values between the background and plant classes at five different spots within the field of study.

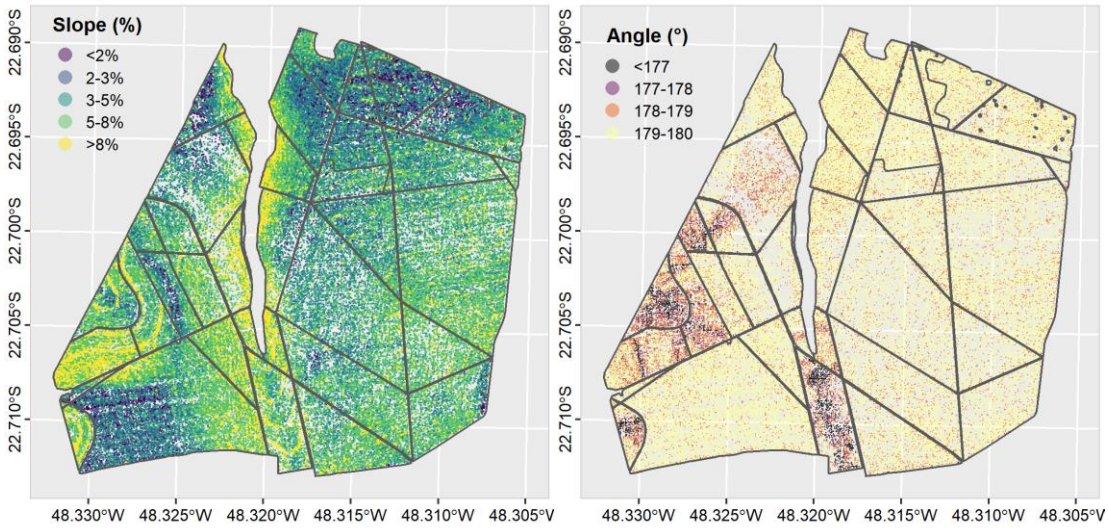

Figure 33. Spatial variability of the slope (%) (left) and path angle (°) (right) in the study fields, generated from RGB images from a camera onboard an unmanned aerial vehicle (UAV).

Reference

Arthur, D., & Vassilvitskii, S. (2006). k-means++: The Advantages of Careful Seeding. In *Proceedings of the eighteenth annual ACM-SIAM symposium on Discrete algorithms* (pp. 1–11). Society for Industrial and Applied Mathematics.

Bell, M. J., & Garside, A. L. (2005). Shoot and stalk dynamics and the yield of sugarcane crops in tropical and subtropical Queensland, Australia. In *Field Crops Research* (Vol. 92). https://doi.org/10.1016/j.fcr.2005.01.032

Bezuidenhout, C. N., O'Leary, G. J., Singels, A., & Bajic, V. B. (2003). A process-based model to simulate changes in tiller density and light interception of sugarcane crops. *Agricultural Systems*, *76*(2), 589–599. https://doi.org/10.1016/S0308-521X(02)00076-8

Cambardella, C. A., Moorman, T. B., Novak, J. M., Parkin, T. B., Karlen, D. L., Turco, R. F., & Konopka, A. E. (1994). Field-Scale Variability of Soil Properties in Central Iowa Soils. *Soil Science Society of America Journal*, *58*(5), 1501–1511. https://doi.org/10.2136/sssaj1994.03615995005800050033x

Chen, R., Chu, T., Landivar, J. A., Yang, C., & Maeda, M. M. (2018). Monitoring cotton (Gossypium hirsutum L.) germination using ultrahigh-resolution UAS images. *Precision Agriculture*, *19*(1), 161–177. https://doi.org/10.1007/s11119-017-9508-7

Cherubin, M. R., Bordonal, R. O., Castioni, G. A., Guimarães, E. M., Lisboa, I. P., Moraes, L. A. A., … Carvalho, J. L. N. (2021). Soil health response to sugarcane straw removal in Brazil. *Industrial Crops and Products*, *163*, 113315. https://doi.org/10.1016/j.indcrop.2021.113315

Cherubin, M. R., Franchi, M. R. A., Lima, R. P. de, Moraes, M. T. de, & Luz, F. B. da. (2021). Sugarcane straw effects on soil compaction susceptibility. *Soil and Tillage Research*, *212*(5), 105066. https://doi.org/10.1016/j.still.2021.105066

Colaço, A. F., Molin, J. P., Rosell-Polo, J. R., & Escolà, A. (2019). Spatial variability in commercial orange groves. Part 2: relating canopy geometry to soil attributes and historical yield. *Precision Agriculture*, *20*(4), 805–822. https://doi.org/10.1007/s11119-018-9615-0

Esteban, D. A. A., de Souza, Z. M., Tormena, C. A., Lovera, L. H., de Souza Lima, E., de Oliveira, I. N., & de Paula Ribeiro, N. (2019). Soil compaction, root system and productivity of sugarcane under different row spacing and controlled traffic at harvest. *Soil and Tillage Research*, *187*, 60–71. https://doi.org/10.1016/j.still.2018.11.015

Gillies, S., Ward, B., & Petersen, A. S. (2013). Rasterio: Geospatial Raster I/O for {Python} Programmers. MapBox.

Girolamo-Neto, C. Di, Sanches, I. D., Neves, A. K., Prudente, V. H. R., Körting, T. S., Picoli, M. C. A., … De Aragão, C. (2019). Assessment of Texture Features for Bermudagrass (Cynodon dactylon) Detection in Sugarcane Plantations. *Drones*, *3*(2), 36. https://doi.org/10.3390/drones3020036

Gnädinger, F., & Schmidhalter, U. (2017). Digital counts of maize plants by Unmanned Aerial Vehicles (UAVs). *Remote Sensing*, *9*(6), 544. https://doi.org/10.3390/rs9060544

Horn, B. K. P. (1981). Hill Shading and the Reflectance Map. *Proceedings of the IEEE*, *69*(1), 14–47. https://doi.org/10.1109/PROC.1981.11918

ISPA, I. S. of P. A. (2019). ISPA Precision Ag definition. Retrieved June 16, 2021, from https://www.ispag.org/about/definition

Jordahl, K., Bossche, J. Van den, Fleischmann, M., Wasserman, J., McBride, J., & Gerard, J. (2020). geopandas/geopandas: v0.8.1. https://doi.org/10.5281/zenodo.3946761

Kapur, R., Duttamajumder, S. K., & Krishna Rao, K. (2011). A breeder's perspective on the tiller dynamics in sugarcane. *Current Science*, *100*(2), 183–189.

Kedzierski, M., Wierzbicki, D., Sekrecka, A., Fryskowska, A., Walczykowski, P., & Siewert, J. (2019). Influence of lower atmosphere on the radiometric quality of unmanned aerial vehicle imagery. *Remote Sensing*, *11*(10). https://doi.org/10.3390/rs11101214

Laclau, P. B., & Laclau, J. P. (2009). Growth of the whole root system for a plant crop of sugarcane under rainfed and irrigated environments in Brazil. *Field Crops Research*, *114*(3), 351–360. https://doi.org/10.1016/j.fcr.2009.09.004

Li, B., Xu, X., Han, J., Zhang, L., Bian, C., Jin, L., & Liu, J. (2019). The estimation of crop emergence in potatoes by UAV RGB imagery. *Plant Methods*, *15*(1), 1–13. https://doi.org/10.1186/s13007-019-0399-7

Lisboa, I. P., Cherubin, M. R., De Lima, R. P., Gmach, M. R., Wienhold, B. J., Schmer, M. R., … Cerri, C. E. P. (2019). Sugarcane straw blanket management effects on plant growth, development, and yield in Southeastern Brazil. *Crop Science*, *59*(4), 1732–1744. https://doi.org/10.2135/cropsci2018.07.0468

Luna, I., & Lobo, A. (2016). Mapping crop planting quality in sugarcane from UAV imagery: A pilot study in Nicaragua. *Remote Sensing*, *8*(6), 1–18. https://doi.org/10.3390/rs8060500

MacQueen, J. (1967). Some methods for classification and analysis of multivariate observations. In *Proceedings of the fifth Berkeley Symposium on Mathematical Statistics and Probability* (Vol. 1, pp. 281–296).

Maldaner, L. F., Molin, J. P., Martello, M., Tavares, T. R., & Dias, F. L. F. (2021). Identification and measurement of gaps within sugarcane rows for site-specific management: Comparing different sensor-based approaches. *Biosystems Engineering*, *209*, 64–73. https://doi.org/10.1016/J.BIOSYSTEMSENG.2021.06.016

Matsuoka, S., & Stolf, R. (2012). Sugarcane tillering and ratooning: key factors for a profitable cropping. In J. F. Goncalves & K. D. Correia (Eds.), *Sugarcane: Production, Cultivation and Uses*. Nova Science Publishers.

Molin, J. P., & Veiga, J. P. S. (2016). Spatial variability of sugarcane row gaps: measurement and mapping. *Ciencia e Agrotecnologia*, *40*(3), 347–355. https://doi.org/10.1590/1413-70542016403046915

Natarajan, S., Basnayake, J., Wei, X., & Lakshmanan, P. (2019). High-throughput phenotyping of indirect traits for early-stage selection in sugarcane breeding. *Remote Sensing*, *11*(24). https://doi.org/10.3390/rs11242952

Neto, J. R., de Souza, Z. M., Kölln, O. T., Carvalho, J. L. N., Ferreira, D. A., Castioni, G. A. F., … Franco, H. C. J. (2018). The Arrangement and Spacing of Sugarcane Planting Influence Root Distribution and Crop Yield. *BioEnergy Research*, *11*(2), 291–304. https://doi.org/10.1007/s12155-018-9896-1

Passalaqua, B. P., & Molin, J. P. (2020). Path errors in sugarcane transshipment trailers. *Engenharia Agricola*, *40*(2), 223–231. https://doi.org/10.1590/1809-4430-ENG.AGRIC.V40N2P223-231/2020

Paula, V. R. de, & Molin, J. P. (2013). Assessing Damage Caused by Accidental Vehicle Traffic on Sugarcane Ratoon. *Applied Engineering in Agriculture*, *29*(2), 161–169. https://doi.org/10.13031/2013.42642

Pedregosa, F., Weiss, R., Brucher, M., Varoquaux, G., Gramfort, A., Michel, V., … Duchesnay, É. (2011). Scikit-learn: Machine Learning in Python. *Journal of Machine Learning Research*, *12*, 2825–2830.

Sanches, G. M., Duft, D. G., Kölln, O. T., Luciano, A. C. dos S., De Castro, S. G. Q., Okuno, F. M., & Franco, H. C. J. (2018). The potential for RGB images obtained using unmanned aerial vehicle to assess and predict yield in sugarcane fields. *International Journal of Remote Sensing*, *39*(15–16), 5402–5414. https://doi.org/10.1080/01431161.2018.1448484

Sandhu, H. S., Singh, M. P., Gilbert, R. A., Subiros-Ruiz, F., Rice, R. W., & Shine, J. M. (2017). Harvest management effects on sugarcane growth, yield and nutrient cycling in Florida and Costa Rica. *Field Crops Research*, *214*, 253–260. https://doi.org/10.1016/j.fcr.2017.09.002

Santos, H. G. dos, Jacomine, P. K. T., Anjos, L. H. C. dos, Oliveira, V. A. De, Lumbreras, J. F., Coelho, M. R., … Cunha, T. J. F. (2018). *Sistema brasileiro de classificação de solos. Embrapa Solos* (5th ed.).

Shendryk, Y., Sofonia, J., Garrard, R., Rist, Y., Skocaj, D., & Thorburn, P. (2020). Fine-scale prediction of biomass and leaf nitrogen content in sugarcane using UAV LiDAR and multispectral imaging. *International Journal of Applied Earth Observation and Geoinformation*, *92*(April), 102177. https://doi.org/10.1016/j.jag.2020.102177

Shirzadifar, A., Maharlooei, M., Bajwa, S. G., Oduor, P. G., & Nowatzki, J. F. (2020). Mapping crop stand count and planting uniformity using high resolution imagery in a maize crop. *Biosystems Engineering*, *200*, 377–390. https://doi.org/10.1016/j.biosystemseng.2020.10.013

Singels, A., & Smit, M. A. (2009). Sugarcane response to row spacing-induced competition for light. *Field Crops Research*, *113*(2). https://doi.org/10.1016/j.fcr.2009.04.015

Sofonia, J., Shendryk, Y., Phinn, S., Roelfsema, C., Kendoul, F., & Skocaj, D. (2019). Monitoring sugarcane growth response to varying nitrogen application rates: A comparison of UAV SLAM LiDAR and photogrammetry. *International Journal of Applied Earth Observation and Geoinformation*, *82*(May), 101878. https://doi.org/10.1016/j.jag.2019.05.011

Sokolova, M., & Lapalme, G. (2009). A systematic analysis of performance measures for classification tasks. *Information Processing and Management*, *45*(4), 427–437. https://doi.org/10.1016/j.ipm.2009.03.002

Song, X. P., Liang, Y. J., Zhang, X. Q., Qin, Z. Q., Wei, J. J., Li, Y. R., & Wu, J. M. (2020). Intrusion of Fall Armyworm (Spodoptera frugiperda) in Sugarcane and Its Control by Drone in China. *Sugar Tech*, *22*(4), 734–737. https://doi.org/10.1007/s12355-020-00799-x

Souza, C. H. W. de, Lamparelli, R. A. C., Rocha, J. V., & Magalhães, P. S. G. (2017). Mapping skips in sugarcane fields using object-based analysis of unmanned aerial vehicle (UAV) images. *Computers and Electronics in Agriculture*, *143*, 49–56. https://doi.org/10.1016/j.compag.2017.10.006

Souza, G. S. de, Souza, Z. M. de, Cooper, M., & Tormena, C. A. (2015). Controlled traffic and soil physical quality of an oxisol under sugarcane cultivation. *Scientia Agricola*, *72*(3), 270–277. https://doi.org/10.1590/0103-9016-2014-0078

Spekken, M., & Molin, J. P. (2018). Uav images as a source for retrieval of machine tracks and vegetation gaps along crop rows. In *Internactional Conference on precision agriculture* (pp. 1–10). Montreal, Quebec, Canada.

Sumesh, K. C., Ninsawat, S., & Som-ard, J. (2021). Integration of RGB-based vegetation index, crop surface model and object-based image analysis approach for sugarcane yield estimation using unmanned aerial vehicle. *Computers and Electronics in Agriculture*, *180*(July 2020), 105903. https://doi.org/10.1016/j.compag.2020.105903

Van Dillewijn, C. (1952). *Botany of Sugarcane. Botany of sugarcane*. Waltham: Chronica Botanica.

Zhang, P., Zhang, W., Sun, H. T., He, F. G., Fu, H. B., Qi, L. Q., … Liu, J. S. (2020). Effects of Spray Parameters on the Effective Spray Width of Single-Rotor Drone in Sugarcane Plant Protection. *Sugar Tech*. https://doi.org/10.1007/s12355-020-00890-3

5. SPATIAL-TEMPORAL ANALYSIS TO INVESTIGATE THE INFLUENCE OF IN-ROW PLANT SPACING ON THE SUGARCANE YIELD

Abstract

Understanding the relationship between plant spacing and sugarcane yield is key to site-specific management of the fields. The objective of this study was to analyze the relationship between sugarcane yield and plant spacing in regions with different yield potentials in commercial fields. Specifically, to verify whether there is a difference between plant spacing in areas with different productive potential and to verify if there is a difference in yield reduction in areas with different productive potential. The analyses were performed over two consecutive years to verify the temporal patterns of plant spacing and yield data in each sugarcane row within the field. The yields from three years (2018 to 2020) were used to perform a spatial-temporal analysis of the yield over the years. The yield of two study field was performed by classifying each part of the field into four homogeneous classes. The plant spacing was calculated and mapped using RGB mosaics with 0.03 m spatial resolution generated from images from a camera onboard an unmanned aerial vehicle (UAV). The yield over the years was classified as high, low, stable, and unstable, and the spacing between plants between these regions varies and can influence the final yield. By performing the regression analysis, it was possible to verify that the yield reduction within the sugarcane rows occurs with the increase in in-row plant spacing. High, stable, and unstable yield sites have the same pattern of yield reduction with increasing plant spacing. Furthermore, spacing in regions with high and stable yields did not result in yields with zero values. Unlike other regions that had no yield on some scales. Low and unstable yield sites had larger angular coefficients in the fitted regression, i.e., the increase in plant spacing has a steeper decrease in yield when compared to high yield sites. Low-yielding regions require a larger plant population and are more susceptible to lose in yield within the row with increasing plant spacing. However, there is a need to conduct studies with other sugarcane cultivars, moreover, with different planting spacing.

Keywords: Precision agriculture; Yield variability; Plant variability

5.1. Introduction

In sugarcane, plant spacing is one of the factors that must be monitored, because maintaining the plant population throughout the harvests is fundamental to the economic and environmental success of the plantation. Although it is conducted as a semi-perennial, sugarcane is a perennial crop, and the inter-row spacing is fixed and follows the gauge of the machinery to avoid damage to the plants by heavy machinery traffic (Paula and Molin, 2013). Thus, the plant population in sugarcane fields depends on the number of plants and the density of tillers per plant within each row. Plant density have a key role in maximizing sugarcane yield and improving its quality in sugarcane fields (Ehsanullah et al., 2011; Rossi Neto et al., 2017).

Monitoring the sugarcane plant population is very important because maintaining the same number of plants throughout the harvest is essential for the longevity of the sugarcane plantations (Matsuoka and Stolf, 2012). Plant population mapping brings detailed information that can help in decision-making for replanting regions with low plant counts or applying agricultural inputs appropriately in defective regions (Shirzadifar et al., 2020). Similarly, sugarcane plant mapping allows the optimization of inputs, reduces costs, and minimizes environmental impacts. In addition, detecting and measuring plant spacing in crop fields or differences in development can allow adjustments in tillage, irrigation, and even replanting (Gasparotto et al., 2020).

Monitoring the factors that influence yield has become increasingly essential for decision-making. Defining the best row spacing and plant spacing to obtain higher yields throughout the harvests is complex, and according to (Gasparotto et al., 2020) the difficulty of conducting experiments is one of the main factors. To this, we can add the difficulty to of spatially investigating the relationship between plant spacing and yield due to the low adoption of specialized yield data. Analysis within the sugarcane row requires the collection of yield data with high spatial resolution. That is, the amount of data at small distances within the row, and yield variability can be influenced by the frequency of data collection by the yield monitor. A low data frequency leads to a smoothing of yield variability on a small scale (Maldaner and Molin, 2020).

The plant population considered ideal is the one that allows the highest sugarcane yield per area and sugar per amount of stalk produced. A study from 1986, and used as a reference by the sugarcane industry until today, shows that yield loss occurs with plant spacing above 0.5 m (Stolf, 1986). A recent study conducted on two fields with clayey and sandy soil showed that the final yield of sugarcane varies according to plant spacing in different soil types (Neto et al., 2018). The hypothesis is that plant spacing can vary in different regions within the same field without yield loss. In other words, to reach the productive and economic potential of each region within the field the ideal plant spacing can vary. Studies have shown that plant populations tend to decrease along ratoons and consequently there is an increase in plant spacing within sugarcane rows (Maldaner et al., 2021; Matsuoka and Stolf, 2012).

However, it is necessary to verify the extent to which the increase in plant spacing influences the loss of yield in regions with different productive potentials within the same field. In this sense, the objective of this study was to analyze the relationship between sugarcane yield and plant spacing in regions with different yield potentials in commercial fields. Specifically, (i) to verify whether there is a difference between plant spacing in areas with different productive potential; (ii) to verify if there is a difference in yield reduction in areas with different productive potential; and (iii) to measure the loss in yield as a function of increasing plant spacing. The analyses were performed over two consecutive years to verify the temporal patterns of plant spacing and yield data in each sugarcane row within the field.

5.2. Material and Methods

5.2.1. Study area

The study was conducted in two commercial fields of 20.9 and 10.4 ha in the municipality of São Manuel, São Paulo, Brazil (22°42'01" S, 48°16´50" W, and 483 m of altitude) (Fig 34). The climate in the study region is mesothermal, Cwa - humid subtropical, which includes drought in the winter (from June to September) and rain from November to April. The average annual rainfall in the municipality is 1433 mm and the annual average temperature is 23ºC. The predominant soil class is the Argisol with a sandy texture (Santos et al., 2018). The variety SP83-2847 was mechanically planted in 2014, with 1.5 m row spacing. The harvest in three years of study (Fig 35) consisted of single row harvesters in the late season (wet time of the year – October and November). Plant spacing was collected in two successive sugarcane growing seasons (2019 and 2020). Considering the previous study (Maldaner et al., 2021c), plant spacing was measured when sugarcane was at the initial tillering stage, approx. 0.30 m canopy height.

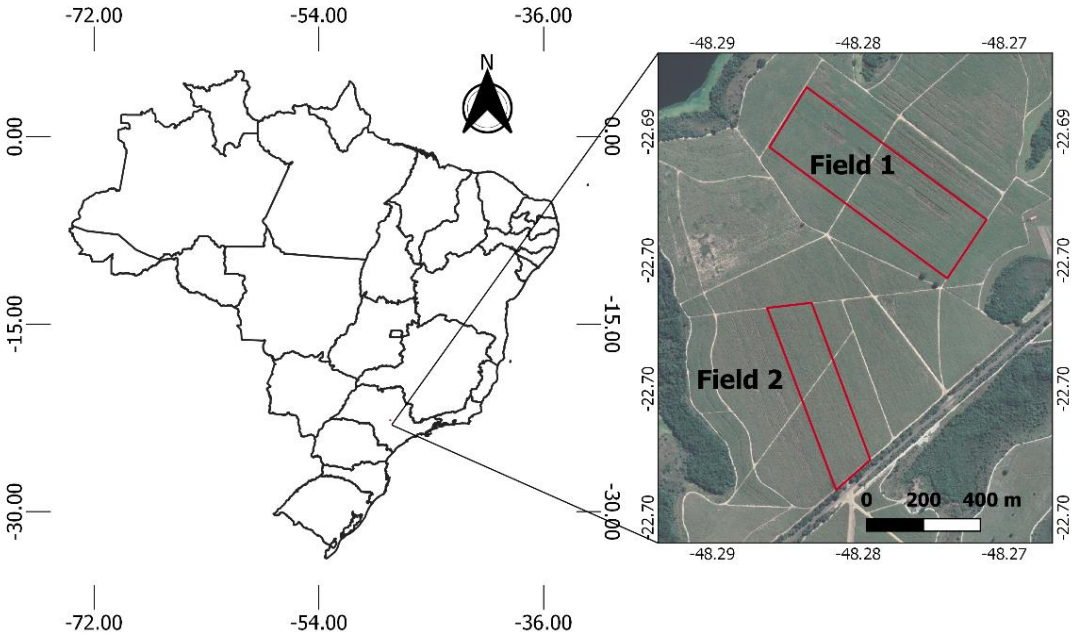

Figure 34. Location map of study fields.

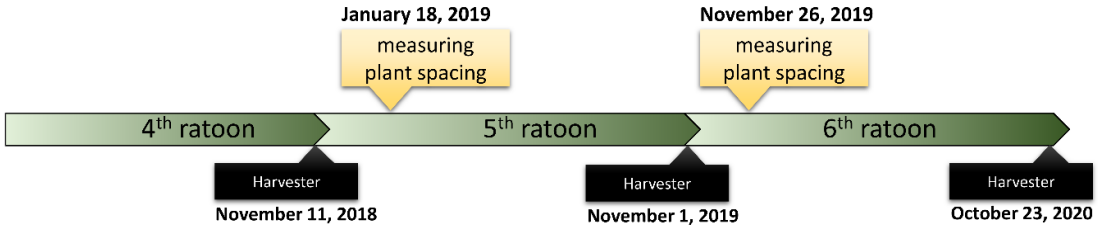

Figure 35. Timeline of data collection.

5.2.2. Yield data collection and processing

The approach to mapping yield is a commercial sensor system (Solinftec, Araçatuba, São Paulo, Brazil) based on the total weight of sugarcane harvested in the studied areas spatially distributed in the field, considering the variations in hydraulic pressure of the chopper system of each harvester. A detailed description of the mapping system and validation of the prediction methodology were carried out in a previous study (Maldaner et al., 2021a). Harvesting is carried out by cutting and processing a single row at a time at an average speed of 1.6 m s^{-1}. Each harvester is equipped with a high-precision global navigation satellite system and is capable of georeferencing yield data every five seconds (0.2 Hz) within each line. Thus, it was possible to generate high-resolution data for each sugarcane over the three years of the study. Each yield data set was subjected to sequential data screening to detect and remove points with erroneous values according to the methodology described by Maldaner & Molin (2020).

The data for each field over all the years were standardized on an in-row grid of 0.5 m (Fig. 36B) that used a 1.0 m search radius (Fig. 36C), to ensure that each point in the grid had at least one yield data and to span the voids left by the removal of erroneous data. Radius above 1.0 m can lead to unexpected intersection of the yield values of neighboring rows. The yield of each point on the grid was the average of multiple yield data within the

search radius. If no yield data were found within the search radius, the average yield of the nearest neighbors within the same sugarcane row was used to estimate the yield (Fig. 36D).

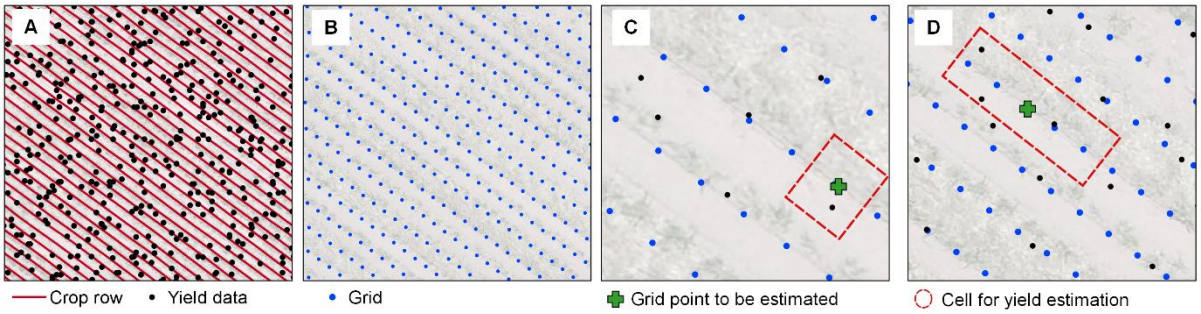

Figure 36. The step to sugarcane yield map using yield data provided by yield monitor (A). In row grid with 0.5 m resolution (B). Search radius (1.0 m) for yield data to estimate at each grid point (C). In-row search radius for yield data to estimate at each grid point when not yield data was found in previous step C (D).

During the analysis, it was noted that there was a large difference between yields from year to year, probably due to overall weather conditions in each year. For this reason, to perform the analyses in this study, the yield of each year was standardized between 0 and 1 according to equation 11.

$$xn_i = \frac{x_i - \min(x)}{\max(x) - \min(x)} \tag{11}$$

where xn_i is the yield standardized and x_i is the yield at each i point in the grid.

5.2.3. Temporal stability

Temporal patterns in the two study fields were calculated following the methodology described by (Blackmore et al., 2003). The spatial and temporal patterning of yield for each field was performed by classifying each part of the field into four homogeneous classes:

A. High yielding area — above the grand mean (for all years) for the field;

B. Low yielding area — below the grand mean (for all years) for the field;

C. Stable area — low inter-year spatial variance (<25%) and

D. Unstable area — high inter-year spatial variance (≥ 25%).

The inter-year spatial variance was calculated by quantifying the variance relative to the mean (point yield minus the field mean) over time (Whelan and McBratney, 2000):

$$\sigma_i^2 = \frac{\sum_{t=2018}^{t=2020} \left(xn_{t,i} - \overline{xn}_t\right)^2}{3} \tag{12}$$

where σ_i^2 is the temporal variance at grid point i, t is the time in years between 2018 and 2020, $xn_{t,i}$ is the yield in years t at point i, and $\overline{xn}_t$ is the mean of the yield for the whole field in years t.

5.2.4. Plant spacing

To calculate and map the plant spacing we used RGB mosaics with 0.03 m spatial resolution generated from images from a camera onboard an unmanned aerial vehicle (UAV). The detail of the RGB mosaic processing is described in Chapter 4. The identification of sugarcane plants in the RGB mosaic consisted of six stages: (i) split the mosaic into tiles; (ii) split each tile into n windows; (iii) convert RGB to L*a*b* color space; (iv) unsupervised classification; (v) identification of the plant class; (vi) and mask layer filtering. The result of this processing is a binary image with two classes: plan and background. Software InfoRow 2.0 (SOMO, Piracicaba, Brazil), commonly used by farmers, was used to extract the sugarcane row from the RGB mosaic. The shapefile with the sugarcane rows (lines) was cropped with the mask classified as a background using the *geopandas* library (Jordahl et al., 2020) with an intersection function (Fig. 37). Then, the length of each segment was calculated, and this length was considered the distance between ratoons within each row of sugarcane.

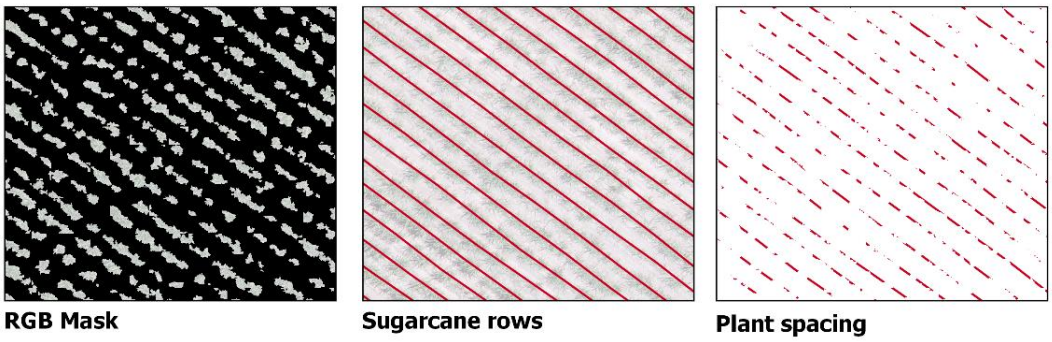

Figure 37. The step to crop sugarcane row with the RGB mask resulted from image segmentation.

5.2.5. Yield losses

Yield loss with increasing plant spacing was calculated using the ratio of yield at spacing without plants (Y_{gap}) to yield at places with plants (Y_{plant}). Y_{plant} is the average of the nearest neighbors to Y_{gap} within the same sugarcane row. In this case, the neighbors within 1.0 m of distance were considered (Fig. 38). In this way, it was possible to calculate the relationship between yields for each spacing *i* found within each sugarcane row.

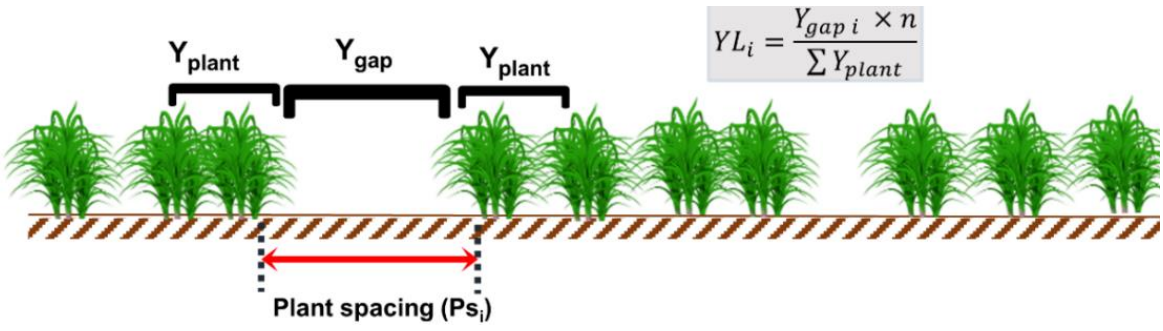

Figure 38. Identification of yield in places with (Y_{plant}) and without plants (Y_{gap}) to calculate losses (YL_i) at each plant spacing *i*.

5.2.6. Analyses

Descriptive statistics and geostatistics followed by a visual assessment of the yield maps were made to identify patterns in the spatial variability. The spatial dependence index was calculated as the relation of the nugget variance, and the sill variance and was interpreted as strong (<0.25), moderate (between 0.25 and 0.75), or weak

(>0.75) (Cambardella et al., 1994). The comparison between the four yield classes was assessed using an analysis of variance (ANOVA) and, when significant differences were found, the average values were compared by the Tukey at 5% probability test. The plant spacing of the two years (2019 and 2020) was analyzed with the respective yields collected posterior. Regression analysis was used to describe the causal effect of plant spacing on yield for every year of study. The models were chosen based on the significance of the regression coefficients using the t-test at a 5% probability level and the coefficient of determination (R^2).

5.3. Results and Discussion

Sugarcane yield shows anisotropic behavior, that is, when its variability is not the same in all directions, or when the pattern of spatial variability changes direction (Fig. 39). In both study fields, yield variability has greater continuity along the direction of the sugarcane rows. A recent study shows that nugget effect values with within-row data are much lower than for considered inter-row yields (Maldaner and Molin, 2020). In other words, sugarcane has high yield variation between rows, which may be correlated with the presence different plant spacing, vegetative vigor, tiller density, among others.

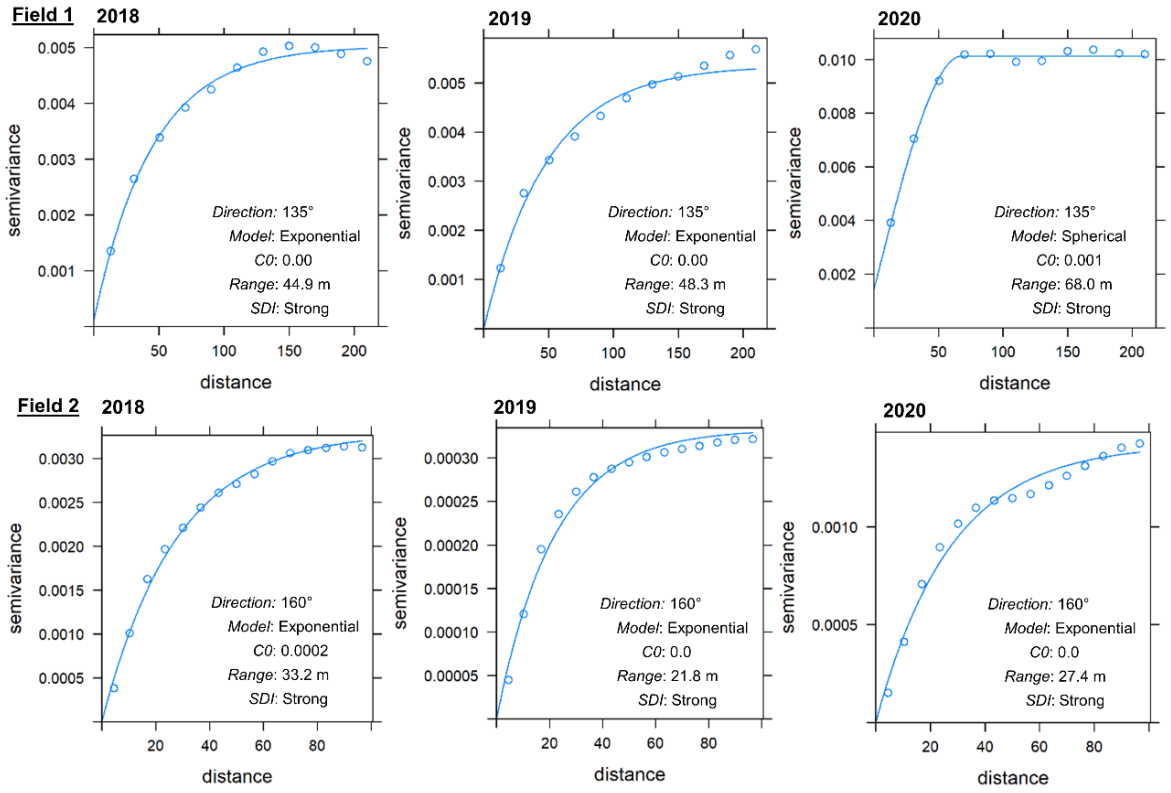

Figure 39. Geostatistic analysis of sugarcane yields each year for the two fields of study.

The variability of sugarcane yield in Field 1 has a strong degree of spatial dependence with a range of 44.9 m in the direction of the sugarcane rows in 2018. The range of spatial variability of yield increased over the years in Field 1. This range increase may be the first evidence that sugarcane yield is correlated with in-row plant spacing and that it increases over the years. The sugarcane yield in Field 2 had strong spatial dependence towards the sugarcane rows. The range is smaller compared to Field 1, and the range of variability in 2018 (33.2 m) was larger than the

other years. Each year, individual yield maps often show significant spatial variability but they appear to cancel out each other over time (Fig. 40). The pattern in high and low yield regions is evident in the maps.

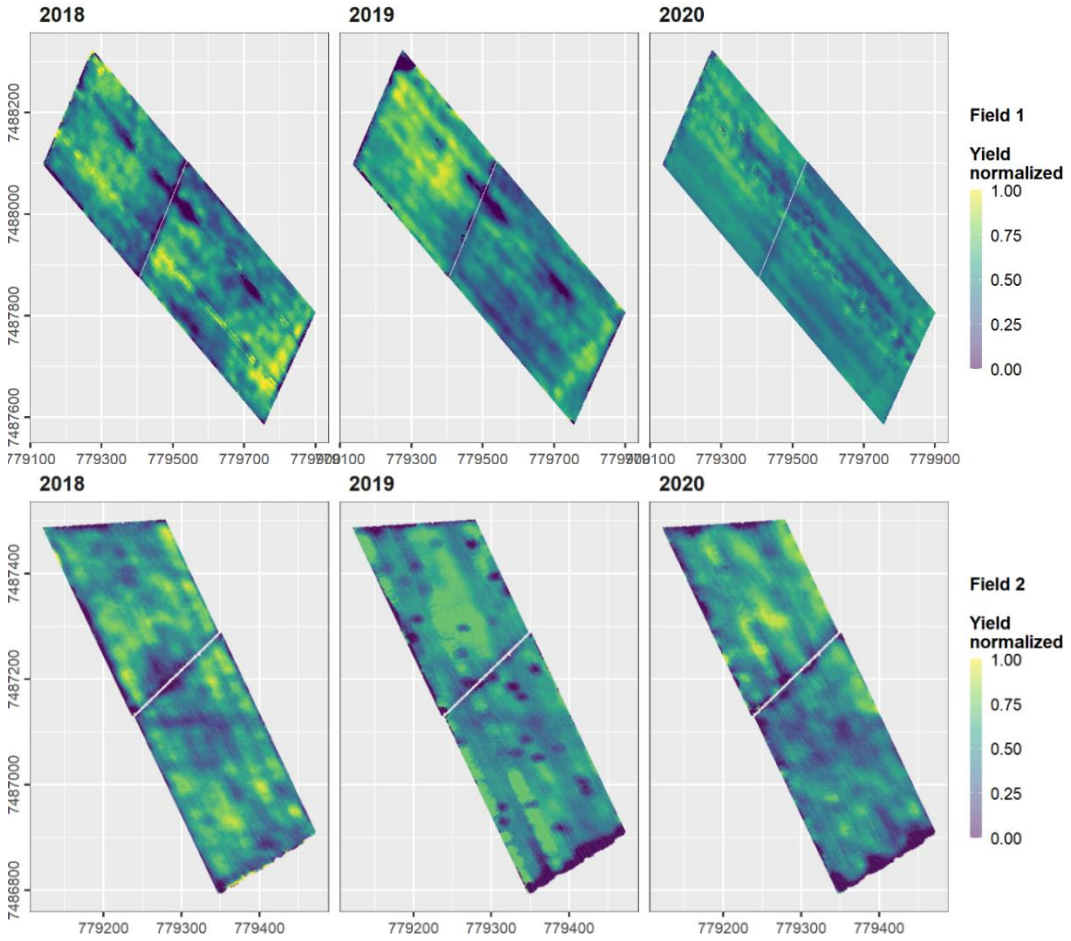

Figure 40. Sugarcane yield over the three years of study in the two fields.

The temporal variability showed strong structuring over the years in regions with low yield in Field 1 and Field 2 (Fig. 41). In Field 2, the predominant class was high and unstable yield over the years. In both study fields, there were few regions with low and unstable yields over the years. Low temporal variability and low yield may be correlated with plant spacing in years before the studies. High temporal variability in regions of high yield may be correlated with the reduction of plants over the years and consequent increase in plant spacing. The different yield classes and temporal variability allows the establishment of a specific treatment pattern for each of them, making the interventions demand a personalized individual management, for example, greater investments in units with greater productive potential, providing savings in inputs, and preserving the environment (Molin et al., 2015). Strategies to save inputs can be used in classes with low yield potential and strategies to intensify the use of these same inputs aiming to increase the sugarcane yield response.

There is a difference in plant spacing between low and high-yielding regions (Fig. 42). High-yielding is regions that have plant spacing smaller than 0.8 m, i.e. shorter spacing between plants than low-yielding regions in both years of study. Low and stable yield spots have greater spacing between plants, with average values close to and above 1.0 m. That is regions with low plant populations present low yield over the years of study. In the study conducted by (Neto et al., 2018), results show that the reduction in plant spacing promotes greater yield gains over the years. Moreover, the authors also show that yields decrease compared to the first year of cultivation. In this

study, plant spacing increased in 2020 compared to 2019 in all yield classes, except in Field 1 where there was no significant difference between the average plant spacing in the low and unstable classes. The increase in plant spacing over the harvest years is already expected, as the plants are subject to damage due to machine traffic (Paula and Molin, 2013), pests, diseases, and weather factors (Luna and Lobo, 2016; Matsuoka and Stolf, 2012).

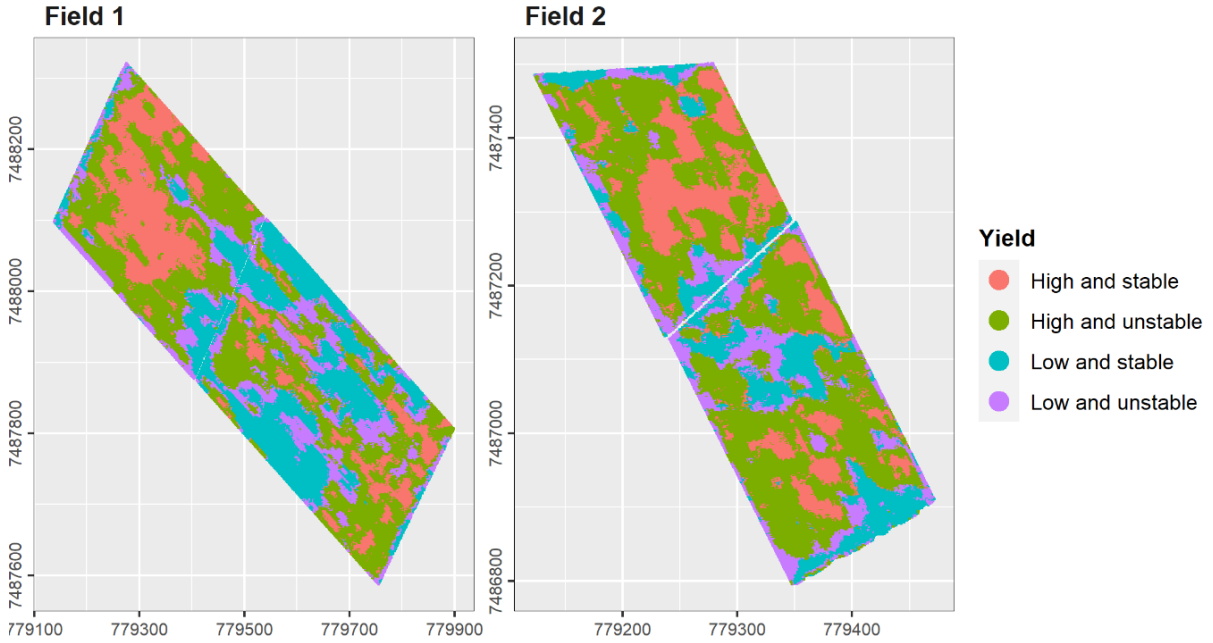

Figure 41. The spatial and temporal yield variability trend maps of the two study fields.

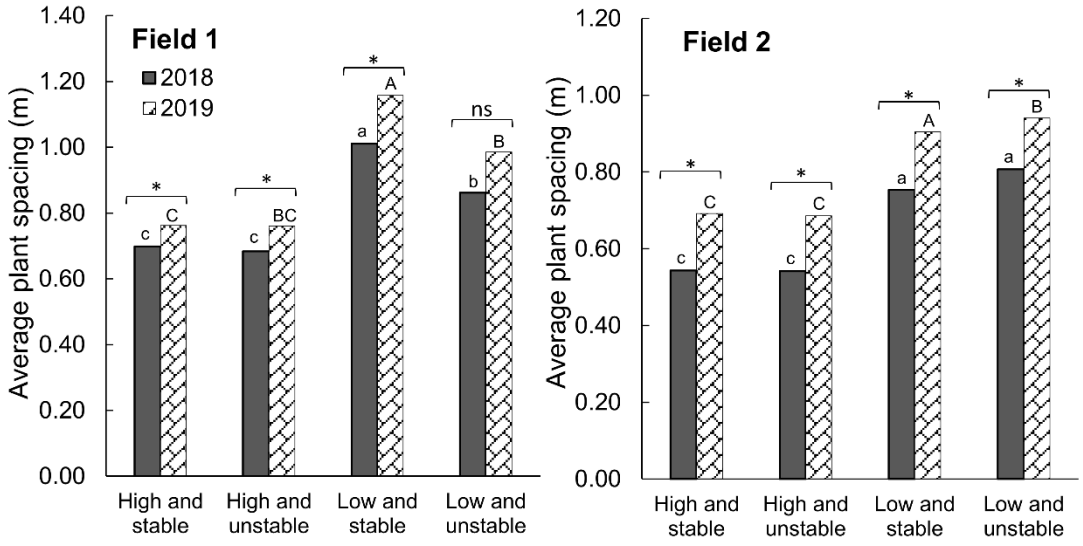

Figure 42. Plant spacing variation for each yield class in the two study fields. Different letters above the box indicate a significant difference between the groups in the same year (Tukey test; $p<0.05$). The symbol above the box indicates that there is a significant difference (*, $p\leq0.05$) in average plant spacing between the two years of studies for each yield class.

No significant difference ($p<0.05$) between the average yield on sites with (Y_{plant}) or without plants (Y_{gap}) in the high and stable yield class was observed within Field 1 in 2020 (Fig. 43). This means that the average plant spacing in this class did not influence the local yield reduction within the row. The same was found in low and unstable yield areas in 2019 and the low and stable yield areas in Field 2 in 2019. Although there is no significant

difference between the locations with and without plants, we cannot state that the average spacing within each class correlates with the yield of each class. Sugarcane is grass and its phenological characteristic is tillering in the early stages of sprouting (Van Dillewijn, 1952), which may vary in density within the field (Kapur, Duttamajumder, & Krishna Rao, 2011). Plants with larger numbers of tillers and greater vegetative vigor can close plant spacing, thus lowering the measured plant spacing and reducing yield loss in locations without plants. Y_{gap} differed among yield classes (see Fig. 43). In both fields and study years, sites with high and stable yields had Y_{gap} higher than the other classes. Moreover, in these regions, the minimum Y_{gap} did not reach zero. In other words, although there was a difference between the yield between locations with and without plants, spacing did not cause a total loss in the final yield. Unlike the other yield classes, some sites without plants had zero yields.

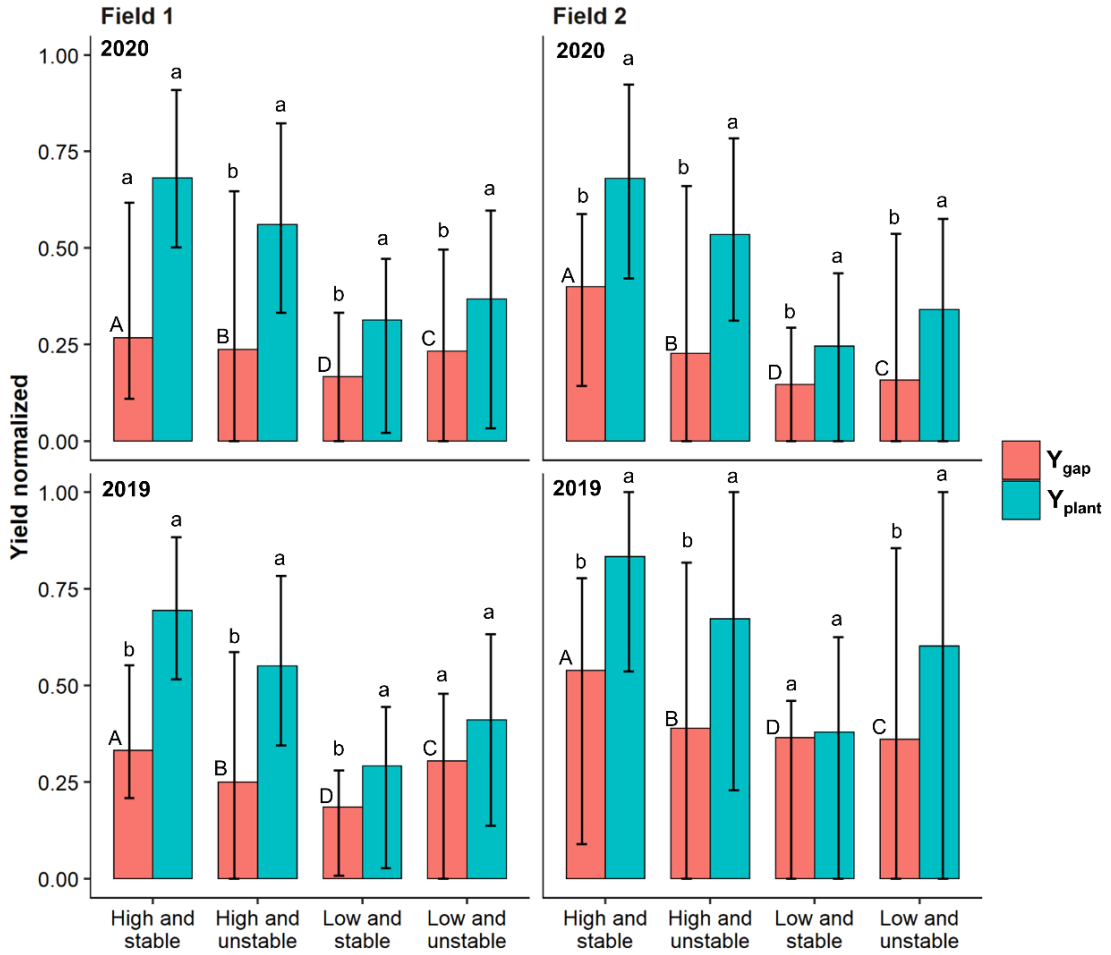

Figure 43. Comparison of yield in each yield class. Y_{gap} – yield in regions without plants. Y_{plant} – yield in regions with plants. Different lowercase letters above the box indicate a significant difference between the groups in the yield class. Different uppercase letters indicate a significant difference in the Y_{gap} between the class (Tukey test; $p<0.05$).

The influence of plant spacing within the row on the final yield of sugarcane has different behavior for different yield potentials (Fig. 44). In high and stable yield regions the increase in plant spacing does not reduce the yield within the row. The same was found for the high and unstable yield regions where yields increased in variation from 3.5 m plant spacing, in contrast to regions of low yield over the years, where increasing plant spacing leads to a gradual reduction in yield. In regions with low and stable yields, the reduction in yield starts at plant spacing greater than 1.0 m, and in regions with low and unstable yields there was a decrease in yield at spacing greater than 1.5 m. Regions with different yield potentials require different plant densities within the row. In this study, in high-yielding

regions, the spacing between plants can be greater compared to low-yielding regions without reducing the final yield within the row. While low yielding regions require a greater number of plants within the row to reach maximum yield potential, and increasing plant spacing gradually reduces final yield. In other words, each region requires an optimum population that maximizes yields. However, there is still a need for more studies with different cultivars and different row spacing and cropping systems.

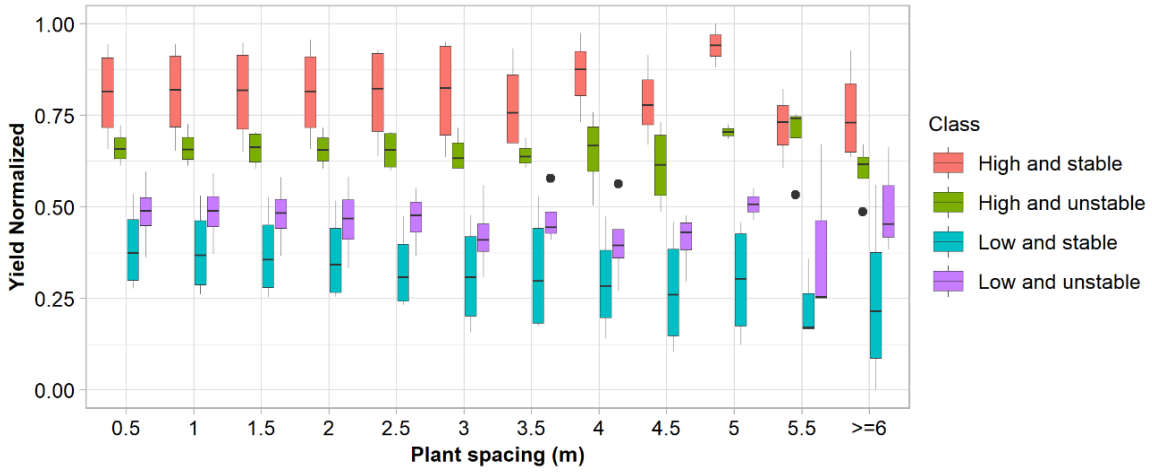

Figure 44. Yield versus plant spacing in the different classes of yield within fields.

By performing the regression analysis, it was possible to verify that the yield reduction within the sugarcane rows occurs with the increase in in-row plant spacing (Fig. 45). High, stable, and unstable yield sites have the same pattern of yield reduction with increasing plant spacing. Being in these regions the linear model had a moderate fit with R2 between 0.5 and 0.6. Low and unstable yield sites had larger angular coefficients in the fitted regression, i.e., the increase in plant spacing has a steeper decrease in yield when compared to high yield sites. The reduction in plant density in these regions and consequently loss in yield, consequently, can decrease its economic return. A recent study by (Neto et al., 2018) shows that the density of sugarcane plants can influence the final yield. From this, regions with a higher probability of yield loss over the years can be identified. However, the authors show that in some fields with larger in-row plant spacing there is a greater tillering in relation to fields with higher plant density.

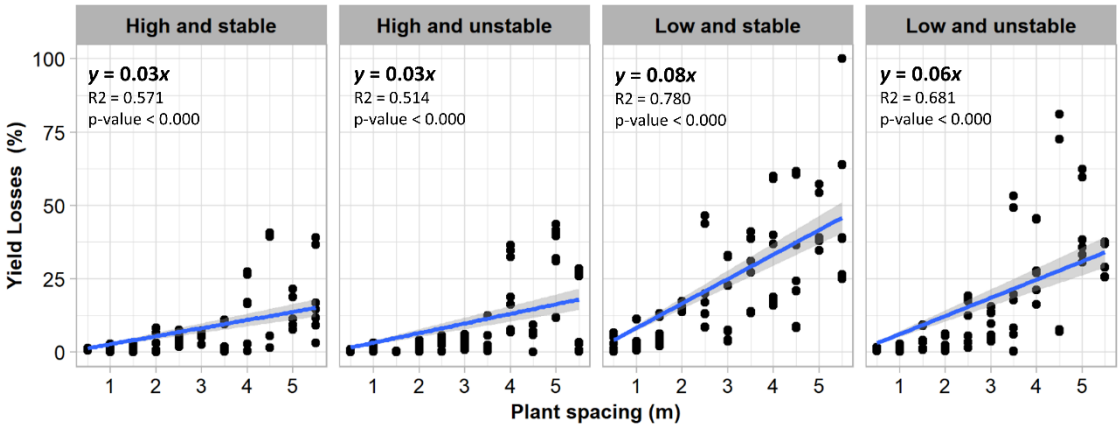

Figure 45. Yield loss within the sugarcane row in relation to plant spacing. Each black dot represents the median loss value for each plant spacing in 2019 and 2020, Field 1, and Field 2. The blue line is the fitted linear model for each yield class.

Increasing or decreasing the plant spacing within the row has a clear effect on the yield. In this influence, there should be a location within the same field where the maximum yield is predictable and which should be at the optimum plant spacing. However, we still need to understand the relationship between vegetative vigor, tiller density, within-row arrangement, and yield to select varieties and plant spacing that will yield more in different specific regions within the same field and/or with different management systems. Optimal plant spacing and/or seedling density during planting is one of the most significant cultural decisions a producer makes. Since sugarcane is a perennial crop, the establishment of the sugarcane field demands special caution, since it becomes the basis for cultivation during the next few years of the crop in the field. At planting it is necessary to establish an optimum plant population, because over the years a reduction of plants may occur due to the traffic of heavy machinery traffic, pests, diseases, and climate factors (Matsuoka and Stolf, 2012). This work showed that the identification of regions of high and low productive potential can guide future planting by varying the plant population. Nevertheless, controlling the sugarcane plant population at planting is not as easy as it is in crop seedlings such as corn, soybeans, or cotton. Sugarcane field establishment is accomplished by vegetative propagation through stalks (setts). After planting the sett (the propagative portion of the stalk), the bud sprouts to form the primary shoot (Matsuoka and Stolf, 2012). On the other hand, sugarcane field establishment with pre-sprouted sugarcane seedlings (dos Santos et al., 2020; Santos et al., 2020; Teixeira et al., 2020), which is increasingly being adopted by farmers, can be a solution for planting with a varied population of seedlings within the sugarcane fields. The sugarcane seedling represents part of the cost of planting, to have smaller spacing between plants a larger number of seedlings is necessary and consequently increases the cost of planting. On the other hand, it is necessary to calculate what is the economic return of reducing the plant spacing, or the cost of replanting plants over the years in places where there has been an increase in plant spacing and yield loss.

5.4. Conclusion

The yield over the years was classified as high, low, stable, and unstable, and the spacing between plants between these regions varies and can influence the final yield. Regions with equal spacing and above 1.0 m have lower yields compared to other yield classes. Furthermore, spacing in regions with high and stable yields did not result in yields with zero values. Unlike other regions that had no yield on some scales. The hypothesis that plant density influences yield was confirmed, with yield loss within the sugarcane row occurring with increasing plant spacing. Regions with different yield potentials require different optimum populations to maximize yield. Low-yielding regions require a larger plant population and are more susceptible to lose in yield within the row with increasing plant spacing. However, there is a need to conduct studies with other sugarcane cultivars, moreover, with different planting media. Moreover, understanding the relationship between plant spacing and yield is fundamental to the decision-making and success of localized sugarcane management.

Reference

Blackmore, S., Godwin, R.J., Fountas, S., 2003. The Analysis of Spatial and Temporal Trends in Yield Map Data over Six Years. Biosyst. Eng. 84, 455–466. https://doi.org/10.1016/S1537-5110(03)00038-2

Cambardella, C.A., Moorman, T.B., Novak, J.M., Parkin, T.B., Karlen, D.L., Turco, R.F., Konopka, A.E., 1994. Field-Scale Variability of Soil Properties in Central Iowa Soils. Soil Sci. Soc. Am. J. 58, 1501–1511.

https://doi.org/10.2136/sssaj1994.03615995005800050033x

dos Santos, L.C.N., Teixeira, G.C.M., Prado, R. de M., Rocha, A.M.S., Pinto, R.C. dos S., 2020. Response of Pre-sprouted Sugarcane Seedlings to Foliar Spraying of Potassium Silicate, Sodium and Potassium Silicate, Nanosilica and Monosilicic Acid. Sugar Tech 2020 225 22, 773–781. https://doi.org/10.1007/S12355-020-00833-Y

Ehsanullah, K.J., Jamil, M., Ghafar, A., 2011. Optimizing the row spacing and seeding density to improve yield and quality of sugarcane. Crop Environ. 2, 1–5.

Gasparotto, L.G., Rosa, J.M., Marin, F.R., 2020. Interrow spacing and sugarcane yield in a diversity of climates: A major review. Agron. J. https://doi.org/10.1002/agj2.20425

Jordahl, K., Bossche, J. Van den, Fleischmann, M., Wasserman, J., McBride, J., Gerard, J., 2020. geopandas/geopandas: v0.8.1. https://doi.org/10.5281/zenodo.3946761

Luna, I., Lobo, A., 2016. Mapping crop planting quality in sugarcane from UAV imagery: A pilot study in Nicaragua. Remote Sens. 8, 1–18. https://doi.org/10.3390/rs8060500

Maldaner, Leonardo Felipe, Canata, T.F., Molin, P.J., 2021a. An approach to sugarcane yield estimation using sensors in the harvester and ZigBee technology. Sugar Tech (Under Rev.

Maldaner, L.F., Molin, J.P., 2020. Data processing within rows for sugarcane yield mapping. Sci. Agric. 77, e20180391. https://doi.org/10.1590/1678-992x-2018-0391

Maldaner, L.F., Molin, J.P., Dias, C.T. dos S., Martello, M., Canata, T.F., 2021. Mapping sugarcane spatial patterns using spatial and temporal analysis of features extracted from UAV images. Biosyst. Eng. (Under Rev.

Maldaner, Leonardo Felipe, Molin, J.P., Martello, M., Tavares, T.R., Dias, F.L.F., 2021b. Identification and measurement of gaps within sugarcane rows for site-specific management: Comparing different sensor-based approaches. Biosyst. Eng. 209, 64–73. https://doi.org/10.1016/j.biosystemseng.2021.06.016

Matsuoka, S., Stolf, R., 2012. Sugarcane tillering and ratooning: key factors for a profitable cropping, in: Goncalves, J.F., Correia, K.D. (Eds.), Sugarcane: Production, Cultivation and Uses. Nova Science Publishers.

Molin, J.P., Amaral, L.R. do, Colaço, A.F., 2015. Agricultura de Precisão, 1st ed. Oficina de Textos, São Paulo.

Neto, J.R., de Souza, Z.M., de Medeiros Oliveira, S.R., Kölln, O.T., Ferreira, D.A., Carvalho, J.L.N., Braunbeck, O.A., Franco, H.C.J., 2017. Use of the Decision Tree Technique to Estimate Sugarcane Productivity Under Edaphoclimatic Conditions. Sugar Tech 19, 662–668. https://doi.org/10.1007/s12355-017-0509-7

Neto, J.R., de Souza, Z.M., Kölln, O.T., Carvalho, J.L.N., Ferreira, D.A., Castioni, G.A.F., Barbosa, L.C., de Castro, S.G.Q., Braunbeck, O.A., Garside, A.L., Franco, H.C.J., Menezes De Souza, Z., Oriel, &, Kölln, T., Luis, J., Carvalho, N., Ferreira, D.A., Guilherme, &, Ferreira Castioni, A., Carneiro Barbosa, L., Sérgio, &, Quassi De Castro, G., Braunbeck, O.A., Garside, A.L., Coutinho, H., Franco, J., 2018. The Arrangement and Spacing of Sugarcane Planting Influence Root Distribution and Crop Yield. BioEnergy Res. 11, 291–304. https://doi.org/10.1007/s12155-018-9896-1

Paula, V.R. de, Molin, J.P., 2013. Assessing Damage Caused by Accidental Vehicle Traffic on Sugarcane Ratoon. Appl. Eng. Agric. 29, 161–169. https://doi.org/10.13031/2013.42642

Santos, H.G. dos, Jacomine, P.K.T., Anjos, L.H.C. dos, Oliveira, V.A. De, Lumbreras, J.F., Coelho, M.R., Almeida, J.A. de, Araujo Filho, J.C. de, Oliveira, J.B. de, Cunha, T.J.F., 2018. Sistema brasileiro de classificação de solos, 5th ed, Embrapa Solos.

Santos, L.S., Braga, N.C.C., Rodrigues, T.M., Neto, A.R., Brito, M.F., da Costa Severiano, E., 2020. Pre-sprouted Seedlings of Sugarcane Using Sugarcane Industry By-products as Substrate. Sugar Tech 22, 675–685.

https://doi.org/10.1007/s12355-020-00798-y

Shirzadifar, A., Maharlooei, M., Bajwa, S.G., Oduor, P.G., Nowatzki, J.F., 2020. Mapping crop stand count and planting uniformity using high resolution imagery in a maize crop. Biosyst. Eng. 200, 377–390. https://doi.org/10.1016/j.biosystemseng.2020.10.013

Stolf, R., 1986. Metodologia de avaliação de falhas nas linhas de cana-de-açúcar. Stab 4, 22–36.

Teixeira, G.C.M., de Mello Prado, R., Rocha, A.M.S., dos Santos, L.C.N., dos Santos Sarah, M.M., Gratão, P.L., Fernandes, C., 2020. Silicon in Pre-sprouted Sugarcane Seedlings Mitigates the Effects of Water Deficit After Transplanting. J. Soil Sci. Plant Nutr. 20, 849–859. https://doi.org/10.1007/s42729-019-00170-4

Whelan, B.M., McBratney, A.B., 2000. The "null hypothesis" of precision agriculture management. Precis. Agric. 2, 265–279. https://doi.org/10.1023/A:1011838806489

6. FINAL CONSIDERATIONS

This research has provided several technological advances to make proximal sensors, high-resolution images, and yield maps more efficient and effective in localized management of sugarcane fields. The use of proximal plant sensors in sugarcane is an emerging technology that may results in the real-time application of inputs and the generation of high-resolution data for localized management of the sugarcane field. The practical application of high-resolution images in sugarcane is growing and produces accurate and spacialized information necessary for the management of the sugarcane field. This thesis had four distinct studies within the same context of generating spacialized information of the plants within the rows to contribute to the most economically viable management and minimizing the environmental impacts of sugarcane production. This research describes the following contributions to knowledge that will make the management of sugarcane fields more effective and efficient:

- A sensor system has been developed in which photoelectric and ultrasonic sensors together with a displacement sensor can detect the plants within a sugarcane row and measure the plant spacing. Growers to manage their sugarcane fields can easily use this system.
- For the first time, a system with photoelectric and ultrasonic sensors was used simultaneously to detect sugarcane plants within the rows. This system can be used to accurately detect plants in each row within the sugarcane field for ON/OFF fertilizer applications and to generate georeferenced information on plant population and plant spacing.
- This thesis presents three different methods to detect, measure, and map the gaps within the sugarcane rows, using proximal plant sensors and the high-resolution image generated by cameras attached to an unmanned aerial vehicle (UAV). Based on the analyses, for each methodology studied it was possible to propose the best time to detect sugarcane plants and measure the plat spacing.
- Through the proposed approach of plant identification by high-resolution images generated by cameras attached to a UAV, it is possible to accurately count plants in the early-grown stages of the crop. Thus, this methodology can help farmers to map the regions with greater susceptibility to plant reduction over the years.
- Based on the spatial-temporal analysis of sugarcane yield it was possible to verify that plant spacing within rows influences final yield and regions with different yield potentials require different optimum plant populations.

For future work, adding an ON/OFF and variable-rate dosing system to the plant detection system will help analyze the economic potential of using these sensors for localized row-by-row and plant-by-plant application within the sugarcane fields. Studies with high-resolution images for mapping plant populations have yet to be conducted using a greater diversity of sugarcane cultivars and different crop types, for example, different row spacing and seedling types during planting. For temporal analysis of plant population, new data layers should be added, such as soil physical attributes, climate, cultivar, and others. Increased adoption of spatialized high-resolution yield data, i.e., row-by-row yield data, is necessary to aid further research. Knowing how much each sugarcane plant is producing within the row will be necessary for the effectiveness and feasibility of localized sugarcane field management.